AN ABSTRACT OF THE DISSERTATION OF

Andrea R. Burton for the degree of Doctor of Philosophy in Integrative Biology presented on April 20, 2020.

Title: Adaptive Potential of Coastal Invertebrates to Environmental Stressors and Climate Change

Abstract approved: _____

Felipe S. Barreto

Climate change presents multiple stressors that are impacting marine life. As carbon dioxide emissions continue to increase in the atmosphere, atmospheric and sea water temperatures increase. In addition, more carbon dioxide is absorbed into the oceans, reducing pH and aragonite saturation state, resulting in ocean acidification (OA). Tightly coupled with OA is hypoxia due to deep stratified sea water becoming increasingly acidified and deoxygenated. The effects of these climate stressors have been studied in detail for only a few marine animal models. However, there are still many taxa and developmental stages in which we know very little about the impacts. Using genomic techniques, we examine the adaptive potential of three local marine invertebrates under three different climate stressors: marine disease exacerbated by thermal stress, OA, and combined stressors OA with hypoxia (OAH). As sea water temperatures rise, the prevalence of marine diseases increases, as seen in the sea star wasting syndrome (SSWS). The causation of SSWS is still widely debated; however reduced susceptibility to SSWS could aid in understanding disease progression. By examining genetic variation in *Pisaster ochraceous* collected during the SSWS outbreak, we observed weak separation between symptomatic and asymptomatic individuals. OA has been widely studied in many marine organisms, including *Crassostrea gigas*. However, limited studies have parsed the effects of OA during settlement, with no studies assessing the functionality of settlement and how it is impacted by OA. We investigated the effects of OA on settlement and gene expression during the transition from larval to juvenile stages in Pacific oysters. While OA and hypoxia are common climate stressors examined, the combined effects have scarcely examined. Further, the impacts of OAH have been narrowly focused on a select few species, with many economically important organisms having no baseline information on how they will persist as OAH severity increases. To address these gaps in our knowledge, we measured genetic variation in metabolic rates during OA for the species *Haliotis rufescens* to assess their adaptive potential through heritability measurements. We discuss caveats and considerations when utilizing similar heritability estimate methods for other understudied organisms. Together, these studies will provide novel information on the biological responses and susceptibility of difference coastal species to stressors associated with global climate change. These experiments provide information on both the vulnerability of current populations and their genetic potential for adaptation to changing ocean conditions.

Adaptive Potential of Coastal Invertebrates to Environmental Stressors and Climate Change

by
Andrea R. Burton

A DISSERTATION

submitted to

Oregon State University

in partial fulfillment of
the requirements for the
degree of

Doctor of Philosophy

Presented April 20, 2022
Commencement June 2022

Doctor of Philosophy dissertation of Andrea R. Burton presented on April 20, 2022

APPROVED:

Major Professor, representing Integrative Biology

Head of the Department of Integrative Biology

Dean of the Graduate School

I understand that my dissertation will become part of the permanent collection of Oregon State University libraries. My signature below authorizes release of my dissertation to any reader upon request.

Andrea R. Burton, Author

ACKNOWLEDGEMENTS

I would like to thank Dr. Felipe Barreto for all his support throughout my PhD. I will always appreciate Felipe welcomed me into the lab despite it requiring learning multiple systems and techniques outside of his comfort zone. Felipe was always approachable and incredibly helpful with all aspects of my research, which really helped me keeping my progress structured. Our meetings felt like a perfect balance between encouraging me to critically think while educating me about complex processes in genomic research. Felipe was instrumental to helping me developing and completing my dissertation despite all the challenges presented during the COVID-19 pandemic.

Becoming a PhD graduate student would have never been possible without Dr. Eli Meyer. Being accepted in Eli's lab gave me a sense of belonging in the scientific world. Thank you for believing in me and supporting me even now when you have no obligation to. Eli introduced me to coding and bioinformatics, which was a steep learning curve for me that I now feel proficient in.

I would like to thank my committee members Drs. Chris Langdon, Francis Chan, Molly Burke, and Stephen Ramsey for all their continuous help over the years. My ability to work with Chris before I was officially a grad student enabled me to get an early start on my dissertation work. Francis always encouraged me to think about the bigger picture, especially when it came to thinking about climate change. Molly was pivotal during my last year both with my dissertation and helping me navigate funding options for my last term. I will always appreciate Stephen's dedication to being an effect graduate representative, despite not have a strong background in my research. My committees' continual insights sand guidance into my dissertation helped me become a better scientist.

I want to sincerely thank Drs. Lindsay Biga, Lori Kays, and Devon Quick for their mentorship while teaching the Introductory Biology and Human Anatomy and Physiology Labs. Working with you all helped me improve my science communication, teaching, and implementing new teaching techniques into my courses. Your dedication towards constantly updating your courses to better facilitate student's needs is a practice I will strive to complement as I move forward in my career.

I am also appreciative of Dr. Sarah Gravem and Hannah Gossner whose collaborated with me on one of my chapters. Hannah Gossner conducted the experiment for one of my chapters and was a reliable resource when I needed to ask questions about her data set. I have worked closely with Sarah Gravem both on publishing my first manuscript but also through the Primary Responders in Marine Emergent Diseases (PRIMED) network. I have enjoyed working with her and having an opportunity to discuss my sea star research on a broader scale.

I would like thank Dr. Katie Dziedzic, Dr. Evan Durland, and Dan Schneck who I have dubbed my "secondary mentors". I can't thank you all enough for all the times I needed help for more trivial questions pertaining to my dissertation. You all were quick to share ideas, codes, and laughs, which made working on my dissertation easier and worthwhile.

I would also like to thank my lab mates, Dr. Holland Elder, Kamron Kayhani, Kris Bauer, and Marine Andriot. You all were instrumental at providing insightful feedback to presentations and papers that made my research stronger. You all provided much needed social breaks from work during the pandemic.

I want to give a special thank members from my cohort, Shumpei Maruyama, Silke Bachhuber, Heather Fulton, and Rebecca Mostow. You all aided in the balance between work and play. Between game nights, coastal trips, hiking adventures were insightful discussion that made graduate life more bearable.

I would also like to thank my family, Andrew Burton, Steven Burton, and Eva Burton. You all are the more amazing family members I cannot imagine, and I truly couldn't have done this without you. You have continually been supportive of me throughout all my academic and non-academic endeavors. Thank you for believing in me even when I didn't believe in myself. I aspire to always make you all proud of me as I move forward with my career.

CONTRIBUTION OF AUTHORS

Dr. Felipe Barreto contributed significantly to analysis from each chapter. He provided equipment, reagents, and funds towards all my Chapters, including sequencing for Chapters 2 and 4. Additionally, Felipe provided feedback on all my writing and helped develop tables and figures.

Dr. Chris Langdon provided facilities to conduct an experiment along with providing feedback on Chapter 3.

Dr. Francis Chan contributed assistance in analyses of Chapters 4.

Dr. Sarah Gravem contributed to sample collection and fieldwork for sea stars in Chapter 2.

Dr. Evan Durland assisted in the experimental design, collection, and analysis of Chapter 3.

Masters Hannah Gossner conducted preliminary experiments for Chapter 4.

TABLE OF CONTENTS

TABLE OF CONTENTS (Continued)

TABLE OF CONTENTS (Continued)

LIST OF FIGURES

LIST OF TABLES

LIST OF APPENDIX FIGURES

LIST OF APPENDIX TABLES

DEDICATION

To my parents. Thank you all for supporting me throughout the years. I wouldn't be the person I am today without your continuous encouragement as I navigated through different educational experiences and travelling the world. I love you both and hope I continue to make you proud.

To my brother, Andrew Burton. You were my first and biggest role model as your love for nature, animals, and science was intoxicating and is the biggest reason I went on to become a Biologist. I love you and thank you for always being there for me.

CHAPTER 1 – General introduction

Background on climate change

Global climate change has negatively impacted marine life in many ways. As carbon and other greenhouse gas emissions continue to increase in our atmosphere, our oceans are experiencing rising seawater temperatures, sea level rise, salination, ocean acidification (OA), and hypoxia (IPCC et al. 2021). Locally, the acidification of California Current Large Marine Ecosystem (CCLME) often coincides with hypoxic conditions due to seasonal upwelling (Chan et al. 2008). OA and hypoxia (OAH) along with rising sea water temperatures are among the greatest threat to the Pacific ocean's eastern boundary (Harley et al. 2006; McClatchie et al. 2010). Since the industrial revolution, global sea surface temperatures have increased 0.88°C (IPCC et al. 2021). Oxygen concentrations in the eastern temperate Pacific have declined 10 to 20 % over the last three decades (Bograd et al. 2008). Ocean temperatures are predicted to rise 1.76C to 5.28C by 2100 (IPCC et al. 2021). While ocean waters are warming, the pH of our oceans has already dropped 0.1 units since the industrial era, meaning acidity is approximately 30% higher (Caldeira and Wickett 2003; Doney et al. 2009; IPCC et al. 2021). Projections of continued carbon emissions predict a decrease of 0.06 to 0.31 pH units by 2100. Concentrations of oxygen in our oceans are declining due to heat-related stratification, reduced oxygen solubility as temperatures increase, and biological processes that produce or consume oxygen (Deutsch et al. 2015, IPCC 2014), resulting in hypoxia (Hoegh-Guldberg et al. 2018).

Increasing sea water temperatures, ocean acidification, and hypoxia pose a major threat to marine ecosystems. Thermal stress has shown to have physiological impacts on marine organisms (Hofmann and Somero 1995; Stillman and Somero 1996). Heat stress can damage molecular structure (Pörtner 2010), induce thermal hypoxemia, transitions to anaerobic energy production, and oxidative stress (Lannig et al. 2010; Sommer et al. 1997). These types of mechanisms may result in marine organisms being more prone to marine diseases as there are thermally stressed. Increased seawater temperatures has resulted in increased susceptibility to diseases in hosts (Harvell et al. 2002). In addition, warmer waters increase pathogen development, rates, transmission, and number of generations per year. As a result, we have seen a higher prevalence of marine diseases over the last few decades (Harvell et al. 2002, 2004).

Ocean Acidification and Hypoxia

Ocean acidification, the result of increased acidified conditions due to increased concentrations of carbon dioxide, has negative impacts on calcifying marine organisms. Absorption of atmospheric CO_2 into the ocean elevates CO_2 partial pressure (pCO_2), resulting in shifts in carbonate chemistry. Dissolved CO_2 in seawater results in the formation of carbonic acid (Caldeira and Wickett 2003; Feely et al. 2009; Orr et al. 2005). Carbonic acid then dissociates, which results in a decrease in

carbonate (CO^{2-}_3) ions and an increase in bicarbonate (HCO^-_3) and hydrogen (H^+) ion concentrations (Eq. 1).

$$CO_{2(g)} \Leftrightarrow CO_{2(aq)} + H_2O \Leftrightarrow H_2CO_3 \Leftrightarrow HCO_3^- + H^+ \Leftrightarrow CO_3^{2-} + 2H^+ \quad \text{[Eq. 1]}$$

Accumulation of H^+ ions result in pH reduction ($pH = -\log[H^+]$), along with shifts in carbonate chemistry. Hydrogen ions have a high affinity towards carbonate, leading to a shift towards the left of Equation 1, which in turn leads to an increase in bicarbonate and a decrease in carbonate ions (Feely et al. 2004; Zeebe and Wolf-Gladrow 2001). The shift in carbonate chemistry results in a decrease in saturation state (Ω) (Feely et al. 2009; Orr et al. 2005). Aragonite saturation state (Ω_{arag}) is calculated as follows is the product of dissolved calcium and carbonate ions, divided by apparent solubility product (K_{sp}) (Eq. 2).

$$\Omega_{arag} = \frac{[Ca^{2+}][CO_3^{2-}]}{K_{sp}} \quad \text{[Eq. 2]}$$

When saturation state is 1 seawater is in equilibrium ($\Omega_{arag} = 1.0$). Decreasing saturation state below 1 ($\Omega_{arag} < 1.0$), seawater is thermodynamically unfavorable for organisms to build their calcium carbonate shells ($CaCO_3$) (Fabry et al. 2008; Feely et al. 2004; Hofmann et al. 2010; Orr et al. 2005).

The California Current Large Marine Ecosystem (CCLME) spans from Vancouver Island, Canada, to Punta Eugenia, Mexico. CCLME experiences seasonal upwelling during the summer (Feely et al. 2008). These upwelling waters contain dissolved inorganic carbon (DIC) (>2190 μmol kg, pH = 7.75), and low calcium carbonate saturation ($\Omega_{arag} < 1.0$) (Chan et al. 2008; Harris et al. 2013; Somero et al. 2016). Aragonite saturation state from upwelled waters has seen decreases in value ($\Omega = 0.66$) (N. Gruber et al. 2012).

Within the CCLME, upwelled water brings nutrient-rich water to the surface (Snyder et al. 2003). Increased productivity due to the influx of nutrients results in higher rates of remineralization of organic carbon into DIC (Feely et al. 2016). As organic matter breaks down, oxygen levels decrease, creating hypoxic zones (Chan et al. 2008). For this reason, OA is intrinsically linked to hypoxia, as DIC is coupled with pH and saturation state (Waldbusser et al. 2015). The coupling of OA and deoxygenation may potentially accelerate acidified condition progression on the Pacific's eastern boundary (Chan et al. 2008). Models predict that coastal upwelling from the CCLME is predicted to reach undersaturated aragonite levels by 2050. Exposure to these OAH conditions make a corrosive and metabolically stressful environment for calcifying organisms (Gruber et al. 2012).

Impacts of Ocean Acidification and Hypoxia

Seawater with an elevated partial pressure of CO_2 (pCO_2) impairs calcification, growth, reproduction, and survival in many marine animals, and these effects vary widely among species

(Kroeker et al. 2010). Increased pCO_2 leads to an increase in carbonic acid (H_2CO_3) forming hydrogen ions (H^+) and bicarbonate ions (HCO_3^-), reducing the pH and saturation state of calcium carbonate ($CaCO_3$) (Broecker and Clark 2001; Caldeira and Wickett 2003; Doney et al. 2009; Orr et al. 2005). (Broecker and Clark 2001; Caldeira and Wickett 2003; Doney et al. 2009; Orr, Fabry, Aumont, Bopp, Doney, Feely, Gnanadesikan, Gruber, Ishida, Key, et al. 2005). Lower saturation states directly affect the calcium carbonate secretion of calcifying organisms, reducing calcification rates and increasing the metabolic costs of calcification (Pan et al. 2015).

Calcification, the process of crystallization of carbonate minerals from solution, is energetically favorable when seawater is over saturated. Shifts in saturation states has been shown to affect calcium carbonate secretion in calcifying organisms (Pan et al. 2015), resulting in reduced shell formation and shell dissolution (Doney et al. 2009, Orr et al. 2005). Calcification in more favorable in calcifying organism when sea water is over saturated ($\Omega > 1.0$) (Feely et al. 2004a, Orr et al. 2005, Fabry et al. 2008, Waldbusser et al. 2015a). Reduced pH and saturation states is especially concerning for organisms found along the Oregon coast as they are also subjected to periodic upwelling. Many marine invertebrates rely on gas exchange from their membranes with the sea water. With increasing acidity, marine organisms need to make adjustments to counteract ion concentrations in the sea water through inner acid-base balance (Fabry et al. 2008). Such adjustments can be energetically expensive and may result in reallocation of cellular processes (Burnett 1997; Pörtner 2008).

There is a growing interest in the effects of OA on early developmental stages. In most marine organisms, early life stages are more vulnerable to OA (Kroeker et al. 2010). Early in development, larvae are more sensitive to environmental conditions (Pechenik 1987), resulting in much higher rates of mortality overall (Gosselin and Qian 1997). It is during these early stages that calcifying organisms first deposit their calcium carbonate shells and skeleton, which is energetically demanding (Kurihara 2008). In particular, metamorphosis is a stage in development where rapid calcification is required (Plough 2018). Studies have demonstrated that OA treatments impair metamorphic transition and reduce settlement success (Kurihara 2008). However, the mechanisms in which metamorphosis is impacted by OA conditions have yet to be explored. In chapter 3, I examine the impacts of OA on the Pacific oyster, *Crassostrea gigas*, during metamorphosis. I identify genes related to settlement that are differentially expressed between ambient have high pCO_2 treatments.

Hypoxic water has been shown to modify organism behavior, along with reducing growth, calcification, and gonad production (Low and Micheli 2020; Riedel et al. 2014), and in prolonged exposure mass mortality (Vaquer-Sunyer and Duarte 2008). Few studies have examined the synergistic effects of OAH on marine organisms (Pörtner 2005; Steckbauer et al. 2015). The blue mussel, *Mytilus edulis,* exhibited additive effects of low pH and hypoxia during short-term exposure (Gu et al. 2019). In 17 species of invertebrates along the Chilean coast, metabolic rates varied across taxa in a multi-factorial OA and hypoxia study (Steckbauer et al. 2015). Overall, Steckbauer (et al. 2015) saw additive effects of hypoxia and high pCO_2, but not consistent synergetic or antagonist effects. More studies are

needed to understand the impacts of OAH on calcifying organism as OA and hypoxia are not mutually exclusive (Chan et al. 2008). We examine the vulnerability and adaptive potential of the red abalone, *Haliotis rufescens*, by comparing four OAH treatments to estimate heritability of variation in metabolic rate for both species in chapter 4.

Increasing Prevalence of Marine Diseases

Marine diseases have become more prevalent due to warmer waters (Harvell et al. 2002). Harvell et al. (2002) predicts that warmer waters provide a more hospitable environment for pathogens to flourish, in addition to hosts being more susceptible as their immune systems are weekend. The impacts of increased sea water temperatures resulting in a higher prevalence of marine disease was apparent when evaluating the spread and occurrence of Sea Star Wasting Syndrome (SSWS). The SSWS epidemic began in 2013, and rapidly spread along the western coast of the United States, ranging from Baja California, Mexico, to the Gulf of Alaska, USA (Hewson et al. 2014, 2018). Sea stars that were impacted by SSWS had higher rates of symptoms in regions with higher sea water temperatures (Bates et al. 2009; Eckert et al. 1999; Eisenlord et al. 2016; Kohl et al. 2016). The spread and severity of SSWS was exacerbated by rising sea water temperatures, which are only going to worsen as global climate change progresses. Over 20 species of sea stars were impacted, including that of the keystone species*, Pisaster ochraceus*.

Purpose of Chapter 2

Chapter 2 is entitled, “Little evidence for genetic variation associated with susceptibility to sea star wasting syndrome in the keystone species *Pisaster ochraceus*”. In this chapter, I investigate genomic differences between wasting and apparently normal *P. ochraceus*". Using restriction site-associated DNA sequencing (2bRAD-seq), I examine genetic variation in ~72,000 SNP loci. No genetic differences were found when analyzing differentiation (F_{st}) between wasting and apparently normal individuals. I also found weak separation between the two disease-status groups through a discriminant analysis of principal components (DAPC). This study suggests that there is little genetic basis for reduced susceptibility to SSWS. However, from the gene regions we identified from the DAPC analyses, future studies can aid in functional studies intending to understand disease progression.

Purpose of Chapter 3

Chapter 3 is entitled, “Assessing how ocean acidification impacts gene expression patterns during settlement of *Crassostrea gigas*”. The purpose of this chapter is to identify genes important for settlement in the Pacific oyster, *Crassostrea gigas*, and how they are impacted by ocean acidification. Using transcriptomics, we were able to isolate 943 differentially expressed genes between ambient and high pCO_2 treatments when accounting for differences in developmental stages. An enrichment test

was run on these 943 genes, where we found 31 GO terms within the three classes: molecular function, biological processes, and cellular components. The enriched genes found in this study add to a growing body of literature of genes important for *C. gigas'* development and how OA impacts settlement.

Purpose of Chapter 4

Chapter 4 is entitled: "Limitations of estimating heritability of variation in respiration rates within a small sample size of *Haliotis rufescens*". For this chapter, we estimated heritability (h^2) in respiration rates as a proxy for metabolic activity in *Haliotis rufescens* when exposed and recovering from four different ocean acidification and hypoxia (OAH) conditions. Estimates of h^2 for respiration rates ranged from negative values to 0.25, indicating that traits for respiration rates are heritable. During OAH exposure, h^2 increased with increasing OAH stress conditions, but dropped in the most extreme OAH treatment. However, constraints in the data set leave us to believe that these h^2 estimates may not accurately reflect the species. In this chapter, we discuss the limitations in estimating heritability within a species lacking a complete genome along with issues that a rise from a small dataset consisting of individuals sampled from aquaculture settings.

References

Bates, A., Hilton, B., & Harley, C. (2009). Effects of temperature, season and locality on wasting disease in the keystone predatory sea star *Pisaster ochraceus*. Diseases of Aquatic Organisms, 86, 245–251.

Bograd, S.J., Castro, C.G., Lorenzo, E.D., Palacios, D.M., Bailey, H., Gilly, W., & Chavez, F.P. (2008). Oxygen declines and the shoaling of the hypoxic boundary in the California Current. Geophysical Research Letters, 35.

Broecker, W, & Clark, E. (2001). A dramatic Atlantic dissolution event at the onset of the last glaciation. Geochemistry, Geophysics, Geosystems, 2.

Burnett, L.E. (1997). The challenges of living in hypoxic and hypercapnic aquatic environments, American Zoologist. 37, 633-40.

Caldeira, K., & Wickett, M.E. (2003). Anthroponotic carbon and ocean pH. Nature 425:365-365.

Chan, F., Barth, J.A., Lubchenco, J., Kirincich, A., Weeks, H., Peterson, W.T., & Menge, B.A. (2008). Emergence of anoxia in the California Current Large Marine Ecosystem. Science 319, 920-920.

Deutsch, C., Ferrel, A., Seibel, B., Pörtner, H., & Huey. R.B. (2015). Climate change tightens a metabolic constraint on marine habitats. Science, 348, 1132-35.

Doney, S.C., Fabry, V.J., Feely, R.A., Kleypas, & J.A. (2009) Ocean acidification: The other CO_2 problem. Annual Review of Marine Science, 1, 169-92.

Eckert, G. L., Engle, J. M., & Kushner, D. J. (1999). Sea star disease and population declines at the Channel Islands. In Proceedings of the Fifth California Islands Symposium (pp. 390–393). Minerals Management Service.

Eisenlord, M. E., Groner, M. L., Yoshioka, R. M., Elliott, J., Maynard, J., Fradkin, S., Turner, M., Pyne, K., Rivlin, N., van Hooidonk, R., & Harvell, D. C. (2016). Ochre star mortality during the 2014 wasting disease epizootic: Role of population size structure and temperature. Philosophical Transactions of the Royal Society B: Biological Sciences, 371(1689).

Fabry, V.J., Langdon, C., Balch, W.M., Dickson, A.G., Feely, R.A., Hales, B., Hutchins, D.A., Kleypas, J.A., & Sabine, C.L. (2008). Ocean acidification's effects on marine ecosystems and biogeochemistry: Ocean carbon and biogeochemistry scoping workshop on ocean acidification research: La Jolla, California, 9-11 October 2007. Eos, Transactions American Geophysical Union, 89, 143.

Feely, R.A., Sabine, C.L., Lee, K., Berelson, W., Kleypas, J., Fabry, V.J., Millero, F.J. (2004). Impact of anthropogenic CO_2 on the $CaCO_3$ system in oceans. Science, 305, 362-66

Feely, R.A., Sabine, C.L., Hernandez-Ayon, J.M., Ianson, D, & Hales, B. (2008). Evidence for upwelling of corrosive "acidified" water onto the continental shelf. Science, 320, 1490-92.

Feely, R.A., Alin, S.R., Carter, B., Bednaršek, N., Hales, B., Chan, F., Hill, T.M., Gaylord, B., Sanford, E., Byrne, R.H., Sabine, C.L., & Greeley, D., Juranek, L. (2016). Chemical and biological impacts of ocean acidification along the west coast of North America. Estuarine, Coastal and Shelf Science, 183, 1-11.

Feely, R.A., Doney, S., & Cooley, S. (2009). Ocean acidification: Present conditions and future changes in a high-CO_2 world. Oceanography, 22, 36-47.

Gosselin, L.A., & Qian, P.Y. (1997). Juvenile mortality in benthic marine invertebrates. Marine Ecology Progress Series, 146, 265-82.

Gruber, N., Hauri, C., Lachkar, Z., Loher, D., Frölicher, T., & Plattner, G. (2012). Rapid progression of ocean acidification in the California Current System. Science, 337, 220-23.

Gu, Huaxin, Shang, Y. Clements, J. Dupont, S., Wang, T., Wei, S., Wang, X., Chen, J., Huang, W., Hu, M., & Wang, Y.(2019). Hypoxia aggravates the effects of ocean acidification on the physiological energetics of the blue mussel *Mytilus Edulis*. Marine Pollution Bulletin, 149, 110538.

Harley, C.D., Hughers, A.R., Hultgren, K.M., Miner, B.G., Sorte, C.J.B., Thornber, C.S., Rodriguez, L.R., Tomanek, L., & Williams, S.L. (2006). The impacts of climate change in coastal marine systems. Ecology Letters, 9, 228-41.

Harris, K.E., DeGrandpre, M.D., Hales, B. (2013). Aragonite saturation state dynamics in a coastal upwelling zone. Geophysical Research Letters, 40, 2720-25.

Harvell, D. C., Mitchell, C. E., Ward, J. R., Altizer, S., Dobson, A. P., Ostfel, R. S., & Samuel, M. D. (2002). Climate warming and disease risks for terrestrial and marine biota. Science, 296(5576), 2158–2162.

Harvell, D., Aronson, R., Baron, N., Connell, J., Dobson, A., Ellner, S., Gerber, L., Kim, K., Kuris, A., McCallum, H., Lafferty, K., McKay, B., Porter, J., Pascual, M., Smith, G., Sutherland, K., & Ward, J. (2004). The rising tide of ocean diseases: unsolved problems and research priorities. Frontiers in Ecology and the Environment, 2(7), 375–382.

Hewson, I., Button, J. B., Gudenkauf, B. M., Miner, B., Newton, A. L., Gaydos, J. K., Wynne, J., Groves, C. L., Hendler, G., Murray, M., Fradkin, S., Breitbart, M., Fahsbender, E., Lafferty, K. D., Kilpatrick, A. M., Miner, C. M., Raimondi, P., Lahner, L., Friedman, C. S., … Harvell, C. D. (2014). Densovirus associated with sea-star wasting disease and mass mortality. Proceedings of the National Academy of Sciences of the United States of America, 111(48), 17278–17283.

Hewson, I., Bistolas, K. S. I., Quijano Cardé, E. M., Button, J. B., Foster, P. J., Flanzenbaum, J. M., Kocian, J., & Lewis, C. K. (2018). Investigating the complex association between viral ecology, environment, and northeast Pacific Sea Star Wasting. Frontiers in Marine Science, 5(MAR).

Hoegh-Guldberg, O.D., Jacob., O., Bindi, D., Brown., M., Camilloni, S., Diedhiou, A., Djalante, R., Ebi, K., Engelbrecht, F., & Hijioka, Y. (2018). Impacts of 1.5°C global warming on natural and human systems. In: Global warming of 1.5°C. An IPCC special report on the impacts of global warming of 1.5C above pre-industrial levels and related global greenhouse gas emission pathways.

Hofmann, G.E., & Somero, G. (1995). Evidence for protein damage at environmental temperatures: Seasonal changes in levels of ubiquitin conjugates and Hsp70 in the intertidal mussel *Mytilus Trossulus*. The Journal of experimental biology, 98, 1509-18.

Hofmann, G.E., Barry, J.P., Edmunds, P.J., Gates, R.D., Hutchins, D.A., Klinger, T., & Sewell, & M.A. (2010). The effect of ocean acidification on calcifying organisms in marine ecosystems: An organism-to-ecosystem perspective. Annual Review of Ecology, Evolution, and Systematics, 41, 127-47.

IPCC (2014). Ocean Systems. In: Climate change 2014: Impacts, adaptation, and vulnerability. Part A: Global and sectoral aspects. Contribution of working group II to the fifth assessment report of the Intergovernmental Panel on Climate Change. Cambridge, United Kingdom and New York, NY.

IPCC (2021). Climate change 2021: The physical science basis. In: Contribution of working group I to the sixth assessment report of the Intergovernmental Panel on Climate Change.

Kohl, W. T., McClure, T. I., & Miner, & B. G. (2016). Decreased temperature facilitates short-term sea star wasting disease survival in the keystone intertidal sea star *Pisaster ochraceus*. PLoS One, 11(4), e0153670.

Kroeker, K.J., Kordas, R.L., Crim, R.N., & Singh, G.G. (2010). Meta-analysis reveals negative yet variable effects of ocean acidification on marine organisms. Ecology Letters, 13, 1419-34.

Kurihara, H. (2008). Effects of CO_2-driven ocean acidification on the early developmental stages of invertebrates. Marine Ecology Progress Series, 373, 275-84

Lannig, G., Eilers, S., Pörtner, H.O., Sokolova, I.M., & Bock, C.(2010). Impact of ocean acidification on energy metabolism of oyster, *Crassostrea gigas*—Changes in metabolic pathways and thermal response. Marine Drugs, 8, 2318-39.

Low, N.H.N, & Micheli, F. (2020). Short- and long-term impacts of variable hypoxia exposures on kelp forest sea urchins. Scientific reports, 10, 2631.

McClatchie, S., Goericke, R., Cosgrove, R., Auad, G., & Vetter, R. (2010). Oxygen in the southern California bight: Multidecadal trends and implications for demersal fisheries. Geophysical research letters, 37.

Orr, J.C., Fabry, V.J., Aumont, O., Bopp, L., Doney, S.C., Feely, R.A., Gnanadesikan, A., Gruber, N., Ishida, A., Joos, F. et al. (2005). Anthropogenic ocean acidification over the twenty-first century and its impact on calcifying organisms. Nature, 437, 681-86.

Pan, T.C.F, Applebaum, S.L., & Manahan, D.T. (2015). Experimental ocean acidification alters the allocation of metabolic energy. Proceedings of the National Academy of Sciences, 112, 4696-4701.

Pechenik, J.A. (1987). Environmental influences on larval survival and growth. Eds. A Giese and J. Pearse. New York: Blackwell Scientific.

Plough, L.V. (2018). Fine-scale temporal analysis of genotype-dependent mortality at settlement in the Pacific oyster *Crassostrea gigas*. Journal of Experimental Marine Biology and Ecology, 501, 90-98.

Pörtner, H. O. (2010). Oxygen-and capacity-limitation of thermal tolerance: A matrix for integrating climate-related stressor effects in marine ecosystems. Journal of Experimental Biology, 213, 881-93.

Pörtner, H. O. (2008). Ecosystem effects of ocean acidification in times of ocean warming: A physiologist's view. Marine Ecology Progress Series, 374, 203-17.

Pörtner, H. O. (2005). Synergistic effects of temperature extremes, hypoxia, and increases in CO_2 on marine animals: From earth history to global change. Journal of Geophysical Research. 110, C09S10.

Riedel, B., Pados, T., Pretterebner, K., Schiemer, L., Steckbauer, A., Haselmair, A., Zuschin, M., & Stachowitsch, M. (2014) Effect of hypoxia and anoxia on invertebrate behaviour: Ecological perspectives from species to community level. Biogeosciences, 11, 1491-1518.

Snyder, M.A., Sloan, L.C., Diffenbaugh, N.S., & Bell, J.L. (2003). Future climate change and upwelling in the California current. Geophysical Research Letters, 30.

Somero, G.B., Beers, J.M., Chan, F., Hill, T.M., Klinger, T., & Litvin, S.Y. (2016) What changes in the carbonate system, oxygen, and temperature portend for the northeastern Pacific Ocean: A physiological perspective. BioScience 66, 14-26.

Sommer, A., Klein, B, & Pörtner, H.O. (1997). Temperature induced anaerobiosis in two populations of the polychaete worm *Arenicola Marina* (L.). Journal of Comparative Physiology B, 167, 25-35.

Steckbauer, A., Hendriks, I.E., Fernandez, M., Lagos, N.A., Prado, L., & Duarte, C.M.(2015). Synergistic effects of hypoxia and increasing CO2 on benthic invertebrates of the central Chilean coast. Frontiers in Marine Science, 2, 49.

Stillman, J.H., & Somero, G.N. (1996). Adaptation to temperature stress and aerial exposure in congeneric species of intertidal porcelain crabs (Genus *Petrolisthes*): Correlation of physiology, biochemistry and morphology with vertical distribution. Journal of Experimental Biology, 199, 1845-55.

Vaquer-Synyer, R., & Duarte, C.M. (2008). Thresholds of hypoxia for marine biodiversity. Proceedings of the National Academy of Sciences, 105, 15452-57.

Waldbusser, G.G., Hales, B., Langdon, C.J., Haley, B.A., Schrader, P., Brunner, E.L., Gray, M.W., Miller, C.A., Gimenez, I., & Hitchinson, G. (2015). Ocean acidification has multiple modes of action on bivalve larvae. PLoS ONE, 10.

Zeebe, R., & Wolf-Gladrow, D. (2001). CO_2 in seawater-equilibrium, Kinetics, Isotopes. No. 65, Gulf Professional Publishing.

CHAPTER 2 – LITTLE EVIDENCE FOR GENETIC VARIATION ASSOCIATED WITH SUSCEPTIBILITY TO SEA START WASTING SYNDROME IN THE KEYSTONE SPECIES *PISASTER OCHRACEUS*

Andrea R. Burton, Sarah A. Gravem, Felipe S. Barreto

Published in:
Molecular Ecology
Pages 197- 205
John Wiley & Sons
111 River Street, 8-02
Hoboken, New Jersey

Abstract

The keystone species *Pisaster ochraceus* suffered mass mortalities along the northeast Pacific Ocean from Sea Star Wasting Syndrome (SSWS) outbreaks in 2013–2016. SSWS causation remains of debate, leading to concerns as to whether outbreaks will continue to impact this species. Considering the apparent link between ocean temperature and SSWS, the future of this species and intertidal communities remains uncertain. Surveys of co-occurring apparently normal and wasting *P. ochraceus* along the central Oregon coast in 2016 allowed us to address whether variation in disease status showed genetic variation that may be associated with differences in susceptibility to SSWS. We performed restriction site-associated DNA sequencing (2bRAD-seq) to genotype ~72,000 single nucleotide polymorphism (SNP) loci across apparently normal and wasting sea stars. Locus-specific analyses of differentiation (F_{st}) between disease-status groups revealed no signal of genetic differences separating the two groups. Using a multivariate approach, we observed weak separation between the groups, but identified 18 SNP loci showing highest discriminatory power between the groups and scanned the genome annotation for linked genes. A total of 34 protein-coding genes were found to be located within 15 kb (measured by linkage disequilibrium decay) of at least one of the 18 SNPs, and 30 of these genes had homologies to annotated protein databases. Our results suggest that the likelihood of developing SSWS symptoms does not have a strong genetic basis. The few genomic regions highlighted had only modest levels of differentiation, but the genes associated with these regions may form the basis for functional studies aiming to understand disease progression.

Introduction

Rising sea water temperatures, due to climate change, are becoming increasingly stressful to marine ecosystems. As a result, marine diseases have become more prevalent in the last few decades (Harvell et al. 2002, 2004). Disease outbreaks can have detrimental downstream effects on marine species due to changes in community structure and age distribution (Behringer, Silliman, and Lafferty 2018; Burge et al. 2014). Many marine taxa have suffered intense population declines as a result of the increasing prevalence of diseases (Burge et al. 2014; Harvell et al. 2004). These declines can result in reduced variation due to population bottlenecks and genetic drift, and possibly from strong directional selection associated with tolerance or resistance to disease (Nei, Maruyama, and Chakrabort 1975; Zenger, Richardson, and Vachot-Griffin 2003).

The Sea Star Wasting Syndrome (SSWS) epidemic event that began in 2013 is believed to be the largest marine wildlife disease on record (Gravem et al. 2021; Harvell et al. 2019). SSWS affected over 20 species of sea stars from Baja California, Mexico, to the Gulf of Alaska, USA (Hewson et al. 2014, 2018), and severely reduced population sizes of several sea star species (Gravem et al. 2021; Harvell et al. 2019; Hewson et al. 2014; Menge et al. 2016; Miner et al. 2018; Montecino-Latorre et al. 2016). Similar SSWS symptoms have been observed in British Columbia in 2008 (Bates, Hilton, and Harley 2009), along the US east coast (Bucci et al. 2017), the South Pacific (Pratchett 1999; Zann,

Brodie, and Vuki 1990), Australia and Yellow Sea (Hewson et al. 2019). While the viral candidate sea star-associated densovirus (SSaDV) has been debunked (Jackson et al. 2020), other possible causative or exacerbating agents remain unknown, with hypotheses including pathogen(s) (Lloyd and Pespeni 2018), inconsistent aetiology stress responses between locations, species and environment (Hewson et al. 2018), microbial dysbiosis (Lloyd and Pespeni 2018), and microbial-driven depletion of oxygen at the animal–water interface (Aquino et al. 2021). There is also mixed evidence for whether anomalously warm waters linked to global warming initiated the outbreak (Aalto et al. 2020; Eisenlord et al. 2016; Menge et al. 2016; Miner et al. 2018; Tracy, Weil, and Harvell 2020). Regardless, it is clear that the disease is exacerbated in warmer conditions (Bates, Hilton, and Harley 2009; Eckert, Engle, and Kushner 1999; Eisenlord et al. 2016; Kohl, McClure, and Miner 2016), and that severe population reductions occurred in warmer southern regions (Gravem et al. 2021; Harvell et al. 2019; Miner et al. 2018). The interplay between climate change and disease is a growing threat to wildlife species, especially when it causes rapid and extreme population declines. What is still unclear is whether tolerance or resistance to some of these diseases has a genetic basis that may allow populations to adapt if outbreaks continue to occur.

The keystone species *Pisaster ochraceus* was severely affected by SSWS over much of its range. In Oregon, their populations declined by 50%–94% (Menge et al. 2016). Because *P. ochraceus* aids in maintaining fast-growing *Mytilus californianus* populations from overgrowing intertidal zones (Paine 1966, 1969, 1974), declines in their populations have resulted in trophic cascades and regime shifts in intertidal regions (Burt et al. 2018; Miner et al. 2018; Schultz, Cloutier, and Côté 2016). Loss of *P. ochraceus* due to SSWS could have detrimental impacts on coastal ecosystems. It is likely that SSWS has exerted strong selection on *P. ochraceus* populations. Recent genetic studies on this and other affected sea star species suggest a genetic component to variation in SSWS susceptibility. Individuals with SSWS symptoms showed elevated expression levels in genes associated with immune response and tissue remodeling (Fuess et al. 2015; Gudenkauf and Hewson 2015; Ruiz-Ramos et al. 2020). In addition, Schiebelhut et al. (2018) observed allele frequency shifts before and after peak SSWS outbreaks in California populations of *P. ochraceus*. More specifically, they detected changes in restriction site-associated DNA sequencing (RAD-seq) haplotype frequencies between pre-SSWS adults and post-SSWS adults, as well as between pre-SSWS adults and recruits in the populations after SSWS. These changes occurred in few loci but were consistent across independent geographical samples (Schiebelhut, Puritz, and Dawson 2018). However, because Schiebelhut et al. (2018) genotyped only apparently normal individuals (asymptomatic), it is still unclear whether the allele shifts were caused by the disease itself or by other co-occurring factors.

Here, we build upon the work of Schiebelhut et al., (2018) by investigating genomic differences between wasting individuals (i.e., presenting with SSWS) and grossly, or apparently normal individuals from the same localities during an outbreak of SSWS. We examine genetic variation in 200 *P. ochraceu*s individuals collected in central Oregon in 2016, 2 years following the

initial spring 2014 SSWS outbreak in Oregon (Menge et al. 2016). At this time, both apparently normal and wasting sea stars were common at each of the six Oregon sites sampled. We reasoned that, by being found on the same transects as wasting individuals and hence probably exposed to similar conditions, sea stars found to be apparently normal may carry genetic variants associated with resistance or tolerance to SSWS. By combining field surveys of natural disease prevalence with high-throughput single nucleotide polymorphism (SNP) genotyping, we assess the contribution of sea star genetic variation to SSWS occurrence. Our data set is the result of a unique opportunity to compare apparently normal and wasting individuals from the same time and place during the SSWS epidemic.

Methods & Materials

Field surveys and tissue sampling

Field surveys aimed at quantifying the prevalence of SSWS were conducted between April and July 2016 in the low intertidal zone at five sites in central Oregon: Fogarty Creek (44.8386, −124.0588), Boiler Bay (44.8303, −124.0608), Yachats Beach (44.3114, −124.1086), Strawberry Hill (44.2492, −124.1154) and Tokatee Klootchman (44.2037, –124.1170). These surveys were conducted using 5 × 2-m belt transects (5–10 transects per site). Animals were collected by hand at low tide. Arm length was recorded (center to longest arm) for each animal, and only adults (with >3 cm arm length) were scored for disease status (Menge et al., 2016). We recorded visual disease symptoms based on the six-level ranking protocol, as per Menge et al. (2016); these included, in order of severity: twisting arms (1), deflated (2), lesions (3), lost arms (4), losing grip on rocks (5), and disintegrating or "melting" (6). Animals were considered apparently normal (rank of 0) if none of these symptoms existed.

We returned to each of these sites to collect tissue for genetic analysis (Table S2.1). We also collected tissue from apparently normal and wasting individuals at a sixth site (Smelt Sands, 44.3212, −124.1081, on August 16, 2016), but we did not conduct transect surveys there. From each individual, tube feet (~5–10) were collected using scrubbed and sterilized forceps, then stored in 1.5-ml microcentrifuge tubes containing 1 ml of 95% ethanol. All samples were stored on ice and then at –20°C until ready for DNA isolation. In total, we collected tissue from 410 sea stars, 92 of which were wasting.

Library preparation and sequencing

For genotyping, we included only individuals with the highest wasting scores from each site, which ranged from ranks 3 to 6 (Table S2.1). In total, 82 individuals were included in the wasting group and 112 in the apparently normal group. DNA was extracted using the E.Z.N.A Tissue DNA kit (Omega Biotek) and quantified using a fluorescence method (Quant-iT dsDNA Assay Kit, ThermoFisher). We used the 2bRAD protocol for genotyping SNPs (Wang et al. 2012), following the

original published protocol, but using the enzyme AlfI. We also used adaptors with "NN" overhangs to target 100% of restriction sites. Multiplexed individuals were pooled at approximately equimolar amounts (after quantification via quantitative PCR [polymerase chain reaction]) and sequenced across five lanes of an Illumina HiSeq 3000 as 50-bp single reads, at the Center for Genome Research and Biocomputing at Oregon State University.

Data filtering

Adaptors were trimmed and low-quality reads were filtered (phred score <30) using publicly available scripts (https://github.com/EliMeyer/2brad_utilities/). Because of the cleavage pattern of the AlfI enzyme, 2bRAD DNA inserts are 34–36 bp in length. Therefore, after adaptor and quality trimming, we filtered out any reads that were shorter than 34 bp to reduce chances of mismapping. Cleaned reads were mapped to the reference *Pisaster ochraceus* genome (NCBI accession GCA_010994315.1) using shrimp (Rumble et al., 2009), reporting the top three maximum hits per read. We used stacks version 1.35 (Catchen et al. 2011, 2013) to call genotypes using default parameters, with samples coded by disease status group (wasting/apparently normal). Additional filtering parameters used included: selection of a single (first) SNP per stack, removal of loci that were genotyped in only one group, minimum minor allele frequency (MAF) set to 0.025, a minimum minor allele count set to 4, and only loci represented in at least 50% of samples were retained. Using vcftools (Danecek et al. 2011), we retained only biallelic loci and only genotypes with a minimum coverage of six reads. Finally, we used plink (Purcell et al. 2007) to remove individuals that were missing more than 50% of loci. This filtering pipeline retained a data set with 133 individuals (74 normal and 59 wasting) and 71,784 SNP loci, which we will refer to as the "full data set."

Population structure

Before comparing genotypic variation between sea stars varying in disease status, we assessed whether significant population genetic structure exists among the sampled sites. We used the Bayesian clustering approach in structure (Pritchard, Stephens, and Donnelly 2000) with the data set of 133 individuals, but we further filtered it to reduce computational burden. For this, we filtered loci that were genotyped in at least 90% of individuals, using vcftools, retaining 4,626 loci. structure runs included 100,000 burn-in and 100,000 Markov chain Monte Carlo (MCMC) sampling replicates, assuming admixture and with sampling locality used as prior information. We ran three values of K to assess whether clustering occurring at the specific site ($K = 6$) or at the subregion level ($K = 3$) were more likely than a large panmictic population ($K = 1$). To confirm that parameters converged, each value of K was run three separate times and likelihoods and clustering patterns were compared across runs. This clustering analysis suggested genetic variation was not structured among sampling sites

(Figure S2.1). We therefore considered our samples as coming from a single population in the subsequent analyses.

Analyses of genetic variation

We used two types of approaches for estimating differentiation between disease status groups. We estimated Weir & Cockerham's F_{st} (Weir and Cockerham 1984) using gpat++ (Shapiro et al. 2013), with significance levels adjusted using the false discovery rate (FDR) in r. To test for F_{st} outliers that may indicate selection, we used bayescan version 2.1 (Foll and Gaggiotti 2008) with the following settings: prior odds of the neutral model of 10, burn-in of 50,000 replicates, a thinning interval of 10, 20 pilot runs for 5,000 iterations, and recorded output of 5,000 iterations. Significance for Bayescan F_{st} outliers was assessed at a *q*-value FDR of 0.01.

We also used a multivariate approach to test for differentiation between grossly normal and wasting sea stars. A discriminant analysis of principal components (DAPC) (Jombart, Devillard, and Balloux 2010) was used, implemented in the r package "adegenet" (Jombart and Collins 2015) and identified outlier loci based on their loadings associated with the discriminant function separating the two groups.

Regions linked to discriminant loci

To identify functional candidates that may be associated with disease status, we scanned for protein-coding genes linked to outlier SNPs. We first determined the appropriate genomic window size for scanning around each SNP by estimating linkage disequilibrium (LD) between pairs of SNPs. The r^2 was calculated using vcftools between pairs of SNPs within 100,000-bp windows. Average r^2 was calculated in bins of 100-bp increments and were plotted against physical distance. This plot showed that LD decays rapidly up to 15 kb, then continues to decrease but at lower rates (Figure S2.2). We hence scanned a 30-kb window centered at each outlier SNP (15 kb on either side) by overlaying the protein-coding genome annotation from Ruiz-Ramos et al. (2020) onto the genome assembly, using the Integrative Genomics Viewer (Robinson et al. 2011).

Results

Field observation

A total of 3,670 *Pisaster ochraceus* were counted in belt transects across five sites, with the incidence of SSWS ranging from 5.2% to 10.0% (Table 2.1). In three of the sites (Boiler Bay, Yachats Beach, and Strawberry Hill), all surveyed wasting sea stars showed either symptoms of lesions or arm loss, while at Tokatee Klootchman, 25% showed the more advanced symptom of grip loss. Fogarty Creek harbored sea stars with the most advanced stage of SSWS; all wasting individuals surveyed were

disintegrating (Table 2.1). Metadata associated with the 410 individuals from which we collected tissue sample can be found in Table S2.1.

Sequencing and genotyping

Illumina sequencing yielded ~1.6 billion reads. After removing low quality reads, 1.4 billion reads remained, with an average of 6.9 million reads per sample. A total of 259,407 RAD stacks passed sample and population filters, surveying a total of 9,526,221 bases (~2.3% of the 401.9-Mb genome) and with mean per-sample coverage of 38.1×. As mentioned above, 71,784 RAD stacks contained at least one polymorphic site, and a single random SNP was retained per stack in the full data set (Table S2.2). Moreover, given our estimated LD block of 15 kb, this full SNP set allowed for an average of 2.5 SNPs sampled per block. This level of coverage suggests our data set may provide sufficient power to detect genomic regions associated with phenotypic differences, if these exist and have a strong genetic component (Lowry et al. 2017b, 2017a).

Analyses of genomic variation

Genomic differentiation between grossly normal and wasting sea stars was very low based on F_{st} estimates. Across the final SNP data set (71,784), Weir & Cockerham's F_{st} had a median value of 0.00314, and nearly 45% of loci had $F_{st} = 0$ (Table S2.2). Moreover, while 362 loci had moderate F_{st} values (≥0.1), no locus showed significant differentiation after FDR adjustments; the lowest adjusted *p*-value was 0.172 (Figure 2.1). Outlier tests with F_{st} using bayescan also showed no evidence of selection in any locus in our data set (Figure S2.3).

DAPC analyses showed modest separation between apparently normal and wasting groups (Figure 2.2a). Based on loading values from the DAPC, we identified 18 SNPs across 10 chromosomes contributing most to the differentiation between the two groups (Figure 2.2b; Table S2.3). Allele frequency differences across these loci ranged from 0.014 to 0.253 (Table S2.3). Using a 30-kb window centered at each of these SNP positions, we detected 34 protein-coding genes predicted by the genome annotation from Ruiz-Ramos et al. (2020). blast searches of these protein sequences against the Uniprot/Swissprot databased revealed that 30 of them have predicted products with known functional annotation (Table S2.4). Chromosomes 3 and 8 harbored the most genes linked to these SNPs (seven genes each); in chromosome 8, one SNP was linked to three genes, and the others to two each (Figure 2.3).

We assessed whether the 18 SNP loci identified as outliers from our DAPC analyses overlapped with haplotypes from Schiebelhut et al. (2018) that were the most discriminatory between post and pre-SSWS adults in their samples from California. For this, we compared the 30-kb ranges encompassing our SNP outliers to the haplotype coordinates from Schiebelhut et al. (2018). We

detected no overlap in the two sets of outliers, with the shortest distance detected as ~257 kb (Table S2.5).

Discussion

The recent outbreaks of SSWS at multiple coastal sites caused severe population declines in several sea star species. Mitigation techniques for addressing outbreaks when the causative agent(s) is unknown should run in parallel with studies attempting to determine the cause (Eisenlord et al. 2016). With rising sea water temperatures resulting in a higher prevalence of marine diseases (Harvell et al. 2002; Tracy et al. 2019), we are likely to see similar scenarios of mass mortality outbreaks impacting marine species more frequently and having little time to address management or conservation plans. Assessing the potential for natural population resilience is a critical step in predicting the long-term fate of affected species and of the communities they in turn influence. For example, selectively rearing disease-resistant oysters in hatcheries has been a useful tool in avoiding disease outbreaks that are decimating wild populations (Agnew et al. 2020; Dégremont, Garcia, and Allen 2015). While many marine species are not amenable for selective breeding, examining genomic variation in natural populations can address whether these species have the genetic makeup for adaptation to marine diseases on their own.

In this study, we took advantage of the co-occurrence of wasting and apparently normal individuals of *Pisaster ochraceus* in central Oregon to scan for genomic regions that potentially predict individual SSWS status. After genotyping nearly 72,000 SNP loci across 133 individuals, we found no strong patterns of differentiation between wasting and apparently normal individuals. Loci with elevated F_{st} were not clearly concentrated as peaks in any genomic region, and no single locus showed a statistically significant level of allele frequency differences. Using a multivariate approach as a complement to the locus-specific F_{st} analyses, 18 SNP loci stood out as contributing to genomic differentiation between the two groups of individuals based on disease status. Overall, we argue that a genetic basis for SSWS resilience in *P. ochraceus* is probably weak, but we identified a list of genomic regions and functional candidates that may serve as a basis for studies of gene expression, physiology or comparative genomics during future SSWS outbreaks.

While the proximate cause(s) of SSWS at the individual level are still unknown, recent experimental studies are consistent with a pathogen agent. For example, individuals that were wasting in the laboratory showed physiological and gene expression responses that suggest innate immunity, cytokine-like systems and tissue remodeling (Fuess et al. 2015; Gudenkauf and Hewson 2015; Ruiz-Ramos et al. 2020). Our findings showed no evidence for a strong genetic component to SSWS tolerance or resistance, but the weakly associated loci we identified may have small but cumulative effects, which is expected for a polygenic trait. This trait may hence require much higher powered studies for detecting associated loci with more precision (Gagnaire and Gaggiotti 2016).

Schielbelhut et al. (2018) detected allelic shifts in grossly normal *P. ochraceus* adults and juveniles before and after the SSWS outbreak in California. They found three loci putatively under selection and reported on 100 discriminatory haplotypes between time periods. Interestingly, the 18 SNP loci we detected as most discriminatory in our samples did not occur within 30 kb of those reported by Schielbelhut et al. (2018), and most were between 250 kb and 2 Mb apart. Lack of overlap in these genomic regions is perhaps not surprising given the multitude of differences between the studies, such as year of sampling, the health status of sea stars and geographical location. For instance, SSWS is known to be associated with spikes in sea water temperature (Bates, Hilton, and Harley 2009; Eckert, Engle, and Kushner 1999; Eisenlord et al. 2016; Kohl, McClure, and Miner 2016), and daily deviations from annual sea water temperatures in Oregon were more prevalent in 2013/2014 than in California (Miner et al. 2018). Such relevant environmental differences between California and Oregon may hence also cause different selective pressures. Moreover, the reduced representation nature of RADseq and the use of different restriction enzymes suggest that a lack of overlap between different study outlier markers is not indicative of a lack of biological relevance.

The scarcity of SSWS-associated loci detected is also possibly a result of reduced coverage from the inherent nature of RADseq methods (Lowry et al. 2017a). While RADseq is an efficient and cost-effect method for producing thousands of SNPs along the entire genome, these markers remain sparse. Despite the limitations, many RADseq studies have found loci attributed to adaptive selection when coverage is adequate (Epstein et al. 2016; Lowry et al. 2017a; McKinney et al. 2017). Marker density aimed at detecting phenotype–genotype associations is recommended to be high relative to LD in the target species (Lowry et al. 2017a). Based on this metric, our RADseq effort in this study adequately covers the full genome, with on average 2.5 SNPs found per every 15-kb linkage block. Therefore, we argue that our results are not due to low marker density, but perhaps may be improved by genotyping a higher number of individuals.

Our study joins that of Schielbelhut et al. (2018) and Ruiz-Ramos et al. (2020) in assessing genomic variation in the keystone species *P. ochraceus* and highlighting the importance of understanding the causes and responses to devastating SSWS outbreaks. While current patterns remain obscure, the accumulation of putative functional genomic regions will serve as invaluable resources for continued field and laboratory studies. In addition to physiological and transcriptomic experiments, we suggest the need for a concerted effort to sample large numbers of wasting and apparently unaffected individuals across several geographical regions, and ideally using low-coverage whole-genome sequencing for substantially increased power (Lou et al., 2021).

Acknowledgements

We thank Kris Bauer, Laurel Field, Skylar Peven, Bruce Menge, Brittany Poirson, Amanda Coração, Melissa Britsch, Jenna Sullivan, Chenchen Shen, and Jonathan Robinson for help with sample collections and DNA extractions. Thanks go to Mark Dasenko for assistance with Illumina sequencing. We would also like to thank Lauren Schiebelhut for access to the genome assembly, and Eli Meyer who provided support on 2bRAD preparation and processing. This work was supported by Oregon State University startup funds to F.S.B. All Pisaster density data were provided by B.A. Menge using research supported by National Science Foundation DEB-LTREB Awards 1050694 and 1554702 to B.A. Menge.

Data Accessibility

Illumina sequence reads are deposited in the NCBI Sequence Read Archive (SRA), in accessions SRR13611638–SRR13611837.

References

Aalto, E. A., Lafferty, K. D., Sokolow, S. H., Grewelle, R. E., Ben-Horin,T., Boch, C. A., Raimondi, P. T., Bograd, S. J., Hazen, E. L., Jacox, M. G.,Micheli, F., & De Leo,G. A. (2020). Models with environmental drivers offer a plausible mechanism for the rapid spread of infectious disease outbreaks in marine organisms. Scientific Reports, 10(1), 5975.

Agnew, M. V., Friedman, C. S., Langdon, C., Divilov, K., Schoolfield, B., Morga, B., Degremont, L., Dhar, A. K., Kirkland, P., Dumbauld, B., & Burge, C. A. (2020). Differential mortality and high viral load in naive Pacific oyster families exposed to OsHV-1 suggests tolerance rather than resistance to infection. Pathogens, 9(12), 1057.

Aquino, C. A., Besemer, R. M., DeRito, C. M., Kocian, J., Porter, I. R., Raimondi, P. T., Rede, J. E., Schiebelhut, L. M., Sparks, J. P., Wares, J. P., & Hewson, I. (2021). Evidence that microorganisms at the animal-water interface drive sea star wasting disease. Frontiers in Microbiology, 11.

Bates, A., Hilton, B., & Harley, C. (2009). Effects of temperature, season and locality on wasting disease in the keystone predatory sea star *Pisaster ochraceus*. Diseases of Aquatic Organisms, 86, 245–251.

Behringer, D. C., Silliman, B. R., & Lafferty, K. D. (2018). In D. C. Behringer, B. R. Silliman, & K. D. Lafferty (Eds.), Marine disease ecology. Oxford University Press. Bucci, C., Francoeur, M., McGreal, J., Smolowitz, R., Zazueta-Novoa, V., Wessel, G. M., & Gomez-Chiarri, M. (2017). Sea star wasting disease in *Asterias forbesi* along the Atlantic Coast of North America. PLoS One, 12(12), e0188523.

Burge, C. A., Mark Eakin, C., Friedman, C. S., Froelich, B., Hershberger, P. K., Hofmann, E. E., Petes, L. E., Prager, K. C., Weil, E., Willis, B. L., Ford, S. E., & Harvell, C. D. (2014). Climate change influences on marine infectious diseases: Implications for management and society. Annual Review of Marine Science, 6(1), 249–277.

Burt, J. M., Tinker, M. T., Okamoto, D. K., Demes, K. W., Holmes, K., & Salomon, A. K. (2018). Sudden collapse of a mesopredator reveals its complementary role in mediating rocky reef regime shifts. Proceedings of the Royal Society B: Biological Sciences, 285(1883), 20180553.

Catchen, J. M., Amores, A., Hohenlohe, P., Cresko, W., & Postlethwait, J. H. (2011). Stacks: Building and genotyping loci de novo from short-read sequences. G3, 1(3), 171–182.

Catchen, J. M., Hohenlohe, P. A., Bassham, S., Amores, A., & Cresko, W. A. (2013). Stacks: An analysis tool set for population genomics. Molecular Ecology, 22(11), 3124–3140.

Danecek, P., Auton, A., Abecasis, G., Albers, C. A., Banks, E., DePristo, M. A., Handsaker, R. E., Lunter, G., Marth, G. T., Sherry, S. T., McVean, G., & Durbin, R., & Group, 1000 Genomes Project Analysis (2011). The variant call format and VCFtools. Bioinformatics, 27(15), 2156–2158.

Dégremont, L., Garcia, C., & Allen, S. K. (2015). Genetic improvement for disease resistance in oysters: A review. Journal of Invertebrate Pathology, 131, 226–241.

Eckert, G. L., Engle, J. M., & Kushner, D. J. (1999). Sea star disease and population declines at the Channel Islands. In Proceedings of the Fifth California Islands Symposium (pp. 390–393). Minerals Management Service.

Eisenlord, M. E., Groner, M. L., Yoshioka, R. M., Elliott, J., Maynard, J., Fradkin, S., Turner, M., Pyne, K., Rivlin, N., van Hooidonk, R., & Harvell, D. C. (2016). Ochre star mortality during

the 2014 wasting disease epizootic: Role of population size structure and temperature. Philosophical Transactions of the Royal Society B: Biological Sciences, 371(1689).

Epstein, B., Jones, M., Hamede, R., Hendricks, S., McCallum, H., Murchison, E. P., Schönfeld, B., Wiench, C., Hohenlohe, P., & Storfer, A. (2016). Rapid evolutionary response to a transmissible cancer in Tasmanian devils. Nature Communications, 7(1), 12684.

Foll, M., & Gaggiotti, O. (2008). A genome-scan method to identify selected loci appropriate for both dominant and codominant markers: A Bayesian perspective. Genetics, 180(2), 977–993.

Fuess, L. E., Eisenlord, M. E., Closek, C. J., Tracy, A. M., Mauntz, R., Gignoux-Wolfsohn, S., Moritsch, M. M., Yoshioka, R., Burge, C. A., Harvell, C. D., Friedman, C. S., Hewson, I., Hershberger, P. K., & Roberts, S. B. (2015). Up in arms: Immune and nervous system response to sea star wasting disease. PLoS One, 10(7), e0133053.

Gagnaire, P.-A., & Gaggiotti, O. E. (2016). Detecting polygenic selection in marine populations by combining population genomics and quantitative genetics approaches. Current Zoology, 62(6), 603–616.

Gravem, S. A., Heady, W. N., Saccomanno, V. R., Alvastad, K. F., Gehman, A. L. M., Frierson, T. N., & Hamilton, S. L. (2021). Sunflower Sea Star (*Pycnopodia helianthoides*). IUCN Red List of Threatened Species.

Groner, M. L., Maynard, J., Breyta, R., Carnegie, R. B., Dobson, A., Friedman, C. S., Froelich, B., Garren, M., Gulland, F. M. D., Heron, S. F., Noble, R. T., Revie, C. W., Shields, J. D., Vanderstichel, R., Weil, E., Wyllie-Echeverria, S., & Harvell, C. D. (2016). Managing marine disease emergencies in an era of rapid change. Philosophical Transactions of the Royal Society B: Biological Sciences, 371(1689), 20150364.

Gudenkauf, B. M., & Hewson, I. (2015). Metatranscriptomic analysis of *Pycnopodia helianthoides* (Asteroidea) affected by sea star wasting disease. PLoS One, 10(5).

Harvell, D., Aronson, R., Baron, N., Connell, J., Dobson, A., Ellner, S., Gerber, L., Kim, K., Kuris, A., McCallum, H., Lafferty, K., McKay, B., Porter, J., Pascual, M., Smith, G., Sutherland, K., & Ward, J. (2004). The rising tide of ocean diseases: unsolved problems and research priorities. Frontiers in Ecology and the Environment, 2(7), 375–382.

Harvell, D. C., Mitchell, C. E., Ward, J. R., Altizer, S., Dobson, A. P., Ostfel, R. S., & Samuel, M. D. (2002). Climate warming and disease risks for terrestrial and marine biota. Science, 296(5576), 2158–2162.

Harvell, D. C., Montecino-Latorre, D., Caldwell, J. M., Burt, J. M., Bosley, K., Keller, A., Heron, S . F., Salomon, A. K., Lee, L., Pontier, O., Pattengill-Semmens, C., & Gaydos, J. K. (2019). Disease epidemic and a marine heat wave are associated with the continental-scale collapse of a pivotal predator (*Pycnopodia helianthoides*). Science Advances, 5(1), eaau7042.

Hewson, I., Bistolas, K. S. I., Quijano Cardé, E. M., Button, J. B., Foster, P. J., Flanzenbaum, J. M., Kocian, J., & Lewis, C. K. (2018). Investigating the complex association between viral ecology, environment, and northeast Pacific Sea Star Wasting. Frontiers in Marine Science, 5.

Hewson, I., Button, J. B., Gudenkauf, B. M., Miner, B., Newton, A. L., Gaydos, J. K., Wynne, J., Groves, C. L., Hendler, G., Murray, M., Fradkin, S., Breitbart, M., Fahsbender, E., Lafferty, K. D., Kilpatrick, A. M., Miner, C. M., Raimondi, P., Lahner, L., Friedman, C. S., … Harvell, C. D. (2014). Densovirus associated with sea-star wasting disease and mass

mortality. Proceedings of the National Academy of Sciences of the United States of America, 111(48), 17278–17283.

Hewson, I., Sullivan, B., Jackson, E. W., Xu, Q., Long, H., Lin, C., Quijano Cardé, E. M., Seymour, J., Siboni, N., Jones, M. R. L., & Sewell, M. A. (2019). Perspective: Something Old, Something New? Review of Wasting and Other Mortality in Asteroidea (Echinodermata). Frontiers in Marine Science, 6.

Jackson, E. W., Wilhelm, R. C., Johnson, M. R., Lutz, H. L., Danforth, I., Gaydos, J. K., Hart, M. W., & Hewson, I. (2020). Diversity of sea star-associated densoviruses and transcribed endogenous viral elements of densovirus origin. Journal of Virology, 95(1).

Jombart, T. (2015). An introduction to adegenet 2.0.0. Retrieved from http://adegenet.r-forge.r-project.org/files/ tutor ial-basics.pdf

Jombart, T., Devillard, S., & Balloux, F. (2010). Discriminant analysis of principal components: A new method for the analysis of genetically structured populations. BMC Genetics, 11(1), 94.

Kohl, W. T., McClure, T. I., & Miner, B. G. (2016). Decreased temperature facilitates short-term sea star wasting disease survival in the keystone intertidal sea star *Pisaster ochraceus*. PLoS One, 11(4), e0153670.

Lloyd, M. M., & Pespeni, M. H. (2018). Microbiome shifts with onset and progression of Sea Star Wasting Disease revealed through time course sampling. Scientific Reports, 8(1), 16476.

Lou, R. N., Jacobs, A., Wilder, A. P., & Therkildsen, N. O. (2021). A beginner's guide to low-coverage whole genome sequencing for population genomics. Molecular Ecology, mec.16077.

Lowry, D. B., Hoban, S., Kelley, J. L., Lotterhos, K. E., Reed, L. K., Antolin, M. F., & Storfer, A. (2017a). Breaking RAD: an evaluation of the utility of restriction site-associated DNA sequencing for genome scans of adaptation. Molecular Ecology Resources, 17(2), 142–152.

Lowry, D. B., Hoban, S., Kelley, J. L., Lotterhos, K. E., Reed, L. K., Antolin, M. F., & Storfer, A. (2017b). Responsible RAD: Striving for best practices in population genomic studies of adaptation. Molecular Ecology Resources, 17(3), 366–369.

McKinney, G. J., Larson, W. A., Seeb, L. W., & Seeb, J. E. (2017). RADseq provides unprecedented insights into molecular ecology and evolutionary genetics: Comment on Breaking RAD by Lowry et al. (2016). Molecular Ecology Resources, 17(3), 356–361.

Menge, B. A., Cerny-Chipman, E. B., Johnson, A., Sullivan, J., Gravem, S., & Chan, F. (2016a). Correction: Sea star wasting disease in the keystone predator *Pisaster ochraceus* in Oregon: Insights into differential population impacts, recovery, predation rate, and temperature effects from long-term research. PLoS One, 11(6), e0157302.

Menge, B. A., Cerny-Chipman, E. B., Johnson, A., Sullivan, J., Gravem, S., & Chan, F. (2016b). Sea star wasting disease in the keystone predator *Pisaster ochraceus* in Oregon: Insights into differential population impacts, recovery, predation rate, and temperature effects from long-term research. PLoS One, 11(6), e0157302.

Miner, C. M., Burnaford, J. L., Ambrose, R. F., Antrim, L., Bohlmann, H., Blanchette, C. A., Engle, J. M., Fradkin, S. C., Gaddam, R., Harley, C. D. G., Miner, B. G., Murray, S. N., Smith, J. R., Whitaker, S. G., & Raimondi, P. T. (2018). Large-scale impacts of sea star wasting disease (SSWD) on intertidal sea stars and implications for recovery. PLoS One, 13(3), e0192870.

Montecino-Latorre, D., Eisenlord, M. E., Turner, M., Yoshioka, R., Harvell, C. D., Pattengill-Semmens, C. V., Nichols, J. D., & Gaydos, J. K. (2016) Devastating transboundary impacts of sea star wasting disease on subtidal asteroids. PLoS One, 11(10), e0163190.

Nei, M., Maruyama, T., & Chakrabort, R. (1975). The bottleneck effect and genetic variability in populations. Evolution, 29, 1–10.

Paine, R. T. (1966). Food web complexity and species diversity. The American Naturalist, 100(910), 65–75.

Paine, R. T. (1969). A note on trophic complexity and community stability. The American Naturalist, 103, 91–93.

Paine, R. T. (1974). Intertidal community structure. Oecologia, 15, 93–120.

Pratchett, M. S. (1999). An infectious disease in crown-of- thorns starfish on the Great Barrier Reef. Coral Reefs, 18(3), 272.

Pritchard, J. K., Stephens, M., & Donnelly, P. (2000). Inference of population structure using multilocus genotype data. Genetics, 155, 945–949.

Purcell, S., Neale, B., Todd-Brown, K., Thomas, L., Ferreira, M. A. R., Bender, D., Maller, J., Sklar, P., de Bakker, P. I. W., Daly, M. J., & Sham, P. C. (2007). PLINK: A tool set for whole-genome association and population-based linkage analyses. The American Journal of Human Genetics, 81(3), 559–575.

Robinson, J. T., Thorvaldsdóttir, H., Winckler, W., Guttman, M., Lander, E. S., Getz, G., & Mesirov, J. P. (2011). Integrative genomics viewer. Nature Biotechnology, 29(1), 24–26.

Ruiz-Ramos, D. V., Schiebelhut, L. M., Hoff, K. J., Wares, J. P., & Dawson, M. N. (2020). An initial comparative genomic autopsy of wasting disease in sea stars. Molecular Ecology, 29(6), 1087–1102.

Rumble, S. M., Lacroute, P., Dalca, A. V., Fiume, M., Sidow, A., & Brudno, M. (2009). SHRiMP: Accurate mapping of short color-space reads. PLoS Computational Biology, 5(5), e1000386.

Schiebelhut, L. M., Puritz, J. B., & Dawson M. N. (2018). Decimation by sea star wasting disease and rapid genetic change in a keystone species, *Pisaster ochraceus*. Proceedings of the National Academy of Sciences, 115(27), 7069–7074.

Schultz, J. A., Cloutier, R. N., & Côté, I. M. (2016). Evidence for a trophic cascade on rocky reefs following sea star mass mortality in British Columbia. PeerJ, 4, e1980.

Shapiro, M. D., Kronenberg, Z., Li, C., Domyan, E. T., Pan, H., Campbell, M., Tan, H., Huff, C. D., Hu, H., Vickrey, A. I., Nielsen, S. C. A., Stringham, S. A., Hu, H., Willerslev, E., Gilbert, M. T. P., Yandell, M., Zhang, G., & Wang, J. (2013). Genomic diversity and evolution of the head crest in the rock pigeon. Science, 339(6123), 1063–1067.

Tracy, A. M., Pielmeier, M. L., Yoshioka, R. M., Heron, S. F., & Harvell, D. C. (2019). Increases and decreases in marine disease reports in an era of global change. Proceedings of the Royal Society B: Biological Sciences, 286(1912), 20191718.

Tracy, A. M., Weil, E., & Harvell, D. C. (2020). Warming and pollutants interact to modulate octocoral immunity and shape disease outcomes. Ecological Applications, 30(2), e02024.

Wang, S., Meyer, E., McKay, J. K., & Matz, M. V. (2012). 2b-RAD: a simple and flexible method for genome-wide genotyping. Nature Methods, 9(8), 808–810.

Weir, B. S., & Cockerham, C. C. (1984). Estimating F-statistics for the analysis of population structure. Evolution, 38(6), 1358–1370.

Zann, L., Brodie, J., & Vuki, V. (1990). History and dynamics of the crown-of-thorns starfish *Acanthaster planci* (L.) in the Suva area, Fiji. Coral Reefs, 9(3), 135– 144.

Zenger, K. R., Richardson, B. J., & Vachot-Griffin, A.-M. (2003). A rapid population expansion retains genetic diversity within European rabbits in Australia. Molecular Ecology, 12(3), 789–794.

FIGURES AND TABLES

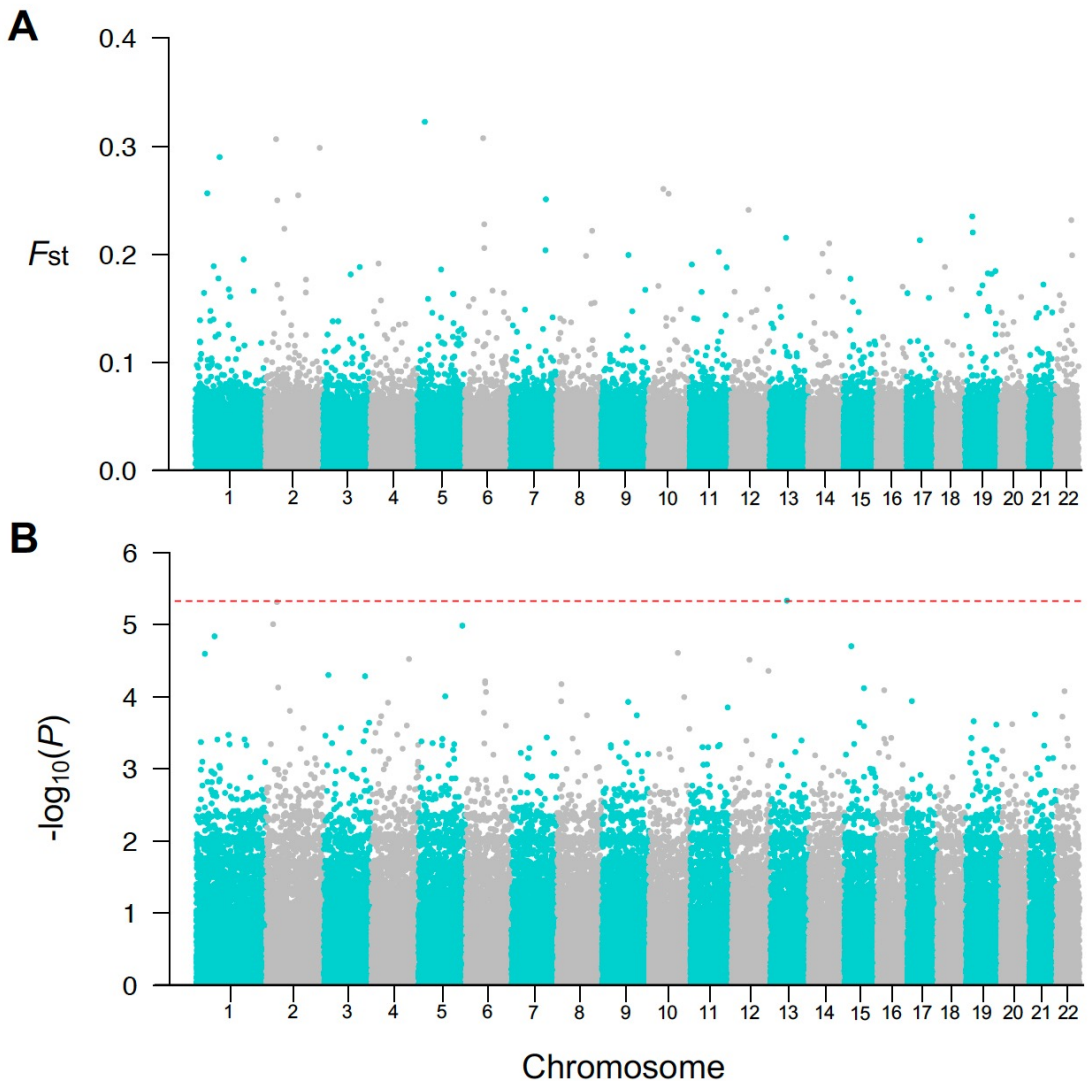

Figure 2.1: Tests of differentiation across SNP loci (n = 71,784) between wasting and apparently normal *Pisaster ochraceus* from central Oregon. (1) Weir & Cockerham's F_{st}. (b) The p-values for differentiation at each locus. Red dashed line marks the lowest FDR adjusted value of 0.172.

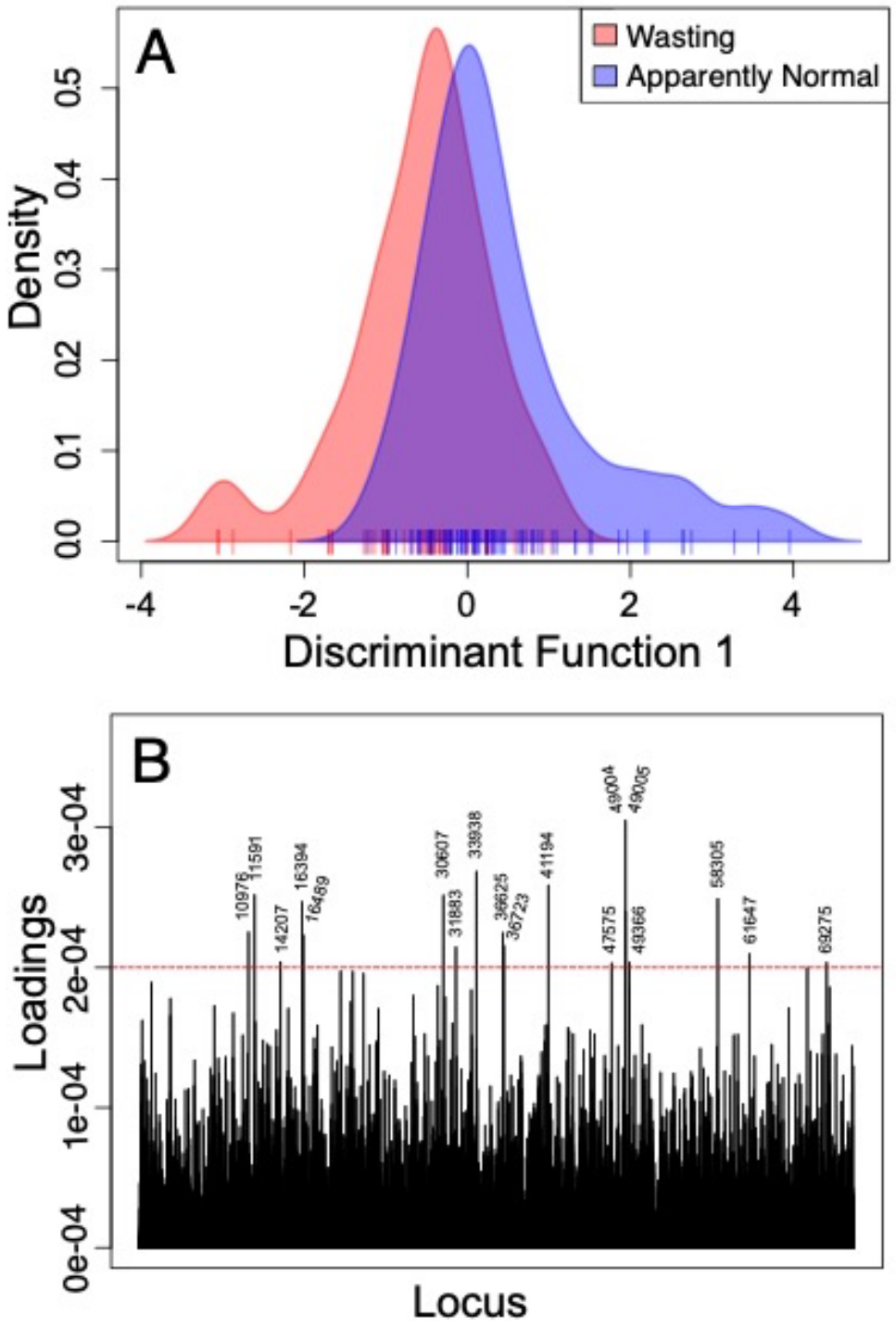

Figure 2.2: Discriminant analyses of principal components (DAPC) comparing apparently normal (n = 74) to wasting (n = 59) sea stars. (a) Distribution of scores for each group. Tick marks on the x-axis represent individual sea stars. (b) Loadings of loci associated with highest between-group variance. Loci above the dashed red line were considered outliers and examined further. Numbers above outlier peaks are locus IDs, which can be found in Tables S2.2 and S2.3.

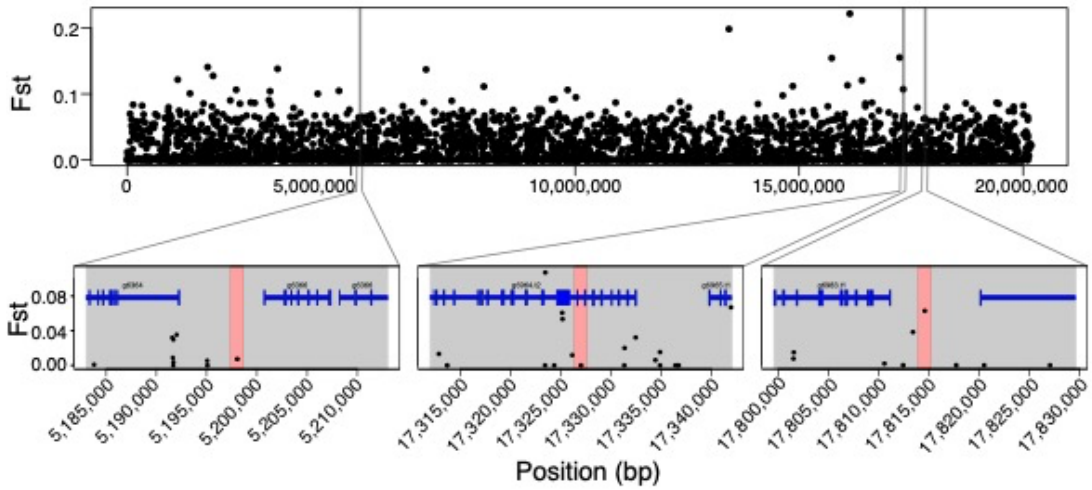

Figure 2.3: Landscape of F_{st} and protein-coding genes surrounding outlier SNPs along chromosome 8. Thin grey bars on the top panel indicate positions of the outlier SNPs (positions 5,198,014, 17,327,004, and 17,814,546 bp). Insets on the bottom panel depict a closeup with a 30-kb window centered at each outlier SNP (highlighted in red). Blue boxes cover the coordinates of protein-coding genes, with thin vertical lines depicting exons.

Table 2.1: Summary of field surveys of prevalence of SSWS in *Pisaster ochraceus* in the central Oregon coast.

Site	Mean total observed	% Apparently Normal	% Wasting	% Lesions	% Arm(s) lost	% Losing grip	% Disintegrating
Fogarty Creek	484	93.9	6.1	0.0	0.0	0.0	100.0
Boiler Bay	316	90.0	10.0	28.6	71.4	0.0	0.0
Yachats Beach	360	93.5	6.5	77.8	22.2	0.0	0.0
Strawberry Hill	495	94.8	5.2	72.3	27.7	0.0	0.0
Tokatee Klootchman	180	90.3	9.7	50	25	25.0	0.0

CHAPTER 3 – OCEAN ACIDIFICATION INFLUENCE ON GENE EXPRESSION PATTERNS DURING SETTLEMENT IN *CRASSOSTREA GIGAS*

Andrea R. Burton, Evan Durland, & Chris Langdon

Abstract

Anthropogenic carbon emissions increase the partial pressure of atmospheric carbon dioxide (pCO_2) which is then dissolved into our oceans, resulting in ocean acidification (OA). OA leads to acidified conditions which can impair the growth of many calcifying species, especially in early developmental stages. Little is known about how this impacts the process of settlement in organisms, such as marine bivalve larvae, that require rapid rates of calcification to attach themselves to a substrate. To investigate functional consequences of OA for settlement i.e., the process of larval attachment, larvae of the Pacific oyster (*Crassostrea gigas*) were grown and induced to settle in either acidified or ambient seawater conditions, using selected families from the Molluscan Broodstock Program. Mechanisms underlying the effects of OA on attachment success were examined through gene expression profiling using RNAseq for non-attached individuals and attached spat from each OA condition. Differences in gene expression were evaluated using a negative binomial contrast model to isolate genes related to attachment that were impacted by OA conditions. There were 44% higher rates of metamorphosed individuals in ambient conditions compared with OA conditions, but no difference in settlement rates. There were 453 differentially expressed genes in the non-attached larvae and spat (i.e., pediveliger larvae and non-attached, metamorphosed spat). There were 943 genes related to attachment process that were differentially expressed in OA conditions, followed by no differences in gene expression in attached spat. Genes from these models were enriched in 13 GO terms differentially expressed between ambient and OA treatments in non-attached individuals and 31 GO terms related to attachment. Three of these GO terms were upregulated in non-attached larvae and spat but were downregulated when isolating genes related to attachment. Differences in the gene expression patterns of non-attached individuals and attachment under OA conditions highlight the need to differentiate between metamorphosis and settlement as they have different physiological processes. These findings identify genes and biological processes associated with effects of OA on settlement in *C. gigas*.

Introduction

Ocean acidification (OA) due to rising carbon dioxide emissions is an increasing threat to marine life. This is especially concerning for organisms found along the West Coast of North America as it is subject to periodic upwelling, which brings CO_2-rich water to surface resulting in coastal OA (Hales et al. 2006). Since the industrial revolution, the ocean's pH has dropped 0.1 units (Caldeira and Wickett, 2003; Hoegh-Guldberg *et al.*, 2007), altering the ocean's carbonate chemistry and negatively impacting marine calcifying organisms. Upwelling brings cool, nutrient-rich waters from depth that are enriched in dissolved carbon dioxide (Barton et al. 2012; Feely et al. 2008). The California Current has

seasonal upwelling during the summer (Feely et al., 2008), which increases the frequency in which coastal organisms are exposed to these conditions. While upwelling of acidified seawater is not a new phenomenon, the continued shift in global carbonate chemistry has exacerbated the acidification from these upwelling events. By 2050, the California Current is predicted to reach undersaturated aragonite levels throughout the instead of periodically (Gruber *et al.*, 2012), leaving many calcifying organisms vulnerable.

The responses of organisms to acidified seawater varies widely among species and life stages, with the most commonly impacted traits being calcification of shells, growth, reproduction, and survival (Kroeker et al., 2010). The biological impacts of OA have been examined in many taxa, ranging from mollusks (Gazeau et al., 2013; Kroeker et al., 2010; Waldbusser et al., 2015), corals (Kleypas *et al.*, 1999), crustaceans (Stillman et al., 2020), echinoderms (Kurihara and Shirayama, 2004; Shirayama, 2005), and calcifying plankton (Riebesell *et al.*, 2000; Orr *et al.*, 2005). Many studies have focused on early developmental stages of invertebrates, such as urchins, bivalves and crustaceans, due to their increased vulnerability to OA (Kroeker *et al.*, 2010). Early in development, larvae of these species are more sensitive to environmental conditions, resulting in overall higher rates of mortality (Gosselin and Qian, 1997). In many bivalve species acidified seawater presents undersaturated conditions in which shell formation is thermodynamically unfavorable (Waldbusser et al. 2015), which then impedes larval development (Timmins-Schiffman et al., 2013; Waldbusser et al., 2015). As a result, OA has been found to decrease larval growth rates, increase shell abnormalities, and decrease survival rates (Byrne & Przeslawski, 2013; Parker et al., 2013; Ross et al., 2011). It is during early developmental stages that calcifying organisms first deposit their calcium carbonate shells and skeleton, which is energetically demanding (Frieder et al., 2017; Kurihara, 2008a).

In bivalves, there are five stages of development before becoming an adult: embryo, D-hinged larvae, veliger larvae, pediveliger larvae, and juvenile (spat) stage (Figure 3.1D). There are two critical stages in which larvae rely mainly on endogenous energy reserves: 1) during embryogenesis, from fertilization until the prodissoconch I larvae start feeding, and 2) during metamorphosis of larvae which become spat (Waldbusser et al., 2015). The prodissoconch I stage is when trochophore larvae first deposit their calcified shells, becoming a D-hinged larvae. Transcriptional changes associated with the formation of the shell of prodissoconch I are strongly affected by OA treatments 8-18 hours post-fertilization (De Wit et all. 2018; Wright-LaGreca et al. 2022). Reduced seawater aragonite saturation (Ω_{arag}) due to high pCO_2 can result in morphological abnormalities of the shells of veliger larvae (Kurihara, 2008b; Waldbusser et al., 2015). In addition, acidification of sea water (lower pH, higher pCO_2 and reduced Ω_{arag}) can create a multi-stressor environment that impacts larval development and metabolism (Dineshram et al., 2012; Waldbusser et al. 2015). Settlement is the final bottleneck during development that indicates successful development. During settlement, individuals attach themselves to a substrate prior to undergoing metamorphosis. Settlement success is highly variable under high pCO_2 conditions and is largely impacted by fitness at different early developmental

stages (Durland et al., 2019). Examining the impacts of environmental pressure, such as OA, only at specific early life stages may miss the overall response. For instance, Durland et al. (2021a) saw reversal of fitness effects across genotypes; frequency of several alleles reversed as juveniles developed from veliger larval stages and went through settlement. This study suggests that fitness of an individual cannot be understood from a single developmental stage, but rather the overall success throughout development to the final stage of attachment and metamorphosis. Therefore, assessing the impact of OA conditions on larval oyster settlement is particularly important. In this study, we focus on genes relating to one of the two processes important to settlement, attachment.

Prior to settlement, veliger larvae develop into pediveliger larvae, indicated by the presence of an eye spot and a ciliated foot. Attachment is the process of individuals cementing themselves to substrate preceding metamorphosis (attached spat). Metamorphosis is an energetically taxing stage in development in which pediveliger larvae transition into juveniles (Haws, 1993). Not all individuals have the physiological capacity to attach prior to metamorphosis, therefore, non-settled or non-attached spat are individuals that have metamorphosed but have not cemented themselves to the substrate prior to metamorphosis. Mortality is high during metamorphosis due to the energetic demands during this stage (Haws, 1993). Improved larval diets prior the metamorphosis has been shown to decrease larval mortality during settlement, suggesting that improving nutritional condition of pediveligers can limit metabolic stress by improving energy reserves (Gallager et al. 1986, Gallager & Mann 1986, Helm 1991, Cooteau 1994, Pernet & Tremblay 2004).

Two important larval developmental states immediately precede metamorphosis: (1) “competency”, in which pediveliger larvae develop an eye spot and ciliated foot and (2) attachment of pediveliger larvae to the substrate (settlement) (Degnan and Morse, 1995; Pawlik, 2020). Cementation, process for attachment, consists of producing a calcium calcite layer from the mantle attaching individual to substrate (Yamaguchi, 1994). Many studies have evaluated the impacts of OA on early life stages including metamorphosis of the Pacific oyster *Crassostrea gigas,* but they have not reported gene expression patterns of settlement under OA conditions (Kurihara, 2008a; Barton *et al.*, 2012; De Wit *et al.*, 2018).

To better understand the cellular physiological processes affecting *C. gigas* during the attachment stage of settlement under OA stress, we quantified genome-wide gene expression levels in controlled experiments. More specifically, we used RNA-seq to profile transcription levels of larvae and spat exposed to high and ambient pCO_2 conditions. Identifying genes related to attachment is important to understand how OA influences the overall success of larval *C. gigas*. Results from this study highlight the importance of cellular processes, relating to calcification and structural changes associated with attachment, that are impacted by OA.

Materials and Methods

Seawater chemistry

Two sea water treatments were prepared for the exposure experiment, high pCO_2 (~1600 μatm CO_2, pH ~7.5-7.6, Ω_{arag} = 0.9-1.2), and ambient pCO_2 (~400 μatm CO_2, pH ~7.9-8.1, Ω_{arag} = 2.3-2.7). Both treatments were produced using 10 μm-filtered seawater at 25°C and salinity of 32. The carbonate chemistry of the high pCO_2 seawater was manipulated by aerating two 200-liter tanks overnight with an air and CO_2 mixture, controlled by a pair of mass flow controllers (Alicat, Tuscon, AZ). During the experiment (described below), water changes were conducted every 2 days, at which point pH and temperature were measured, and seawater from each replicate was sampled for carbonate analyses to account for shifts in carbonate chemistry due to off-gassing or respiration during the 48-hour cultivation period between water changes. Seawater samples were stored in sealed, gas-tight 350 ml amber glass bottles and fixed with 30 μl of saturated mercuric chloride ($HgCl_2$). Dr. Burke Hales' lab at Oregon State University analyzed these seawater samples following their carbonate chemistry measurements protocol (Bandstra et al., 2006; Hales et al., 2005). Parameters measured were total dissolved carbon dioxide (TCO_2), pCO_2, and seawater pH, and these were then used to calculate the saturation states of aragonite (Ω_{arag}) and calcite (Ω_{calc}) (Table S3.1). Measurements of TCO_2 and pCO_2 are known to be highly accurate (Waldbusser *et al.*, 2013), with <0.2% and <5% uncertainty, respectively.

Larval culture

Larval oysters were produced by strip-spawning male and females from broodstock produced by the Molluscan Broodstock Program (MBP). MBP families were largely unrelated having a coefficient of co-ancestry of less than 10% (De Melo et al. 2016). Using a semi-factorial cross design, 19 males and 19 females were crossed, with each male fertilizing 4-6 individual females, forming 95 unique full-sibling families. Eggs from each family were initially kept in 100-ml beakers in standard seawater (same as ambient pCO_2) for one-hour to validate fertilization success. Fertilized eggs were then rinsed on a 25-μm screen to remove excess sperm before egg concentration of each family was quantified and added to a combined pool with equal egg contributions from each family. Pooled eggs were then mixed and distributed across 12 10-liter polycarbonate containers (BearVault, San Diego, CA) at a density of 20 eggs ml^{-1}, allowing for six replicate containers for each pCO_2 treatment. The containers were sealed with a lid and silicone sealing ring (McMaster-Carr, Santa Fe Springs, CA) to prevent gas exchange with the atmosphere.

Larvae were fed daily, beginning at the D-hinge stage 48 hours after fertilization. Larval diets started with 100% *Isochrysis spp*. (C-Iso) at 20,000 cells ml^{-1}. Feeding rates increased by 5,000 cells ml^{-1} per day. Beginning on day 2, 5% of the algal diet (by cell number) was substituted with the diatom *Chaetoceros gracilis* (Cg) and this substitution was increased by 5% day^{-1} until C-Iso and Cg cell concentrations were equal on day 11.

To reduce the effects of bacterial respiration on pCO_2 in the culture units, antibiotics were applied prophylactically. Antibiotics were added at each water change starting from day 2, alternating between chloramphenicol (2 ppm) or a mixture of ampicillin (10 ppm) and streptomycin (20 ppm). To retain slow growing larvae, screen sizes of 25 μm were used up to day 4, 37 μm on day 6, 45 μm on day 8, and 64 μm on all subsequent days. Larvae were checked throughout this period to monitor when different stages of development first appeared. On day 12, larvae larger than 64 μm were separated from non-growing "runts" by sieving. The larvae > 64 μm were aliquoted into smaller 1-liter sealed jars at a density of approximately 2,000 larvae liter^{-1}. The jars were set up to be sampled on days 14, 16, 18, 20, and 22, with four replicates for each time point and treatment (Figure 3.1), resulting in a total of 20 jars per pCO_2 treatment (40 jars in total). Pediveliger larvae, identified as having eye spots, were first observed on 14, indicating that the larvae had reached competency for settlement. Once pediveligers were observed, larval sampling commenced with the goal of estimating metamorphic and attachment rates.

Metamorphosis and settlement rates

To identify genes related to the first step in settlement (i.e., attachment process seen in attached spat), larvae were induced to settle using epinephrine. Epinephrine is a hormone which induces settlement and it allowed us to obtain in a high proportion of larvae undergoing settlement at the same time (Bonar et al., 1990). Given that hormonal stimulus is likely to have additional impacts to gene expression, prior to sampling, we transferred half of the candidate larvae to another 1-litre jar (500 mL each) for two treatments: with epinephrine (Epi) added and a control (Con) which did not have epinephrine added. For the Epi treatment, 0.18 mM of epinephrine was added to the jar and mixed. Larvae in both the Epi and Con treatments were held in the dark for 2 hours to allow epinephrine to take effect (Bonar *et al.*, 1990) (Figure 3.1B, 3.1C).

To measure metamorphic and attachment rates, sampling was carried out on days 14, 16, 18, 20 and 22 to count the number of individuals in different life stages (Figure 3.1). Following the 2-hour epinephrine (and control) exposure, a subset of 200 mL (~400 individuals) of the 500 mL cultures (cultures were split in half before epinephrine exposure) were poured off onto a 64 μm mesh screen after mixing. The remaining 300 mL were not used, except on day 22 when we sampled a subset of cultures for transcriptomics (see below). Excess cultures were poured on 25 μm sieve to remove debris for carbonate measurements. The 64 μm mesh screen collected veliger, pediveliger, and non-attached spat (non-attached larvae and spat) and were fixed in formalin for counting. Pediveliger larvae were distinguished from veliger as having an eye spot, while non-attached spat was identified as having a newly formed shell margin (Figure 3.1D). Attached spat that had cemented themselves on the jar wall remained in the jar and were counted separately. The numbers of veliger, pediveliger, non-attached and attached spat were used to estimate proportions of metamorphosed and attached spat across the total number of living individual oysters larger than 64 μm. The effects of day and pCO_2 treatment on

metamorphosis rates (non-attached and attached spat) and settlement rates (attached spat) success were evaluated by ANOVA (models: Proportion settled or metamorphosed ~ Day + pCO_2 treatment + Day: pCO_2 treatment) (Table 3.1). Prior to the ANOVAs, we confirmed the assumptions of data normality (Shapiro-Wilks W = 0.87, p = 0.68) and homogeneity of variances (Breusch-Pagan BP = 4.31, df = 9, p = 0.14). Any significant results from the ANOVAs were further assessed by a Tukey honest significant difference test to compare settlement (metamorphosis and attachment) between pCO_2 treatments on each sampling day.

Transcriptomic analyses

On day 22, additional sampling from each culture was carried out to preserve individuals for transcriptomics (Figure 3.1C). Non-attached individuals and spat were collected from the water column, while settled spat were those that remained attached to the jar wall after filtering jar contents. From the remaining 300 mL, 200 mL (~400 individuals) cultures were poured onto a 240-µm to collect non-attached individuals larger than that size, and the run-through water was then poured through 25µm sieve to remove debris for carbonate measurements (Table S3.1). The > 240 µm mesh screen captured pediveliger and non-attached spat (together non-attached individuals) and were then preserved in RNAlater. The remaining 100 mL from the ambient and high pCO_2 treatments were not used. Attached spat were counted before being scraped off the jar wall and preserved in RNAlater. Attached spat found in the no-epinephrine (control) exposure treatment were counted, but there was insufficient attached spat for RNA analysis. Overall, each replicate (day x pCO_2 treatment) produced three samples for transcriptomics in attached spat and non-attached individuals: 1) exposure to epinephrine, 2) no-epinephrine exposure (control) (~400 non-attached), and 3) settled (attached) spat (0 to 113 oysters), totaling 36 samples.

To quantify gene expression, a tag-based sequencing method was used (Meyer et al. 2011). This approach uses oligo-dT primers to target 3' ends of mRNA molecules, generating short (~100 bp) cDNA pools that permit accurate quantification of transcript levels. Total RNA was isolated with the Omega Bio-tek E.Z.N.A. tissue RNA Kit (Omega Bio-tek, Norcross, GA). Fragmentation was done by heating RNA to 95°C for 15 minutes, which fragments RNA to a size range of 200-300 bp. Amplification of cDNA was carried out with 13 cycles (90°C for 5 seconds, annealing 60°C for 30 seconds, then 72°C for 30 seconds), which was the minimum number of runs required to have each sample appear on a gel. During amplification reaction, each sample was barcoded with dual indices to allow for pooling. In total, 36 samples were pooled at equimolar amounts and then sequenced across two lanes of a HiSeq2500 at the Oregon Health & Science University. Sequenced reads were then filtered using publicly available scripts (https://github.com/Eli-Meyer/rnaseq_utilities from), first to remove non-template sequences and homopolymer regions greater than 20 bp. Low-quality reads were then removed, using a threshold Phred score less than 30. Using SHRiMP (Anderson *et al.*, 2016), the remaining high-quality reads were mapped to gene models predicted from the *C. gigas* reference

genome (Zhang *et al.*, 2012), plus adjacent 1-kb regions to allow for imperfections in the limits of the gene models. Unique reads aligning to genes were counted, producing a count data set for analyses of gene expression.

Two samples with fewer than 150,000 reads were removed due to insufficient coverage, leaving 34 samples in total. Each treatment combination was still represented by at least 3 replicates. Pre-processing of the data and differential expression were performed in edgeR (Robinson, McCarthy, Smyth 2010). Genes with low counts were removed using the 'filterByExpr' function, and expression levels estimated after normalization with trimmed mean of M-values (TMM; Robinson & Oshlack, 2010). We did not test for epinephrine effects within each pCO_2 treatment due to the difficulty of parsing factors which differed between these two treatments while also accounting for background differences arising from larval development. For instance, cultures exposed to epinephrine likely has more non-attached spat than pediveligers due to induction to metamorphose. Measuring differences in gene expression between Epi and Con may result in differences in earlier (largely pediveliger larvae) and later (having non-attached spat) stages in development rather than the epinephrine exposure alone. However, oyster larvae with differentially expressed genes due to epinephrine exposure were expected to have similar differences regardless of pCO_2 treatments due to both being given the same Epi treatment. The interactive effects of seawater acidification and epinephrine are unknown and potentially confounding for these analyses. To confirm that differential expression found when comparing pCO_2 treatments was not due to the interactive effects of epinephrine and pCO_2 exposure, a multifactorial negative binomial model was used. Expression patterns of non-attached individuals from the two exposure (Epi or Con) and pCO_2 (High and Amb) treatments to determine if there whether epinephrine had an interactive effect with pCO_2. The epinephrine-effect model (model 1; Table 3.2):

$$[(Epi_{high} - Con_{high}) - (Epi_{amb} - Con_{amb})] \quad (1)$$

allowed testing for epinephrine effects while accounting for pCO_2 conditions. Out of 15,474 genes included in the analysis, no differentially expressed genes were detected, suggesting there was no interaction effect of epinephrine and pCO_2 treatment. This confirmed that we do not need to account for epinephrine effects in non-attached individuals when assessing differential gene expression between pCO_2 treatments. We could not confirm that epinephrine did not have an interactive effect on attached spat as we did not have enough spat from the control treatment to run the same contrast model.

To quantify the main effect of *p*CO2 treatments on gene expression associated with attachment (first stage in settlement), expression in attached spat (Att.Spat) were compared across *p*CO2 levels while accounting for effects on non-attached individuals (Non.Att) (model 2):

$$(Att.Spat_{high} - Non.Att_{high}) - (Att.Spat_{amb} - Non.Att_{amb}) \quad (2)$$

Heatmaps were produced to illustrate patterns of gene expression between the two pCO_2 treatments for the settlement model (model 2) for the top 60 differentially expressed genes, and the three functional categories of GO terms (Biological, Molecular, and Cellular) (Table 3.2). Gene expression patterns affected by pCO_2 treatment were examined between the high and ambient pCO_2 treatments for both attached spat and non-attached individuals separately to assess the impacts high pCO_2 within these different developmental stages (Table 3.2: models 3, 4).

Enrichment analysis was carried out using TopGO (Alexa and Rahnenführer, 2016) to test whether certain cellular functions were over- or underrepresented among differentially expressed genes. Fisher's Exact Tests were run using the 'elim' method from TopGO to determine significance levels at $\alpha = 0.01$. There were not enough GO terms to look at both up- and down-regulation for both the attachment (model 2) as there were only 94 up-regulated and non-attached individuals (model 3) with 13 down-regulated genes (Table 3.2). For this reason, all GO terms were enriched regardless of directionality of fold change (Table 3.3). GO terms that were downregulated were enriched for attachment (model 2) (849 down-regulated genes) while upregulated GO terms enriched from the non-attached (model 3) (440 up-regulated genes) models (Table 3.2). Any GO terms that were enriched but was not unilaterally up- or down-regulated were included with individual genes and their direction of change reported (Table S3.2). Gene ontology terms were separated into three classes: molecular function, biological processes, and cellular components, producing heatmaps for each class.

Results

Larval settlement and metamorphosis variation under OA

Attached spat was seen on days 18, 20, and 22. Attachment rates among attached spat differed on day of sampling ($F_{1,30} = 78.59$, $p << 0.01$), but had no significant difference in pCO_2 treatment ($F_{1,30} = 1.89$, $p = 0.18$), with 2.6, 23.6 and 21.1 percent settlement in both ambient and high pCO_2 conditions for days 18 through 22, respectively (Table 3.1) (Figure 3.2A). Rates of metamorphosis varied significantly across days ($F_{4,30} = 175.76$, $p < 10^{-16}$) and pCO_2 levels ($F_{1,30} = 20.76$, $p = 8.1 \times 10^{-5}$). An interaction effect between the two factors was also detected ($F_{4,39} = 4.84$, $p = 0.0039$) (Table 3.1). A post-hoc Tukey HSD test indicated that days 14, 16, and 18 had similar metamorphic rates for high and ambient pCO_2 treatments (Tukey HSD, $p > 0.985$ for each). Combined percentages of non-attached individuals that were induced to metamorphose were 1.0 on day 14, 3.9 day 16, and 12.6 on day 18 for both ambient and high pCO_2 (Figure 3.2B). Metamorphic rates were lower in the high pCO_2 treatments for days 20 and 22 (Tukey HSD, p = 1.1x10-4, $p = 6.6 \times 10^{-4}$), with settled and non-attached spat being 59 percent higher on day 20 and 28 percent higher on day 22 in the ambient treatment.

Transcription profiling

Sequencing captured 1.5 billion reads (mean of ~17.7 million per sample). After filtering, 516 million reads were left (~5.9 million per sample), of which 60.5 million reads (687 thousand per sample) mapped to the reference transcriptome extracted from Zhang's et al. (2012) genome. There were 934 genes important to attachment (model 2) which were differentially expressed in high and ambient pCO_2 conditions after correction for developmental stage (Figure 3.3). Test of GO term enrichment in these genes detected 31 GO terms (13 molecular function, 9 biological process, 9 cellular processes; Table 3.2 and Figure 3.4). The 31 GO terms relating to settlement had the following common categories: binding (n=6), catalytic activity (n=3), cellular anatomical entity (n=9), cellular process (n=4), and metabolic process (n-4) (Table S3.2). Overrepresented GO categories with Fisher adjusted p-values less that 0.001 with in the cellular processes category "ribosome" (GO: 0005840, *p*-value = 1.20E022), the molecular function category "RNA binding" (GO:0003723, p-value = 8.70E-09), "ubiquinol-cytochrome-c reductase activity" (GO:0008121, p-value = 6.20E-05), "translation elongation factor activity" (GO:0003746, p=0.00015), and in the biological process "translation" (GO: 0006412, p = 3.10E-06), among more listed in Table 3.1.

We detected no significant differences in gene expression between attached spat (model 4) in ambient and high *p*CO2 treatments (Table 3.2). However, high pCO_2 seawater had a strong effect on gene expression of pediveligers and non-attached spat, significantly altering the expression of 453 genes (model 3). These genes were enriched for 13 GO terms (Table 3.1). We compared these 13 GO terms to those related to settlement (model 2). Of these GO terms, 10 were not seen in the attachment (model 2): "microtubule-based movement" (GO:0007018), "exodeoxyribonuclease III activity" (G):0008853, "ATP=dependent microtubule motor activity" (GO: GO:0008569), "guanyl-nucleotide exchange factor activity" (GO:0005085), "RNA-directed DNA polymerase activity" (GO:0003964), "actin binding" (GO:0003779), "cytoplasm" (GO:0005737), "cytoskeleton" (G):0005856), and "myosin complex" (GO:0016459). The three remaining GO terms were shared across the two models but were up-regulated in the water non-settled individuals (model 3) and down-regulated when looking at genes related to settlement (model 2). These three GO terms were "RNA binding" (GO:0003723), "RNA helicase activity" (GO:0003724), and "ribosome" (GO:0005840).

Discussion

Larvae reared in high pCO_2 seawater showed lower metamorphic rates, but no differences in attachment rates i.e., final percent attached spat. The reduced rates in metamorphosis are consistent with previous studies which demonstrated the negative effects of high pCO_2 exposure on larval development (Barton *et al.*, 2012; Frieder *et al.*, 2017). Similar rates of larval settlement for ambient and high pCO_2 treatments were also observed in Durland et al. (2019) in their experiment done in 2015. Metamorphosis requires rapid shell formation along with re-organization of body plan (Hadfield, 2000; Heyland and Moroz, 2006; Li *et al.*, 2019) that would occur in both non-attached and attached

spat. Biological processes relating to settlement are not well understood, conceivably due to attachment occurring asynchronously with metamorphosis and being difficult to sample in real time (Xu and Zhang, 2020). In addition, metamorphosis and settlement are often confusingly used interchangeably in many studies (Joyce and Vogeler, 2018), making it difficult to parse our mechanisms relating to attachment. This study highlights the need to make the distinction between these stages of development along with a better understanding of the mechanisms for settlement.

We found numerous gene expression levels related to the attachment process that differed between high and ambient pCO_2 conditions (model 2), however the function of these genes and how they related to attachment and settlement are poorly understood. There are a range of physiological functions occurring during settlement that have been reported in similar transcriptomic studies during larval development (O'Donnell *et al.*, 2010; Huan, Wang and Liu, 2012; De Wit and Palumbi, 2013; De Wit *et al.*, 2018; Durland *et al.*, 2021). In this study, we found gene ontology terms associated with a suite of genes enriched in functions relating to binding, catalytic activity, cellular anatomical entity, cellular process, and metabolic process (Table 3.3). Among these, cellular anatomical activity, localization, and transporter activity are poorly understood in *C. gigas* and other marine invertebrates as their GO terms were not seen in other literature reviews.

We know that calcification is important to settlement and can be impacted by high pCO_2 (Yamaguchi, 1994). We saw that high pCO_2 downregulated three GO terms relating to catalysis activity, structural molecule activity, and cellular processes including "NADH dehydrogenase (ubiquinone) activity" (GO:0008137), "transcription corepressor activity" (GO:0005198), and "protein folding" (GO:0006457). In similar studies, "NADH dehydrogenase (ubiquinone) activity" was differentially expressed in different pCO_2 treatments in larval purple sea urchin, *Strongylocentrotus purpuratus* (Wong *et al.*, 2018). The hard-shelled mussed, *Mytilus coruscus*, exhibited reduced shell formation in high pCO_2 treatments, along with downregulation for the GO term "transcription corepressor activity" (Zhao *et al.*, 2020). Genes enriched for "protein folding" were differentially expressed between competent pediveligers who settled and larvae (Xu and Zhang, 2020). Genes related to these functions are predicted to promote DNA transcription and protein synthesis important to attachment. This suggests that attachment stage of settlement and calcification may be impeded by high pCO_2.

Three GO terms that were downregulated in high pCO_2 treatment relating to the process of attachment were upregulated in other studies. GO term "translation" (GO:0006412) were upregulated in atlantad heteropods (atlandtidae, Pterotracheoidea), suggesting these genes are related to calcification during attachment and are impeded by high pCO_2 conditions. In addition, *M. coruscus* had "actin filament binding" (GO:0051015) upregulated in high pCO_2 conditions (Zhao *et al.*, 2020). Zhao et al. (2020) predicts that there may be a compensatory response against mantle tissue injury, resulting in weakened shell formation when exposed to high pCO_2. Both studies indicate a species-specific response to high pCO_2 and differences in allocation of cellular processes to mitigate acidified stress.

Among the genes related to attachment, three switched from being upregulated in non-attached individuals to downregulated in spat, including: “ribosome” (GO:0005840) and “RNA binding” (GO:0003723). The GO term “ribosome” was differentially expressed in between larval and juvenile stages of *Montastaea faveolata* (Reyes-Bermudez *et al.*, 2009). “RNA binding’ was also upregulated in atlantad heteropods (Atlantidae, Pterotracheoidea) when exposed to high pCO_2 treatments (Wall-Palmer *et al.*, 2021). Together, these studies suggest that these genes are important for metamorphosis and or calcification. These same genes were upregulated in non-attached individuals, similarly to *M. faveolate* and atlantad heteropods, likely to overcompensate to high pCO_2 conditions. However, post-settlement, these genes were downregulated, indicating that these genes oscillate from one stage to another. Oscillating gene expression along with stage-specific expression patterns allow for improved fitness from one stage to the next (Conaco *et al.*, 2012; Hendriks *et al.*, 2014; Durland et al. 2021). We see similar patterns of oscillating gene expression in pre-settlement and post-attached spat, suggesting that these genes important for different stages. It could be advantageous to down-regulate these genes during attachment to conserve energy and these processes for metamorphosis.

The lack of differentially expressed genes between ambient and high pCO_2 treatments in attached spat stages is likely due to variation across replicates as attached spat in the ambient treatment did not exhibit similar expression levels between replicates (Figure 3.3, 3.4). Assuming data to be true, similarity in gene expression between pCO_2 treatments could be attributed to selective pressures prior to settlement. Settlement success in MBP stocks was not impacted by high pCO_2 in a similar trial conducted in 2015 but resulted in 42% fewer spat in 2016 (Durland et al. 2019). However, mortality among larvae during metamorphosis was higher in 2016. Durland et al. (2019) concludes that the higher rates of mortality in 2016 were due to pediveliger competency and not high pCO_2 conditions. This suggests that pCO_2 may act as a bottleneck during developmentally demanding stages, while high pCO_2 has little to no negative impacts on post-settled larvae. However, carryover effects have been observed in juveniles reared in high pCO_2 conditions (Hettinger *et al.*, 2012). Sampling a few hours post settlement may capture genes important to settlement but have not yet negatively been impacted by pCO_2. However, our dataset is unable to address this hypothesis. Future studies would benefit from sampling post settled larvae over time to see if and when these carryover effects present themselves.

Another explanation for the lack of differential gene expression in settled spat in high pCO_2 conditions may be due to MBP stock used have be unintentionally selected for greater tolerance to acidified conditions (Durland et al. 2019, and 2021b). Durland et al. (2021b) compared MBP larvae to those spawned from wild oyster stocks and found that MBP larvae both survived and settled at a higher proportion and exhibited substantially less genetic changes across larval development than wild oysters. In this same study, they also found that high pCO_2 seawater had greater genetic and phenotypic impacts on wild stocks, compared to the selected MBP lines. The overall differences in genetic changes during larval development suggests that MBP oysters may be adapted to hatchery

conditions and, possibly, sub-lethal exposures to acidified seawater. Durland et al. (2019, and 2021b) explains that MBP stocks have inadvertently been selected to reduce genetic load, having many deleterious alleles. Crosses of family lines managing inbreeding in MBP stocks, there may have been a more uniform distribution of negative alleles among families. Having dispersed negative alleles may reduce compounding effects of multiple loci, along with possibly reducing the effects of genetic drift. Together, these studies highlight the advantages to selectively breeding organisms towards resilience to future climate stressors such as OA. More broadly, other studies have demonstrated that standing genetic variation of many invertebrate species possesses a range of phenotypes for traits related to OA resilience (Barrett & Schluter, 2008; Bitter et al. 2019; Brennan et al., 2021; Pespeni et al., 2013). Post-attached spat in this study may have similar expression patterns in both pCO_2 treatments because they are better adapted to such conditions.

Our study contributes to the growing body of literature identifying genetic components of stress due to OA conditions. OA likely has multiple interactive effects in function processes including: “binding”, “catalytic activity”, “cellular anatomical entity”, “cellular processes”, “localization”, “metabolic process”, “structural molecular activity”, and “transporter activity”. However, the overall complexity makes isolation and description of these effects challenging. Previous studies have evaluated how pCO_2 influences gene expressions in marine invertebrates and are consistent with our findings. However, expression patterns may differ depending on developmental stage. The complexity of physiology during settlement process and non-attached individuals highlights the need to distinguish processes associated with different developmental stages in future studies

Acknowledgement

We are grateful to Blaine Schoolfield, Jackie Dixon, and Marilyn Leary who aided in maintaining larval cultures and seawater. Thank you to Dr. Eli Meyer who helped with method development and providing assistants with processing reads. This research project was funded by Oregon Sea Grant under award (grant) number NA14OAR4170064 (project number R/SAQ-20) from the National Oceanic and Atmospheric Administration's National Sea Grant College Program, U.S. Department of Commerce, and by appropriations made by the Oregon State Legislature. We would also like to thank the Hatfield Marine Science Center who provided facilities for this experiment.

References

Alexa, A., & Rahnenführer, J. (2009). Gene set enrichment analysis with topGO. Bioconductor Improv, 28, 1-26.

Anderson, D.A., Walz, M.E., Weil, E., Tonellato, P., & Smith, M.C. (2016). RNA-Seq of the Caribbean reef-building coral *Orbicella faveolata* (Scleractinia Merulinidae) under bleaching and disease stress expands models of coral innate immunity. PeerJ, 4, e1616.

Bandstra, L., Hales, B., & Takahashi, T., (2006). High-frequency measurements of total CO_2: Method development and first oceanographic observations. Marine Chemistry, 100, 24-38.

Barrett, R., & Schluter, D. (2008). Adaptation from stranding genetic variation. Trends in Ecology & Evolution, 23, 38-44.

Barton, A., Hales, B., Waldbusser, G.G., Langdon, C., & Feely, R.A. (2012). The Pacific oyster, *Crassostrea gigas*, shows negative correlation to naturally elevated carbon dioxide levels: Implications for near-term ocean acidification effects. Limnology and Oceanography, 57, 698-710.

Bitter, M.C., Kapsenberg, L., Gattuso, J.P., & Pfister, C.A. (2019). Standing genetic variation fuels rapid adaptation to ocean acidification. Nature Communications, 10, 5821.

Bonar, D.B., Coon, S.L., Walch, M., Weinger, R.M., & Fitt, W. (1990) Control of oyster settlement and metamorphosis by endogenous and exogenous chemical cues. Bulletin of Marine Science, 46, 484-198.

Brennan, R.S., deMayo, J.A., Dam, H.G., Finiguerra, M., Baumann, H., Buffalo, V., & Pespeni, M.H. (2021). Experimental evolution reveals the synergistic genomic mechanisms of adaptation to ocean warming and acidification in marine copepods. bioRxiv.

Byrne, M., & Przeslawski, R. (2013). Multistressor impacts of warming and acidification of the ocean on marine invertebrates'' life histories. Integrative and Comparative Biology, 53, 582-596.

Caldeira, K., & Wickett, M.E. (2003). Anthroponotic carbon and ocean pH. Nature 425:365-365.

Conaco, C. Neveu, P., Zhou, H., Arcila, M.L., Degnan, S.M., Degnan, B.M., & Kosik, K.S. (2012). Transcriptome profiling of the demosponge *Amphimedon queenslandica* reveals genome-wide events that accompany major life cycle transitions. BMC Genomics, 13, 209.

De Wit, P., Durland, E., Ventura, A., & Langdon, C.J. (2018). Gene expression correlated with delay in shell formation in larval Pacific oysters (*Crassostrea gigas*) exposed to experimental ocean acidification provides insights into shell formation mechanisms. BMC Genomics, 19, 160.

De Wit, P., & Palumbi, S.R., (2013). Transcriptome-wide polymorphisms of red abalone (*Haliotis rufescens*) reveal patters of gene flow and local adaptation. Molecular Ecology, 22, 2884-2897.

Degnan, B.M., & Morse, D.E. (1995). Developmental and morphogenetic gene regulation in *Haliotis rufescens* larvae at metamorphosis. American Zoologist, 35, 193-398.

Dineshram, R., Wong, K.K., Xiao, S., Yu, Z., Qian, P.Y., & Thiyagarajan, V. (2012) Analysis of Pacific oyster larval proteome and its response to high-CO_2. Marine Pollution Bulletin, 64, 2160-2167.

Durland, E., De Wit, P., Meyer, E., & Langdon, C. (2021). Larval development in the Pacific oyster and the impacts of ocean acidification: Differential genetic effect sin wild and domesticated stocks. Evolutionary Applications, 14, 2258-2272.

Durland, E., Waldbusser, G., & Langdon, C. (2019). Comparison of larval development in domesticated and naturalized stocks of the Pacific oyster *Crassostrea gigas* exposed to high pCO_2 conditions. Marine Ecology Progress Series, 621, 107-125.

Durland, E., De Wit, P., & Langdon, C. (2021) Temporally balanced selection during development of larval Pacific oysters (*Crassostrea gigas*) inherently preserves genetic diversity within offspring. Proceedings of the Royal Society B: Biological Sciences, 288, 20203223.

Feely, R.A., Sabine, C.L., Hernandez-Ayon, J.M., Ianson, D, & Hales, B. (2008). Evidence for upwelling of corrosive "acidified" water onto the continental shelf. Science, 320, 1490-92.

Frieder, C.A., Applebaum, S.L., Pan, T.C.F, Hedgecock, D., & Manahan, D.T. (2017). Metabolic cost of calcification in bivalve larvae under experimental ocean acidification. ICES Journal of Marine Science. 74, 941-954.

Gazeau, F., Paker, L.M., Corneau, S., Gattuso, J.P., O'Connor, W.A., Martin, S., Pörtner, H.O., & Ross, P.M. (2013) Impacts of ocean acidification on marine shelled molluscs. Marine Biology, 160, 2207-2245.

Gosselin, L.A., & Qian, P.Y. (1997). Juvenile mortality in benthic marine invertebrates. Marine Ecology Progress Series, 146, 265-82.

Gruber, N., Hauri, C., Lachkar, Z., Loher, D., Frölicher, T., & Plattner, G. (2012). Rapid progression of ocean acidification in the California Current System. Science, 337, 220-23.

Hadfield, M.G. (2000). Why and how marine-invertebrate larvae metamorphose so fast. Seminars in Cell & Developmental Biology, 11, 437-443.

Hales, B., Karp-Boss, L., Perlin, A., & Wheeler, P.A. (2006) Oxygen production and carbon sequestration in an upwelling coastal margin. Global Biogeochemical Cycles, 20.

Hales, B., Takahashi, T., & Bandstra, L. (2005). Atmospheric CO_2 uptake by a coastal upwelling system. Global Biogeochemical Cycles, 19.

Haws, M. (1993) Survival and biochemical changes during metamorphosis of the American oyster *Crassostrea virginica* (Gmelin) and the Pacific oyster *Crassostrea gigas* (Thunberg). Doctoral dissertation, Texas A&M University.

Hendriks, G.J., Gaidatzis, D., Aeschimann, F., & Groβhans, H. (2014). Extensive oscillatory gene expression during C. elegans larval development. Molecular Cell, 53, 380-392.

Hettinger, A., Sanford. E, Hill, T.M., Russell, A.D., Sato, K.N., Hoey, J., Forsch, M., Page, H.N., & Gaylord, B. (2012). Persistent carry-over effects of planktonic exposure to ocean acidification in the Olympia oyster. Ecological Society of America, 93, 2738-3768.

Heyland, A., Moroz, L.L. (2006). Signaling mechanisms underlying metamorphic transitions in animals. Integrative and Comparative Biology, 46, 743-759.

Hoegh-Fuldberg, O., Muller-Parker, G., Cook, C.B., Gates, R.D., Gladfelter, E., Trench, R.K, & Weis, V.M. (2007). Len Muscatine (1932-2007) and his contributions to the understanding of algal-invertebrate endosymbiosis. Coral Reefs, 26, 731-739.

Huan, P., Wang, H., & Liu, B. (2012). Transcriptomic analysis of the clam Meretrix on different larval stages. Marine Biotechnology, 14, 69-78.

Joyca, A., & Vogeler, S. (2018). Molluscan bivalve settlement and metamorphosis: Neuroendocrine inducers and morphogenetic responses. Aquaculture, 487, 64-82.

Kleypas, J.A., Buddemeier, R.W., Archer, D., Gattuso, J.P., Langdon, C., & Opdyke, B.N. (1999) Geochemical consequences of increased atmospheric carbon dioxide on coral reefs. Science, 284, 118-120.

Kroeker, K.J., Kordas, R.L., Crim, R.N., & Singh, G.G. (2010). Meta-analysis reveals negative yet variable effects of ocean acidification on marine organisms. Ecology Letters, 13, 1419-34.

Kurihara, H. (2008). Effects of CO_2-driven ocean acidification on the early developmental stages of invertebrates. Marine Ecology Progress Series, 373, 275-84

Kurihara, H., & Shirayama, Y. (2004). Effects of increased atmospheric CO_2 on sea urchin early development. Marine Ecology Progress Series, 274, 161-169.

Li, H., Li, Q., Yu, H., & Du, S. (2019). Developmental dynamics of myogenesis in Pacific oyster *Crassostrea gigas.* Comparative Biochemistry and Physiology Part B: Biochemistry and Molecular Biology, 227, 21-30.

O'Donnell, M.J., Todgham, A.E., Sewell, M.A., Hammond, L.M., Ruggiero, K., Fangue, N.A., Zippay, M.L., & Hofmann, G.E. (2010). Ocean acidification alters skeletogenesis and gene expression in larval sea urchins. Marine Ecology Progress Series, 298, 157-171.

Orr, J.C., Fabry, V.J., Aumont, O., Bopp, L., Doney, S.C., Feely, R.A., Gnanadesikan, A., Gruber, N., Ishida, A., Joos, F. et al. (2005). Anthropogenic ocean acidification over the twenty-first century and its impact on calcifying organisms. Nature, 437, 681-86.

Parker, L.M., Ross, P.M., O'Connor, W.A., Pörtner, H.O., Scanes, E., & Wright, J.M. (2013). Predicting the response of molluscs to the impact of ocean acidification. Biology, 2, 651-692.

Pawlik, J.R. (2020). Chapter 6. Induction of marine invertebrate larval settlement: Evidence for chemical cues. In: Ecological Roles of Marine Natural Products, Cornell University Press, 189-236.

Pespeni, M.H., Sanford, E., Gaylord, B., Hill, T.M., Hosfelt, J.D., Jaris, H.K., LaVigne, M., Lenz, E.A., Russell, A.D., Young, M.K., & Palumbi, S.R. (2013). Evolutionary change during experimental ocean acidification. Proceedings of the National Academy of Sciences, 110, 6937-6942.

Plough, L.V. (2016) Genetic load in marine animals: a review. Current Zoology, 62, 567-579.

Reyes-Bermudez, A., DeSalvo, M.K., Voolstra, C.R., Sunagawa, S., Szmant, A.M., Iglesias-Prieto, R., & Medina, M. (2009). Gene expression microarray analysis encompassing metamorphosis and the onset of calcification in the scleractinian coral *Montrastraea faveolata*. Marine Genomics, 2, 149-159.

Riebesell, U., Zonderva, I., Rost, B., Tortell, P.D., Zeebe, R.E., & Morel, F.M. (2000). Reduced calcification of marine plankton in response to increased atmospheric CO_2. Nature, 407, 364-367.

Ross, P.M., Parker, L., O'Connor, W.A., & Bailey, E.A. (2011). The impact of ocean acidification on reproduction, early development and settlement of marine organisms. Water, 3, 1005-1030.

Shirayama, Y. (2005). Effect of increased atmospheric CO_2 on shallow water marine benthos. Journal of Geophysical Research, 110, C09S08.

Stillman, J.H., Fay, S.A., Ahmad, S.M., Swiney, K.M., & Foy, R.J. (2020). Transcriptomic response to decreased pH in adult, larval and juvenile red king crab, *Paralithodes camtschaticus*, and interactive effects of pH and temperature on juveniles. Journal of the Marine Biological Association of the United Kingdom, 100, 251-265.

Timmins-Schiffman, E., O'Donnell, M.J., Friedman, C.S., Roberts, S.B. & (2013). Elevated pCO_2 causes developmental delay in early larval Pacific oysters, *Crassostrea gigas*. Marine Biology, 160, 1973-1982.

Waldbusser, G.G., Brunner, E.L, Haley, B.A., Hales, B., Langdon, C.J., & Prahl, F.G. (2013). A developmental and energetic basis linking larval oyster shell formation to acidification sensitivity. Geophysical Research Letters, 40, 2171-2176.

Waldbusser, G.G., Hales, B., Langdon, C.J., Haley, B.A., Schrader, P., Brunner, E.L., Gray, M.W., Miller, C.A., Gimenez, I., & Hitchinson, G. (2015). Ocean acidification has multiple modes of action on bivalve larvae. PLoS ONE, 10.

Waldbusser, G.G., Hales, B., Langdon, C.J., Haley, B.A., Schrader, P., Brunner, E.L, Gray, M.W., Miller, C.A., & Gimenez, I., (2015). Saturation-state sensitivity of marine bivalve larvae to ocean acidification. Nature Climate Change, 5, 273-280.

Wall-Palmer, D., Mekkes, L., Ramos_Silva, P., Dämmer, L.K., Goetze, E., Bakker, K., Duijm, E., & Peijnenburg, K.T. (2021). The impacts of past, present and future ocean chemistry on predatory planktonic snails. Royal Society Open Science, 8, 2022265.

Wong, J.M., Johnson, K.M., Kelly, M.W., & Hofmann, G.E. (2018). Transcriptomics reveal transgenerational effects in purple sea urchin embryos: Adult acclimation to upwelling conditions alters the response of their progeny to differential pCO_2 levels. Molecular Ecology, 27, 1120-1137.

Wright-LaGreca, M., Mackenzi, C., & Green, T.J. (2022). Ocean acidification alters developmental timing and gene expression of ion transport proteins during larval development in resilient and susceptible lineages of the Pacific oyster (*Crassostrea gigas*). Marine Biotechnology, 14, 1-9.

Xu, F., & Zhang, G., (2020). Transcriptomic and proteomic dynamics during metamorphosis of Pacific oyster *Crassostrea gigas*. BioRxiv.

Yamaguchi, K. (1994). Shell structure and behavior related to cementation in oysters. Marine Biology, 118, 89-100.

Zhang, G., Fang, X., Guo, X., Li, L.I., Luo, R., Xu, F., Yang, P., Zhang, L., Wang, X., Qi, H., & Xiong, Z. (2012). The oyster genome reveals stress adaptation and complexity of shell formation. Nature, 490, 49-54.

Zhao, X., Han, Y., Chen, B., Xia, B., Qu, K., & Liu, G. (2020). CO_2-driven ocean acidification

weakens mussel shell defense capacity and induces global molecular compensatory responses. Chemosphere, 243, 125415.

FIGURES AND TABLES

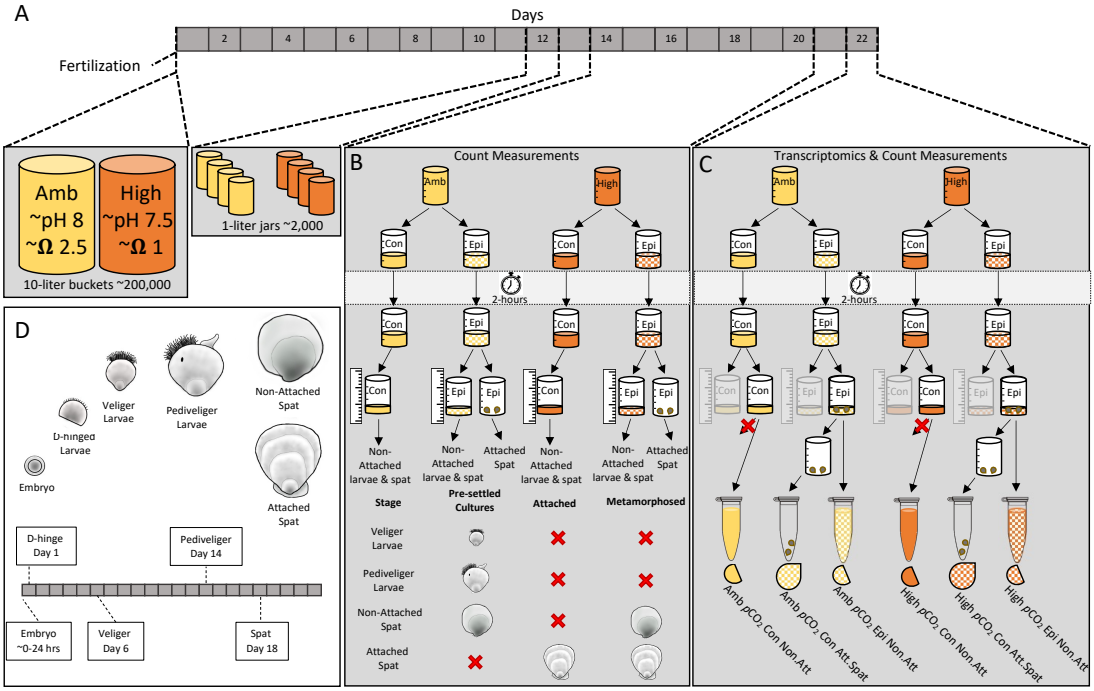

Figure 3.1: Timeline of experimental design and sampling procedure of *C. gigas* on the day of sampling larvae used for counting and for RNA preservation. (A) Larvae were reared in either ambient (yellow) or high pCO_2 (orange) treatments for a total of 22 days. Larvae were transferred into 1-liter jars on day 12. (B) Sampling for count data occurred on days 14 through 22. Cultures were split in half into epinephrine (Epi, checker colored) and non-epinephrine (control, Con, solid colored) treatments. Following 2-hours epinephrine exposure, a fifth of the individuals were sampled for counting. Non-attached individuals were stored and used to count the number of veliger, pediveliger, and non-attached spat. Attached spat had cemented themselves on the walls of jars and were counted separately. The total number of metamorphosed spat in the >64 µm group and attached spat were used to calculated percent metamorphosis (non-attached and attached spat) and settlement (attached spat only). (C) Transcriptomic along with count measurement sampling occurred on day 22. Non-attached individuals were poured off into 240 µm, 64 µm and 25 µm sieves to collect individuals > 240 µm for transcriptomics, > 64 µm for count measurements, and < 25 µm for seawater. Filtered seawater was then used to measure carbonate chemistry (Table S3.1). Epinephrine exposure and count data was sampled using the same procedure from figure 3.1B. The remaining one fifth of cultures were stored in RNA later. Attached Spat were kept separate from non-attached individuals by pouring off non-attached individuals into tube (colored tubes) and scraping spat off the jar wall (clear tubes). (D) The different larval stages and when they first appeared are shown in the same 22-day timeline for embryo, D-hinged, veliger, pediveliger larvae which metamorphosed into non-attached and attached spat.

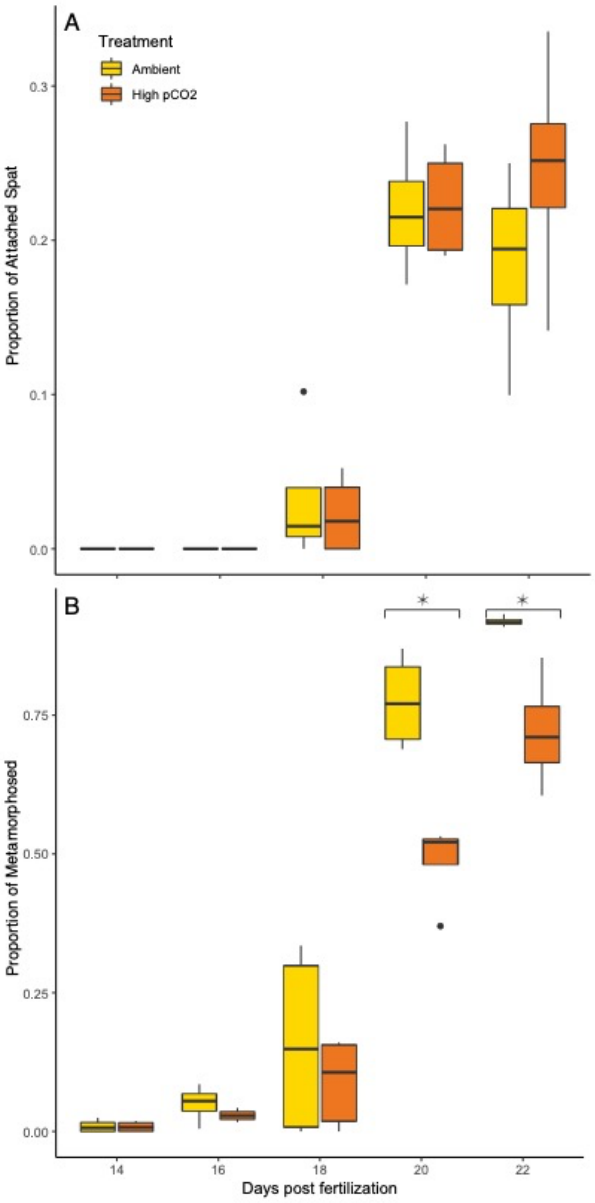

Figure 3.2: Proportion of individuals > 64 µm who (A) settled (attached spat) and (B) metamorphosed (non-attached larvae and non-attached spat) on days 14 through 22, separated by high and ambient pCO_2 conditions.

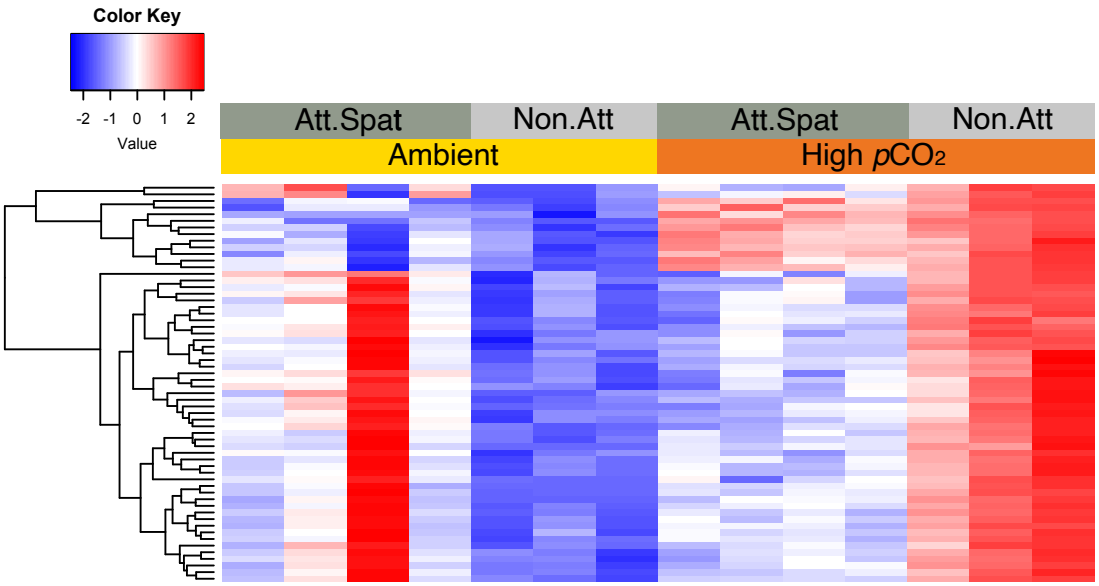

Figure 3.3: Heatmap showing expression of genes per replicate (attached spat n=4; non-attached individuals n=3) for the top 60 differentially expressed genes between high pCO_2 (orange) and ambient (yellow) treatments, separated by the two stages of attached spat (dark grey) and non-attached individuals (pediveligers and non-attached spat) (light grey). Blue indicates low expression, white moderate expression, and red indicates high expression.

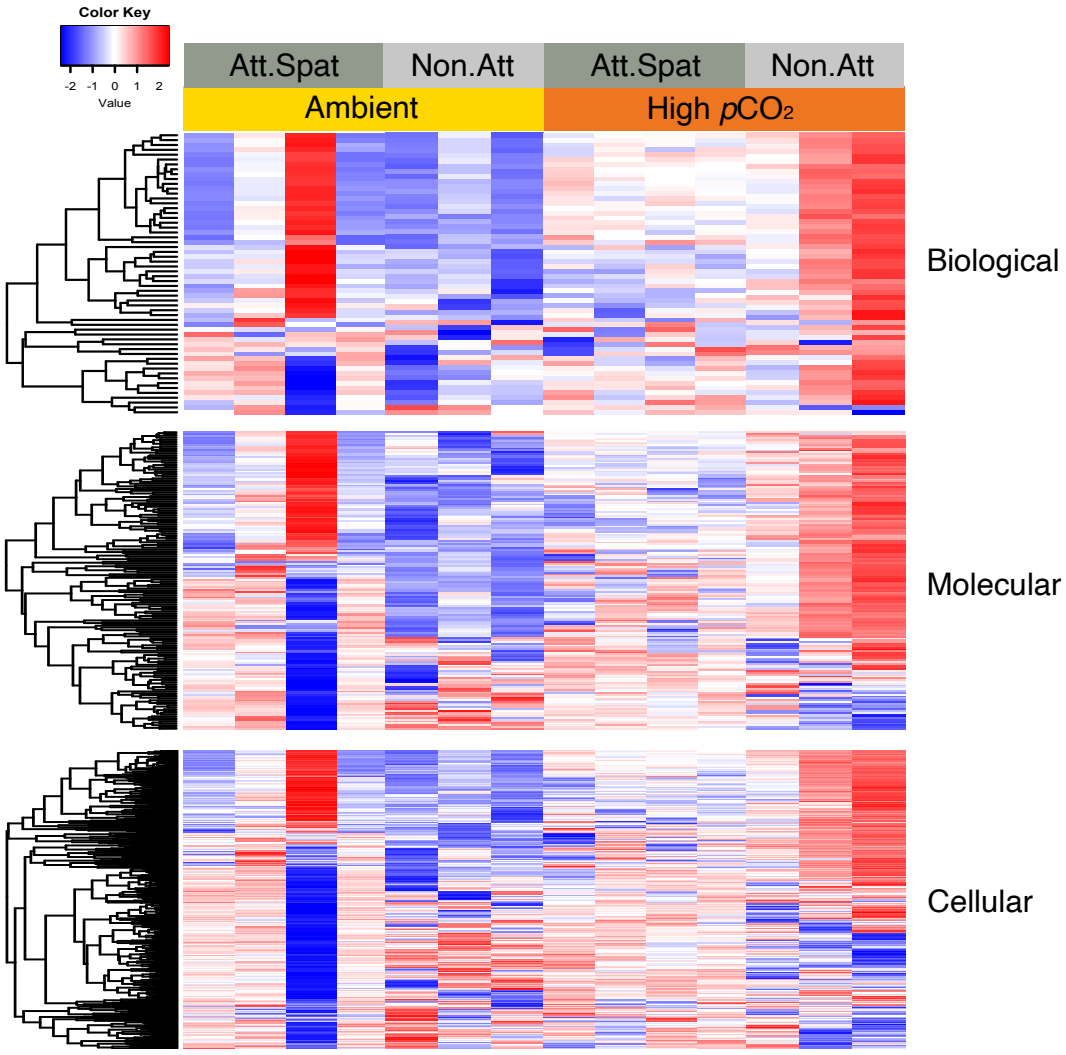

Figure 3.4: Heatmap showing expression of genes per replicate (attached spat n=4, non-attached individuals n=3) for the three functional categories of GO terms (Biological, Molecular, and Cellular) differentially expressed between high pCO_2 (orange) and ambient (yellow) treatments, separated by the two stages of attached spat (dark grey) and non-attached individuals (light grey). Blue indicates low expression, white moderate expression, and red indicates high expression.

Table 3.1: Results from 2-way ANOVA for effect of day and treatment on percent of larvae that settled (attached spat) or metamorphosed (non-attached and attached spat).

Model	Term	DF	F-value	p-value
Settled ~ Day + Treatment + Day:Treatment	Day	4	78.59	1.86e-15
	Treatment	1	1.89	0.18
	Intercept	4	1.37	0.27
Metamorphosed ~ Day + Treatment + Day:Treatment	Day	4	175.76	<2.2e-16
	Treatment	1	20.76	8.14e-05
	Intercept	4	4.84	0.0039

Table 3.2: Summary of models used to estimate differential gene expression from non-attached individuals (Non.Att) and attached spat (Att.Spat) along with epinephrine (Epi) and non-epinephrine exposure (Con) of pediveliger larvae and spat sampled on day 22 within their pCO_2 treatments (high and ambient, amb). The number of replicates, genes used after filtering, and the number of significantly different up- and down-regulated genes are reported.

Model	Test	Model	Sample Num.	Num. of genes	Up-regulated	Down-regulated
1	Epinephrine	$(Epi_{high} - Con_{high}) - (Epi_{amb} - Con_{amb})$	Epi_{high} n = 3 Epi_{amb} n = 3 Con_{high} n = 4 Con_{amb} n = 4	15474	0	0
2	pCO_2 on attachment with correction for developmental stage	$(Att.Spat_{high} - Non.Att_{high}) - (Att.Spat_{amb} - Non.Att_{amb})$	$Att.Spat_{high}$ n = 4 $Att.Spat_{amb}$ n = 4 $Non.Att_{high}$ n = 3 $Non.Att_{amb}$ n = 3	11880	94	849
3	pCO_2 on Non-attached larvae & spat	~ pCO_2 treatment	$Non.Att_{high}$ n = 3 $Non.Att_{amb}$ n = 3	7527	440	13
4	pCO_2 on Attached Spat	~ pCO_2 treatment	$Att.Spat_{high}$ n = 4 $Att.Spat_{amb}$ n = 4	9740	0	0

Table 3.3: List of GO terms from enriched genes which were down regulated from attachment model with correction for developmental stage (model 2) looking at ambient versus high pCO_2 treatments while accounting for stage (attached spat and non-attached individuals) on day 22. GO terms that were down-regulated are reported in this Table while individual genes that were either up- or down-regulated are reported in Table S3.2.

Other	GO.ID	Term	Ann.	Sign.	Exp.	Fisher	Cat.	Reg.
	GO:0003723	RNA binding	200	33	7.93	8.70E-09	Mol	Down
	GO:0003746	translation elongation factor activity	8	4	0.32	0.00015	Mol	Down
binding	GO:0051015	actin filament binding	9	3	0.36	0.00433	Mol	Down
(GO:0005488)	GO:0003743	translation initiation factor activity	31	5	1.23	0.00687	Mol	Down
	GO:0008083	growth factor activity	11	3	0.44	0.00802	Mol	Down
	GO:0031369	translation initiation factor binding	4	2	0.16	0.00891	Mol	Down
	GO:0008121	ubiquinol-cytochrome-c reductase activity	3	3	0.12	6.20E-05	Mol	Down
catalytic activity	GO:0008137	NADH dehydrogenase (ubiquinone) activity	11	4	0.44	0.00064	Mol	Down
(GO:0004824)	GO:0003724	RNA helicase activity	61	7	2.42	0.00995	Mol	Down
	GO:0099512	supramolecular fiber	83	11	3.06	0.0014	Cell	Down
	GO:0043226	organelle	1575	105	58.1	0.0022	Cell	Down
	GO:0005685	U1 snRNP	3	2	0.11	0.004	Cell	Down
cellular anatomical	GO:0005852	eukaryotic translation initiation factor...	10	3	0.37	0.0049	Cell	S2
entity	GO:0015629	actin cytoskeleton	9	5	1.18	0.0058	Cell	S2
(GO:0110165)	GO:0043229	intracellular organelle	1485	100	54.78	0.0064	Cell	Down
	GO:0005874	microtubule	76	8	2.8	0.0065	Cell	Down
	GO:0016282	eukaryotic 43S preinitiation complex	11	3	0.41	0.0066	Cell	Down
	GO:0005840	ribosome	114	34	4.21	1.20E-22	Cell	Down
	GO:0006457	protein folding	30	6	1.23	0.0011	Bio	Down
cellular process	GO:0060271	cilium assembly	15	4	0.61	0.0026	Bio	Down
(GO:0009987)	GO:0006879	cellular iron ion homeostasis	8	3	0.33	0.0032	Bio	Down
	GO:0060285	cilium-dependent cell motility	4	2	0.16	0.0094	Bio	Down
localization (GO:0051179)	GO:0006826	iron ion transport	7	3	0.29	0.0021	Bio	Down
	GO:0006412	translation	70	13	2.86	3.10E-06	Bio	Down
metabolic process	GO:0006120	mitochondrial electron transport, NADH	2	2	0.08	0.0017	Bio	Down
(GO:0008152)	GO:0015986	ATP synthesis coupled proton transport	2	2	0.08	0.0017	Bio	Down
	GO:0022904	respiratory electron transport chain	9	5	0.37	0.002	Bio	Down
structural molecule	GO:0005200	structural constituent of cytoskeleton	19	5	0.75	0.00069	Mol	Down
activity	GO:0003735	structural constituent of ribosome	20	5	0.79	0.0009	Mol	Down
(GO:0005198)	GO:0003714	transcription corepressor activity	3	2	0.12	0.00457	Mol	Down
transporter activity (GO:0005215)	GO:0015078	proton transmembrane transporter activity	19	5	0.75	0.00069	Mol	Down

Table 3.4: List of GO terms from enriched genes from high pCO_2 and ambient model (model 3) for day 22 non-attached individuals. Up regulated GO terms indicated, all other enriched genes regardless of direction of expression are summarized in Table S3.3. GO terms that were also seen in the settlement model are specified, all others were unique to non-attached individuals.

GO.ID	Term	Ann.	Sign.	Exp.	Fisher	Test	Shared	Reg.
GO:0007018	microtubule-based movement	73	41	24.94	8.00E-05	Bio	Unique	S3
GO:0008853	exodeoxyribonuclease III activity	97	64	28.62	8.20E-14	Mol	Unique	S3
GO:0005524	ATP binding	665	258	196.22	4.00E-08	Mol	Unique	S3
GO:0008569	ATP-dependent microtubule motor activity	24	17	7.08	3.30E-05	Mol	Unique	S3
GO:0005085	guanyl-nucleotide exchange factor activity	24	17	7.08	3.30E-05	Mol	Unique	S3
GO:0003723	RNA binding	200	85	59.01	5.00E-05	Mol	Settlement	Up
GO:0003964	RNA-directed DNA polymerase activity	90	44	26.56	7.70E-05	Mol	Unique	S3
GO:0003779	actin binding	57	30	16.82	0.0002	Mol	Unique	S3
GO:0003724	RNA helicase activity	61	30	18	0.00091	Mol	Settlement	Up
GO:0005737	cytoplasm	848	310	261.21	5.90E-05	Cell	Unique	S3
GO:0005856	cytoskeleton	237	115	73	8.90E-05	Cell	Unique	Up
GO:0005840	ribosome	114	53	35.12	0.00028	Cell	Settlement	Up
GO:0016459	myosin complex	13	10	4	0.00081	Cell	Unique	S3

CHAPTER 4 – METHODS TO ASSESS VULNERABILITY AND ADAPTIVE POTENTIAL OF UNDERSTUDIED ORGANISMS TO OCEAN ACIDIFICATION AND HYPOXIA: ESTIMATING HERITABILITY OF VARIATION IN RESPIRATION RATES IN *HALIOTIS RUFESCENS*

Andrea R. Burton, Hannah Gossner, Francis Chan

Abstract

Coastal upwelling along the US West Coast plays a vital role in coastal ecosystems by suppling nutrient-rich waters to the surface. However, upwelling also brings acidified and hypoxic seawater that can negatively impact calcifying organisms. Stressful upwelling conditions are projected to increase in severity as carbon emissions are predicted to lead to further ocean acidification (OA) along with more frequent hypoxic zones. These combined stressors (OA and hypoxia, OAH) are not mutually exclusive in the California Current Large Marine Ecosystem (CCLME) yet are often studied separately. In addition, the impacts of OAH have only been studied in a select few taxa, leaving gaps in our knowledge of how OAH will influence several economically and ecologically important species. The adaptive potential of such species to select for traits tolerant of OAH can be examined through estimating heritability. Expanding the work of Gossner et al. (2018), we estimate the heritability of respiration rates to infer traits related to metabolic processes in different OAH treatments, as metabolic processes are tightly coupled with respiration rates. Using the red abalone, *H. rufescens,* as a model for other understudied calcifying organisms, we measure respiration rates to understand metabolic responses to four different OAH scenarios: pre-industrial, baseline upwelling, contemporary upwelling, and distant future upwelling conditions. Results from Gossner et al. (2018) indicated that the tolerance threshold to OAH has already been reached in current populations, as respiration rates were similar across all current and future upwelling scenarios. Variation in respiration rates and genotyping of the same individuals were then used to estimate narrow-sense heritability (h^2). We found that individuals of *H. rufescens* bred from an aquaculture setting can have h^2 of respiration rate as high as 0.24 under contemporary upwelling, which suggests they have the potential to respond to selective pressure from certain OAH conditions. However, heritability estimates were close to zero under OAH scenarios projected for the distant future. Our study introduces methods and considerations for studying OAH in understudied species which can be transferable to other understudied organisms. We also discuss what steps should be considered when trying to estimate heritability in other understudied organisms that may lack resources such as a genome assembly and features.

Introduction

Red abalone, *Haliotis rufescens*, are motile benthic molluscs found from southern Oregon to Baja California (Estes, Lindberg and Wray, 2005). Individuals of *H. rufescens* are both economically important to the United States, for being a source of food for humans, as well as culturally iconic species to the West Coast (Leighton, 2000; Field, 2020). Shellfish aquaculture, including abalone farming, is a sustainable alternative to terrestrial animal protein (Gentry *et al.*, 2017; Froehlich *et al.*,

2018). In California, recreational harvest of fish and shellfish generates an estimated $230M-$610 in direct expenditures each year (Pendleton and Rooke, 2006). Abalone were once abundant, but after widespread population collapses due to overharvesting, most species are protected by law and no longer harvested (Rogers-Bennett et al., 2000; Rogers-Bennett et al., 2004). The species *H. rufescens* are now the last remaining abalone species with commercial viability in the U.S. West Coast through commercial aquaculture (Reid *et al.*, 2016; Karpov *et al.*, 2000).

In order to generate viable adults of *H. rufescens*, commercial production has focused on increasing larval and juvenile cultures (Utting and Spencer, 1997). These early life stages can be particularly impacted by increased acidity due to ocean acidification (OA) (Kurihara, 2008; Byrne *et al.*, 2011; Barton *et al.*, 2012; Griffith and Gobler, 2017), leading to uncertainties as to how OA will affect shellfish production (Ellis et al. 2017). The impacts of hypoxia are less examined, but not mutually exclusive with OA. Due to upwelling brought on from the California Current Large Marine Ecosystem (CCLME), coastal organisms are readily exposed to both acidified and hypoxic conditions (OAH) during summer months (Chan *et al.*, 2008; Somero *et al.*, 2016; Feely *et al.*, 2018), which can also impact aquaculture facilities with commercial water intake systems (Booth *et al.*, 2012). Low oxygen can trigger stressful responses in organisms, resulting in reduced ATP production and putting strain on metabolic functions, often resulting in high mortalities (Guppy and Withers, 1999). Both veliger and juveniles stages are negatively impacted by high pCO_2 (Zippay and Hofmann, 2010; Gazeau *et al.*, 2013). For example, prolonged exposure to reduced pH 7.5 results in reduced growth rates in juveniles (Kim, Barry and Micheli, 2013), which would be highly detrimental to wild and cultured stocks.

While most studies examine the effects of hypoxia and pH independently, few studies have examined the potential synergistic effects of OAH. Due to OA and hypoxic conditions being intrinsically linked in the CCLME upwelling system (Chan *et al.*, 2017), decoupling these processes does not reflect how future climate scenarios will impact marine organisms. Vulnerability and tolerance to OAH conditions may be assessed through metabolic response. Energy provisions can be limited by the availability of O_2 (Brett, 1971; Pörtner and Farrell, 2008), along with energetic demands of maintaining internal acid-base balance in high pCO_2 conditions (Orr *et al.*, 2005; Kroeker *et al.*, 2013). Acidified conditions along with reduced oxygen concentrations stimulate constant internal adjustments to counteract these conditions (Fabry *et al.*, 2008; Penn *et al.*, 2018). Mechanisms for correcting these imbalances can be energetically expensive (Burnett, 1997; Pörtner and Farrell, 2008), which can be reflected in respiration rates (Deutsch *et al.*, 2015; Deutsch, Penn and Seibel, 2020).

In particular, calcifying organisms are of concern as OA reduces calcification of their shells, growth, and survival (Kroeker *et al.*, 2010). The species *H. rufescens* is among the many calcifying organisms with gaps in our knowledge concerning OAH effects. Currently, our understanding of the impacts of OAH is restricted to a small handful of taxa. Further, gaps in our current knowledge make it difficult to determine which species are more vulnerable than others as climate change stressors

progress. Quick and simple mechanisms for assessing the adaptive potential of understudied organisms is of interest to policy makers and conservation efforts. By utilizing recent SNP-based genotyping methods to evaluate adaptive capacity, we estimate heritability of respiration rates in different OAH conditions and discuss caveats and considerations when applying similar methods to other understudied organisms.

Using respiration rates as a proxy for metabolic rates, Gossner et al. (2018) assessed the vulnerability or resilience of the species *H. rufescens* to the combined stressors of OAH. Four OAH upwelling scenarios were selected based on pre-industrial, baseline, contemporary, and distant future OAH conditions. On average, individuals of *H. rufescens* exhibited reduced metabolic performance for all current and future upwelling scenarios in comparison to pre-industrial OAH conditions (Gossner, 2018). In addition, there was no difference in metabolic rates among the three current and future upwelling conditions. Results from this study suggest the physiological threshold for OAH tolerance has already been reached and that the populations have little metabolic plasticity as OAH conditions worsen. However, Gossner et al. (2018) observed wide variation in responses among individuals. If such phenotypic variation is associated with genetic variation, these populations of *H. rufescens* may be able to respond to selection from OAH changes. Further, northern Californian populations demonstrate a range of responses to shifts in pH and oxygen concentrations, suggesting their harbor genetic variation for survival and growth under OAH (Kim et al. 2013). In addition, wild populations frequently exposed to strong upwelling were found to be more tolerant to high pCO_2 treatments than captive-raised populations that were not reared in frequent upwelling conditions (Swezey *et al.*, 2020). Together, these studies suggest that the species *H. rufescens* possess genetic variation that may aid in adaptation to OAH, but none have measured this potential.

In this study, we aim to expand on Gossner's et al. (2018) work to examine the vulnerability of the species *H. rufescens* by assessing the adaptive capacity of metabolic processes in the same four OAH scenarios. In this chapter, we develop a simplified method to examine the adaptive potential of individuals of *H. rufescens* by quantifying genetic variation and to test whether this variation can explain some of the respiration rate variation observed by Gossner et al. (2018). Adaptation requires genetic variation for selection to act upon. Phenotypic variation from respiration rates measured by Gossner et al. (2018) may be driven in part by non-genetic factors including environmental history, and in part by genetic factors. Heritability of a quantitative trait, such as respiration rate, is defined as the proportion of the phenotypic variation (V_P) in a trait that can be explained by additive genetic variation (V_A); formally this is known as narrow-sense heritability: $h^2 = V_A/V_P$ (Falconer and Mackay, 1996). Estimations of heritability have been used to predict how natural populations may undergo evolutionary change in a trait (Mousseau and Roff, 1987; Falconer and Mackay, 1996; Thomas, 2005; Bairos-Novak *et al.*, 2021). In this study, we measure *H. rufescenses'* adaptive potential in future OAH by estimating heritability of respiration rates in different OAH conditions. In addition, we discuss

considerations needed when replicating these methods when assessing vulnerability of understudied marine organisms to future OAH scenarios.

Although heritability has long been utilized for agricultural purposes, its application to natural populations in which relatedness is often unknown has had mixed success due to variation and uncertainty with how to calculate genetic relatedness. Genetic relatedness can be correlated with phenotypic similarity, enabling the estimation of heritability (Falconer and Mackay, 1996). Several estimators for relatedness have been developed, aiming to address variation and noise in datasets such as levels of inbreeding, outbreeding, and admixture within study populations (Queller and Goodnight, 1989; Li, Weeks and Chakravarti, 1993; Ritland, 1996; Lynch and Ritland, 1999; Wang, 2002, 2007; Milligan, 2003). The performance of each relatedness estimator depends on characteristics of the data which are difficult to predict prior to estimating relatedness (Van De Casteele et al. 2001; Wang, 2002; Csilléry *et al.*, 2006). Relevant characteristics of the data include sample size (Yang *et al.*, 2015), the number of loci (Yang *et al.*, 2010), as well as with population genetic parameters such as such as minor allele frequencies (MAF) or linkage disequilibrium (LD) (Speed *et al.*, 2012, 2017). MAF is the frequency in which the second most common allele occurs in a population. MAF and LD can be biased, with both higher frequencies alleles (Speed *et al.*, 2017) and regions of strong LD tending to overestimate heritability. The accuracy of heritability estimates can be improved when considering such characteristics but may be limiting in non-model organisms. For instance, the species *H. rufescens* has a reference genome that lacks linkage groups (Masonbrink *et al.*, 2019) that removes methods of stratification of loci based on linkage disequilibrium, a genomic characteristic that may improve heritability estimates (Evans *et al.*, 2018).

In this chapter, we estimate heritability of respiration rates under four different OAH conditions. Seawater was manipulated to reflect pCO_2 and oxygen concentrations in pre-industrial, baseline upwelling, contemporary upwelling, and distant future upwelling conditions. We examine different dataset parameters and different relatedness estimators for calculating heritability, with the additional aim of understanding the feasibility of using these methods given the limitations of non-model organisms. Heritability estimates were conducted on metabolic response to OAH in individuals of *H. rufescens.* Further, we discuss the viability and accuracy of methods used in this study to other non-model organisms.

Materials and Methods

Measuring metabolic rates

Respiration rate experiments were carried out by Hannah Gossner for her Masters of Science work, and was completed as described in Gossner (2018). Here, we overview these methods. Approximately 250 Juvenile *H. rufescens, ranging from 10-15 mm,* were shipped overnight from Moss Landing Research Lab, CA, in an insulated box containing ice packs. These juveniles were bred from crosses of twelve females from the Ab Farm (Cayucos, CA) and six males from American Abalone

(Davenport, CA), likely making them distantly related. Upon arrival, individuals of *H. rufescens* were split into two shellfish bags (125 juveniles each) and fed on *Palmaria mollis*. *H. rufescenses'* health and food availability were monitored daily while being held in an outdoor flow-through tanks at Hatfield Marine Science Center in Newport, OR. Respiration rates were measured for 128 juveniles randomly selected individuals to be exposed to one of the four OAH conditions during exposure and allowed to recover before measuring respiration rates again.

Approximately 28 individuals were divided into one of the four OAH treatments: pre-industrial (pH = 8.17, 297 μmol/L, baseline upwelling (pH = 7.56, 75 μmol/L), contemporary upwelling (pH = 7.50, 40 μmol/L), and distant future upwelling (pH = 7.27, 20 μmol/L) (Table 4.1). Baseline upwelling is present day OAH conditions in which seawater is already seen pH reduced by 0.12, and aragonite saturation reduced 0.5 (Gruber *et al.*, 2012; Harris, DeGrandpre and Hales, 2013). Contemporary upwelling represents both modern seawater conditions at a deeper depth or near-future conditions. Distant future represents the worst-case scenario of pH, aragonite saturation, and oxygen concentrations for the year 2100 (Feely *et al.*, 2004; Chan *et al.*, 2017). Seawater was collected from a flow-through system at the Hatfield Marine Science Center, where it was filtered (400 μm). Seawater was manipulated by first removing dissolved gasses using nitrogen gas and bubbling with carbon dioxide until the desired pH was met. Oxygen was added through agitation or diffusion. Dissolved inorganic carbon and alkalinity were back calculated using pH and temperature on CO2Sys (CO2SYS Program, version 2.3, Ernie Lewis) (Gray et al. 2011). Total alkalinity was assumed to be 2250 µM/kgSW and salinity to be 33.5 psu, while temperature was targeted at 8°C. Manipulated seawater was added to 15-mL gas-tight ground-glass vials. Oxygen consumption was measured for 35 to 44 minutes for each individual using Fibox 3 Oxygen Meter and corresponding oxygen-sensitive optode sensor dots (PreSens Precision Sensing, Regensburg, Germany) and acquired with Fibox 3 for PSt3 software (version 6.02). Respiration rates were measured at two different times, first while juveniles were in their pH treatments (exposure treatment), then again after there were given time to recover (recovered treatment). Respiration rates were not recorded for 11 individuals and were not used for sequent analyses. Following the respiration in each OAH experiment, juveniles were stored in ethanol until needed for DNA extractions.

To test whether respiration rates were impacted by OAH treatments, a series of ANOVAs were performed. A Shapiro-Wilk test showed that untransformed rate values had unequal variance and deviated from normality ($p = 0.04$). Respiration rates were hence log-transformed prior to ANOVA tests. A 2-way ANOVA examined the effect of pH treatment and date of experiment to confirm that day of experiment did not affect respiration rates. Date had no effect in the exposure treatment ($F_{3,104} = 0.332$, $P = 0.97$) or in the recovery treatment ($F_{3,104} = 0.25$, $P = 0.61$) (Table 4.2). Therefore, date was not used as a factor for any analyses downstream.

Multilocus SNP genotyping

To estimate heritability of metabolic rates, we first conducted multilocus SNP genotyping for the 117 samples in which respiration rates were measured. Tissue samples from the foot of the juvenile were cut away. DNA from these tissue samples were extracted using the Omega bio-tek E.Z.N.A. Tissue D Kit (Omega Bio-tek, Norcross, GA). Sequencing libraries was prepared using the 2bRAD protocol for genotyping SNPS (Wang et al. 2012) using the AlfI enzyme. A reduced tag representation method was used by selecting adaptors with a "NR" overhang to target a fourth of the AlfI sites (Wang et al. 2012). Samples were pooled in two groups of 64 at equimolar amounts and each pool was sequenced on a lane of HiSeq 3000 as 50-bp single reads at Oregon State University's Center for Genome Research and Biocomputing (now the Center for Quantitative Life Sciences).

Sequenced reads were processed using publicly available scripts (https://github.com/Eli-Meyer/2brad_utilities/). First, adaptors were trimmed and low-quality reads with a phred score less than 30 were removed. Approximately 1.7 billion reads were sequenced (~13.5 million reads per sample), with 1.6 billion reads remaining after filtering (~13 million reads per sample). Cleaned reads were mapped to a reference *H. rufescens* species genome (Masonbrink et al. 2019) which was indexed using BWA (Li & Durbin 2010) and bowtie (Langmead et al. 2009). Reads were then mapped using SHRiMP (Rumble et al. 2009), reporting the top 3 maximum hits per read. Roughly 18.8 million reads successfully mapped (~145 thousand reads per sample).

Genotypes were called based on nucleotide frequencies at each position with permissive threshold of greater than or equal to 5 times coverage. This was done by calling loci homozygous if the minor allele was present at less than 1%, heterozygous if present at more than 25%, and undetermined at intermediate frequencies (Wang et al. 2012). Addition filtering was done to eliminate samples with fewer than 5,000 missing loci, which removed 7 samples. Loci that were genotyped in 10 or fewer samples were also removed. Lastly, only bi-allelic SNPs were retained. The final dataset contained 110 individuals with 343 loci for downstream analyses.

Estimating relatedness and heritability

To estimate heritability of variation in respiration rate, we first estimated genetic relatedness between each individual. Using the 343 SNP loci, we inferred genetic relatedness among samples using the package 'related' (Pew *et al.*, 2015). To determine which estimator of relatedness worked best with this dataset along with determining how related our samples were, we compared six different estimators available through the 'related' package (Frasier 2018): Lynch & Li (LL), Lynch & Ritland (LR), Ritland (R), Wang (W), Queller (Q), and Dyad (D) (Pew et al. 2015). Using the 'FAMILYSIM' function in the 'related' package (Pew *et al.*, 2015), allele frequency data was used to generate 100 iterations of simulated pairs of individuals within the following relatedness groups: parent-offspring, full-sibling, half-sibling, and unrelated. Results from relatedness simulations indicated that Wang (W) and Lynch and Li (LL) had a means closest to the true value (0.5 full sibs, 0.25 half sibs, 0.5 parent to

offspring, and 0 for unrelated), with relatedness estimates falling within 0.1% of the true values for three of the four relatedness groups (Figure 4.1). The abalone individuals we assayed were received from a farm where inbreeding is actively avoided by selecting female parents from one farm and males from another. The individual samples were confirmed to be unrelated as the simulation for unrelated relatedness group having narrow confidence intervals, indicating simulated estimates for unrelated pairs had the least error (Figure 4.1D). The same function 'COANCESTRY" was used to calculated 95% confidence intervals. Each estimator has different ranges for relatedness estimations (Pew *et al.*, 2015), all of which fall outside of the 0 to 1 range in order to add more weight towards unrelated individuals (below 0) (Queller and Goodnight, 1989; Ritland, 1996; Lynch and Ritland, 1999) and for closely related individuals (above 1) (Milligan, 2003).

After selecting W and LL methods, a genetic relatedness matrix was derived from the genotypes using each of these relatedness estimators and these used for all heritability calculations (Queller & Goodnight 1989, Tavalire et al. 2018). Prior to estimating heritability (h^2), a principal component analysis (PCA) including all genotypes was run using the 'prcomp' function in R to examine whether genetic stratification existed in the dataset, which could introduce biases to the analysis. Results from the PCA showed no clear stratification, and that PC1 explained 31% of the variance (Figure S4.1). Variation in respiration rates during exposure and after recovering was partitioned into genetic and non-genetic components using a restricted maximum likelihood model (REML) using the R package 'regress' (Clifford, McCullagh and Clifford, 2014), with PC1 used as a fixed effect due to population structure being a function of genetic ancestry and is the same for all samples (Price *et al.*, 2010). A REML model was performed with respiration rates from each treatment level in both exposure and recovered experiments. We then estimated narrow-sense heritability (h^2) associated with standard errors based on phenotypic variation remaining after accounting for known sources of variance using the h2G function in 'gap' (Zhao, 2007).

Challenges and solutions for h^2 estimation

Estimates of h^2 for the pre-industrial and contemporary treatments were not obtained because the models did not find a variance coefficient (Table 4.3). The variance coefficient is calculated from the variance matrices derived from the related matrix and should be "positive definite". However, if the variance matrix is largely not positive definite, the coefficient cannot be calculated (Yang *et al.*, 2010). Yang et al. (2010) explains that having a non-positive definite variance matrix may be attributed to having small number of loci (e.g. less than 1000) or having a data set where individuals are largely unrelated. For our data set, we have less than 1000 loci and unrelated individuals (Table S4.1). We examined how incrementally incorporating these steps impacts the ability to estimate relatedness and heritability and their uncertainty.

Methods for filtering the dataset so that it may be "positive definite" include removing samples with high confidence intervals calculated from the relatedness matrix, removing loci with

minor allele frequencies (MAF) less than 0.05, and stratifying loci based on MAF (Speed *et al.*, 2012; Evans *et al.*, 2018). First, for each genetic relatedness matrix (W and LL), we compared 95% confidence intervals among individuals. Individuals that were in more than two paired comparisons in which confidence intervals (CI) ranges (upper limit – lower limit) were greater than 5 were removed (Table S4.2). The value of 5 was selected as it related to an ideal number of individuals for removal as 4 resulted in hundreds of pairs with 32 individuals being removed, while 6 was too stringent with only 5 individuals being removed. We next filtered loci based on minor allele frequency (MAF), since those with very low values are known to bias relatedness estimates (Speed *et al.*, 2012). We used vcftools (Danecek et al. 2011) to remove loci with MAF < 0.05 (four were removed from the dataset), and then re-calculated LL and W estimators. Finally, the remaining loci (> 0.05) were binned based on their MAF across the following bins: 0.05-0.10, 0.10-0.20, 0.20-0.30, 0.30-0.40, and 0.40-0.50. LL and WW relatedness estimators were run and heritability estimates re-calculated. A fourth recommend step is to incorporate LD in the relatedness models (Evans *et al.*, 2018). Unfortunately, the current reference genome for the species *H. rufescens* does not contain linkage groups or chromosomal information (Masonbrink et al. 2019), and it is too fragmented. For this reason, the influence of LD on heritability estimates was not assessed.

Results

During exposure to the different experimental OAH levels, respiration rates of *H. rufescens* individuals in the pre-industrial level were 2.5X higher than in the other three levels (Figure 4.2) ($F_{3,96}$ = 36.615, p = $8.25e^{-25}$, Tukey HSD, p = 0.022-0.046). Individuals of *H. rufescens* in the pre-industrial treatment had respiration rates ranging from 0 to 285 μmol O_2/ind/day, while the other three upwelling scenarios 2 to 102 μmol O_2/ind/day. Respiration rates sharply declined in the baseline upwelling treatment, which had similar respiration rates to the contemporary and future upwelling conditions (Tukey HSD, p = 0.997-0.999), with no pattern or shifts in respiration rate as exposure severity increased. During the recovery experiment, respiration rates did not differ significantly among treatment conditions, and ranged from 0 to 276 μmol O_2 g^{-1} d^{-1} ($F_{3,97}$ = 0.199, p = 0.897).

As already mentioned, the Lynch and Li (LL) and Wang (W) relatedness estimators performed best among the six relatedness estimators used for this study (Figure 4.1), and readily produced estimates of h^2 under baseline and future upwelling conditions in both experiments (Table 4.4). Further analyses involved testing filtering steps to permit estimations under pre-industrial and contemporary conditions, and to improve calculations overall. First, removal of 8 individuals with highly overlapping CI for relatedness values (102 remaining) improved the model fits and allowed for calculation of h^2 for respiration rate in the contemporary upwelling in the exposure experiment (Table 4.4). However, relatedness matrices remained non-positive definite for the pre-industrial treatments, and hence h^2 was still not obtained. Removal of MAF < 0.05 improved heritability estimates of contemporary OAH exposure, however, did not improve heritability estimates in pre-industrial

exposure. MAF < 0.05 likely made some relatedness estimates less than zero, making the relatedness matrix non-positive definite. Binning MAF resulted in all but one bin (MAF 40-50%) not being able to estimate heritability (Table S4.3). Binning the loci based on MAF reduced the number of loci per bin ranging from 33 two 172 (Table S4.3), reducing the power for estimating relatedness (Park *et al.*, 2011). For this reason, we decided to not include these steps in the final analyses but will be discussed when assessing the limitations of this data set when doing this type of analyses.

After removing samples with high confidence intervals and MAF less than 0.05, LL and W produced similar heritability estimates with differences in estimates ranging from 0.0003 to 0.1012 (Table 4.4). For both estimators, h^2 increased slightly with increasing OAH stress conditions during exposure, but then decreased in the future OAH treatment (Table 4.4, Figure 4.3a). The highest h^2 estimates were in the contemporary upwelling scenario, in which h^2 was 0.23 ($\pm$ 0.29) and 0.25 ($\pm$0.33) for W and LL, respectively. During recovery, h^2 were all low, with all but the baseline upwelling condition falling below zero (Table 4.4, Figure 4.3b). Overall, uncertainty in estimation of h^2 remained high, as illustrated by wider error bars (Figure 4.3).

Discussion

Here, we report that respiration rates are lower in the decreased pH and oxygen concentration, suggesting that metabolic demand is reduced in *H. rufescens* individuals. Decreased respiration rates have been reported to be correlated with reduced metabolic processes in response to higher levels of stress to OAH (Deutsch *et al.*, 2015; Deutsch et al. 2020). Respiration rates were highest in the preindustrial OAH treatment, but sharply declined and stayed the same in the subsequent treatments. The lack of continued respiration rate decline as OAH condition worsened suggests individuals in the baseline upwelling experienced the same level of stress response to those in the distant future upwelling (Gossner, 2018). Individuals in acidified and hypoxic conditions require metabolic processes to correct for imbalances that are energetically expensive (Burnett 1997, Pörtner 2008, Gruber et al. 2012). Increased stress response to the three future OAH conditions resulted in metabolic depression, but this metabolic depression plateaus with the smallest shift in seawater chemistry that was used in this study. These results suggest that the physiological threshold for OAH stress was reached with the least severe upwelling conditions (Gossner, 2018). Similarity of respiration rates following all the OAH exposures could mean that those exposed to the different upwelling scenarios fully recovered after 30 minutes in ambient seawater conditions. Individuals from all OAH conditions were able to reacclimate back to benign conditions relatively quickly.

Heritability Estimates

With roughly 120 species produced in North American aquacultures, of which 50 are calcifying organisms, there is a need to understand how these organisms will be impacted by future climate change projections (Garibalid, 1996; FAO, 2010). Resource managers and policymakers in

Oregon have expressed the need to understand the risks of OAH in a variety of economically and ecologically important species to predict management efforts towards toward these species. This study provides the first quantitative estimates for heritability of variation in respiration rates in the species *H. rufescens*. The highest heritability estimate for metabolic stress was seen in individuals exposed to the contemporary OAH treatment, with h^2 ~0.24. This level of heritability may allow individuals of *H. rufescens* to respond to selection for traits associated with metabolic processes, at least to some near future OAH scenarios. Notably, heritability estimates for respiration rates were below zero in the most stressful OAH condition. Distant future upwelling conditions appear to be too severe, and individuals exposed to these treatments lacked quantitative genetic variation that could explain their respiration rates. This may indicate limited adaptive potential to the projected levels of OAH in more distant time frames. During recovery post OAH stress, no level of OAH were associated with measurable heritability of respiration rates, suggesting that mechanisms for reacclimating to ambient conditions are do not have a quantitative genetic component, at least in the samples used.

The physiological threshold to OAH occurred prior to any future upwelling scenarios. However, we see that *H. rufescenses'* capability to acclimate to normal seawater conditions occurs rapidly once future upwelling conditions are removed. In addition, we conclude from our heritability estimates that the species *H. rufescens* has the capacity to adapt to all but the worst-case future upwelling scenarios predicted to occur by 2100. In addition, we expected heritability estimates to decline gradually, rather we observed sudden declines from contemporary upwelling to the next. However, heritability estimates had high error that overlapped between OAH treatments, suggesting that the sudden decline in heritability estimates may be an artifact of the data. Assuming the sudden reduction of heritability estimates in the distant future OAH condition is true, this suggests that these conditions are too severe for individuals to mitigate these conditions through metabolic processes. While current aquaculture *H. rufescens* individuals may not adapt to future upwelling conditions, we observe they have metabolic traits for selection in current and closer future projections. Selection of these traits may shift metabolic processes so that individuals of *H. rufescens* may be more tolerant, with future populations have higher adaptive potential over generations. Together, we find that individuals of *H. rufescens* are vulnerable to future OAH conditions but have the capacity to select for metabolic traits to be more tolerant to all but distant future OAH conditions.

To date, this is the first study to examine the combined impacts of OAH on *H. rufescens* species. Previous work on OA allude to heritability potential of increased survival and growth within these conditions (Kim et al. 2013; Swezey *et al.*, 2020), but none have examined hypoxia. For instance, F_2-generations of *H. rufescens* individuals had reduced survival and increased lipid reserves under high pCO_2 conditions, suggesting larval lipid metabolism is potentially heritable (Swezey *et al.*, 2020). However, heritability estimates of growth or metabolic responses in hypoxic conditions has been limited to fish (Anttila *et al.*, 2013; Ferrari *et al.*, 2016) and some marine invertebrates (Dam, 2013; Zhang *et al.*, 2017). Fewer studies have examined the combined effects of OAH (Dam, 2013).

This study, as far as we know, is the first to address the impacts of OAH and the adaptive potential of *H. rufescens* individuals to predicted OAH conditions. Estimating variation in respiration rate observed with genetic variation to estimate heritability provides insight into metabolic response in current and future OAH scenarios. This approach could be a powerful tool in understanding how the species *H. rufescens* and other understudied species will fare under future OAH conditions. However, there are limitations of estimating heritability in non-model taxa, such as *H. rufescens* individuals, that stem from lower availability of genetic resources and difficulty in controlling and estimating genetic relatedness. Other population-level factors and limitations also impact the reliability of heritability estimates. For example, individuals used for this study were obtained from a breeding program, and thus may not reflect individuals of *H. rufescens* in natural populations. Inbreeding was systematically avoided in these populations, making accuracy of heritability estimates more uncertain because of the reduced range of genetic relationships across which to model. In addition, heritability estimates are population-specific and vary both based on standing genetic variance within that population and environmental heterogeneity to which that population is exposed (Visscher et al. 2008). Therefore, our estimates may only represent populations found in the aquaculture farms from where our samples were obtained. Heritability can also differ between life stages; for instance, juveniles of a coral species had lower heritability of bleaching and growth than larvae and adults (Bairos-Novak et al. 2021). In this study, we only estimated heritability in juveniles, which may show very different sensitivity to OAH variation than earlier life stages (Hofmann *et al.*, 2010). Similar methods from this study should be utilized on other life stages to provide a broader picture of the adaptive potential for the species as a whole, especially for early larval developmental stages that are more vulnerable to OA (Kroeker *et al.*, 2010). Early larval stages are readily impacted by environmental factors as they are undergoing variety of developmental processes that are energetically taxing. Metabolic demands during larval stages are high but may have a variable response to OAH. If variation in metabolic response is measured, this could provide heritability estimates of metabolic processes for this life stage. A thorough understanding of how this species will fare with future OAH will require follow-up studies of multiple natural populations at different life stages. Finally, estimates of heritability would greatly benefit from linkage group information (Speed *et al.*, 2012, 2017). The only reference genome sequence for the species *H. rufescens* is ~1.5 Gb of the estimated 1.8 GB genome (Gallardo-Escárate and Del Río-Portilla, 2007) includes around 8,000 scaffolds with no chromosomal or linkage group information (Masonbrink *et al.*, 2019). For this reason, improving heritability estimates through stratification of LD and MAF were limited in this species. We discuss these limitations and how they may apply to other understudied organisms in the next section.

Considerations when estimating heritability in understudied species

Despite the limitations discussed above, we identified a set of data filtering steps that ameliorate calculations of genetic relatedness prior to obtaining h^2. Consideration of which population

to sample along with the number of individuals needs to be taken. Breeding programs often prioritize outbreeding. In this study, we see the biggest limitation for estimating heritability was sample size. While there are other studies that have fewer individuals (e.g. Dziedzic *et al.* 2019 n = 43, Alcapán et al. 2007 n = 95), limitations in our dataset arose when estimating heritability in unrelated individuals. When assessing the adaptive potential of a species to environmental conditions with unknown relatedness, large sample sizes of individuals across multiple populations will increase representation of the species. When estimating heritability among unrelated individuals as we did, around 3,000 samples are required to decrease standard errors to below 0.1 (Visscher *et al.*, 2014). When standard error is greater than 0.1, the 95% confidence interval will cover the whole parameter space, and cannot produce meaningful estimates (Yang *et al.*, 2015) as seen in our dataset (Figure 4.3). Breeding programs may have similar issues when estimating relatedness in breeding programs that are largely unrelated. Either 3,000 individuals need to be sampled (Yang *et al.*, 2015), or selective breeding schemes with some related individuals will improve statistical power for estimating heritability.

In addition, a small data set yielded a limited number of markers to estimate relatedness. Fewer markers prevented MAF binning analyses that has been shown to increase the accuracy of heritability estimates (Evans *et al.*, 2018). Heritability varies with MAF, with performance of models improving by change how genotypes are scaled based on their MAF (Speed *et al.*, 2017). Park et al. (2011) found that the contribution of alleles to genetic variance was highest in 0.3-0.4 or 0.4-0.5 while allele-frequencies between 0.05-0.1 and 0.1-0.2 explained little of the genetic variance. A power-adjusted analysis of the impact of MAF indicated that alleles that are less common likely have larger effects of heritability estimates while explaining little of the variance. This bias in MAF is impacted by the number of SNPs and their collective contribution to genetic variance (Park *et al.*, 2011). Performance of models estimating heritability improved when genotypes were scaled based on MAF (Park *et al.*, 2011; Speed *et al.*, 2017). In our study, we attempted to examine the influence MAF by binning loci in 10% increments. However, due to the limited number of loci, the power of our analyses decreased substantially, resulting in standard errors so large that the estimators for heritability could not be performed for many of our models. Accounting for MAF while estimating heritability could have aided in more reliable estimates, but we were limited by sample size and limitations in our data set. Power analyses suggests that a relatively large number of markers (~2,000-5,000) must be genotyped for heritability estimates (Hu and Yang, 2014). Mechanisms for increasing markers sequenced should be considered, and these include sequencing longer reads (2bRAD is limited to 34-36 bp) and optimizing bioinformatic parameters for balancing number of loci and genotyping error rate (Catchen *et al.*, 2013; O'Leary 2018).

Conclusion

Together, measuring respiration rates as a proxy for metabolic response along with estimating the heritability of this trait could be useful for assessing the vulnerability of non-model and understudied organisms to different OAH scenarios. Gossner's et al. (2018) work isolates the physiological threshold for metabolic depression, our heritability estimates indicate that these physiological responses are related to genetic composition in individuals of *H. rufescens*. Traits relating to these physiological responses can thus drive adaptation given selective pressures from OAH. However, considerations for improving our methods for assessing the vulnerability and adaptive potential should be addressed. Natural populations should be utilized when addressing questions concerning the adaptive potential of a species. In addition, the more representation of these genetic pools will more accurately reflect the species, meaning individuals samples should come from a variety of populations spanning geographic ranges. Methods of how heritability is estimated should be considered, including what population(s) is sampled, the number of individuals and markers being targeted, availability of reference genome and genome characteristics, and what model to use to estimate heritability.

Acknowledgements

The authors of this chapter would like to thank Dr. Eli Meyer and Dr. Katie Dziedzic for sharing their pipeline on how to estimate heritability. We would also like to thank Dr. Molly Burke for her suggestions on what techniques may aid in estimating heritability. Lastly, we would like to thank Dr. Felipe Barreto for providing feedback on how to structure this chapter. Funding for this chapter was provided by the Oregon Sea Grant Omnibus Grant-Funded Projects (ICODE: 2500).

References

Alcapán, A.C., Nespolo, R.F., & Toro, J.E. (2007). Heritability of body size in the Chilean blue mussel (*Mytilus chilensis* Hypé 1854): effects of environmental ageing. Aquaculture Research, 38, 313-320.

Anttila, K., Dhillon, R.S., Boulding. E.G, Farrell, A.P., Glebe, B.D, Elliott, J.A., Wolters, W.R., & Schulte, P.M. (2013). Variation in temperature tolerance among families of Atlantic salmon (*Salmo salar*) is associated with hypoxia tolerance, ventricle size and myoglobin level. Journal of experimental biology, 216, 1183-90.

Bairos-Novak, K., Hoogenboom, M.O., van Oppen, M.J., & Connolly, S.R. (2021). Coral adaptation to climate change: Meta-analysis reveals high heritability across multiple trats. Global Change Biology, 27, 5694-710.

Barton, A., Hales, B., Waldbusser, G.G., Langdon, C., & Feely, R.A. (2012). The Pacific oyster, *Crassostrea gigas*, shows negative correlation to naturally elevated carbon dioxide levels: Implications for near-term ocean acidification effects. Limnology and Oceanography, 57, 698-710.

Booth, J.A.T., McPhee-Shaw, E.E., Chua, P., Kingsley, E., Denny, M., Phillips, R., Bograd, S.J., Zeidberg, L.D., & Gilly, W.F. (2012) Natural intrusions of hypoxic, low pH water into nearshore marine environments on the California coast, Continental Shelf Research, 15, 108-15.

Brett, J.R. (1971). Energetic responses of salmon to temperature. A study of some thermal relations in the physiology and freshwater ecology of sockeye salmon (*Oncorhynchus nerkd*). American Zoologist, 1, 99-113.

Burnett, L.E. (1997). The challenges of living in hypoxic and hypercapnic aquatic environments, American Zoologist. 37, 633-40.

Byrne, M., Ho, M., Wong. E., Soars, N.A., Selvakumaraswamy, P., Shepard-Brennand, H., Dworjanyn, S.A., & Davis, A.R. (2011). Unshelled abalone and corrupted urchins: development of marine calcifiers in a changing ocean. Proceedings of the Royal Society B: Biological Sciences, 278, 2376-2383.

Van De Casteele, T., Galbusera, P., & Matthysen, E. (2001). A comparison of microsatellite-based pairwise relatedness estimators. Molecular Ecology, 10, 1539-49.

Catchen, J. M., Hohenlohe, P. A., Bassham, S., Amores, A., & Cresko, W. A. (2013). Stacks: An analysis tool set for population genomics. Molecular Ecology, 22(11), 3124–3140.

Chan, F., Barth, J.A., Lubchenco, J., Kirincich, A., Weeks, H., Peterson, W.T., & Menge, B.A. (2008). Emergence of anoxia in the California Current Large Marine Ecosystem. Science 319, 920-920.

Chan, F., Barth, J.A., Blanchette, C.A., Byrne, R.H., Chavez, F., Cheriton, O., Feely, R.A., Friederich, G., Gaylord, B., Couhier, T., & Hacker, S. (2017). Persistent spatial structuring of coastal ocean acidification in the California Current System. Scientific Reports, 31, 107.

Clifford, D., McCullagh, P., & Clifford, M.D. (2014). The regress package. R package version, 1.3-14.

Csillery, K., Johnson, T., Beraldi, D., Clutton-Brock, T., Coltman, D., Hansson, B., Spong, G., & Pemberton, J.M. (2006). Performance of marker-based relatedness estimators in natural populations of outbred vertebrates. Genetics, 173, 2091-2101.

Dam, H.G. (2013). Evolutionary adaptation of marine zooplankton to global change. Annual Review of Marine Science, 5, 349-370.

Deutsch, C., Ferrel, A., Seibel, B., Pörtner, H., & Huey. R.B. (2015). Climate change tightens a metabolic constraint on marine habitats. Science, 348, 1132-35.

Deutsch, C., Penn, J.L., & Seibel, B. (2020). Metabolic trait diversity shapes marine biogeography. Nature, 585, 557-562.

Dziedzic, K.E, Elder, H., Tavalire, H., & Meyer, E. (2019). Heritable variation in bleaching responses and its functional genomic basis in reef-building corals (*Orbicella faveolata*). Molecular Ecology, 28, 2238-2253.

Ellis, R.P., Urbina, M.A., & Wilson, R.W. (2017). Lessons from two high CO_2 worlds, future oceans and intensive aquaculture. Global Change Biology, 23, 2141-2148.

Estes, J., Lindberg, D., & Wray, C. (2005) Evolution of large body size abalones (*Haliotis*): patterns and implications. Paleobiology, 31, 591-606.

Evans, L.M., Tahmasbi, R., Vrieze, S.I., Abecasis, G.R., Das, S., Gazal, S., Bjelland, D.W., De Candia, T.R., Goddard, M.E., Neale, B.M., & Yang, J. (2018). Comparison of methods that use whole genome data to estimate the heritability and genetic architecture of complex traits. Nature Genetics, 50, 737-745.

Fabry, V.J., Langdon, C., Balch, W.M., Dickson, A.G., Feely, R.A., Hales, B., Hutchins, D.A., Kleypas, J.A., & Sabine, C.L. (2008). Ocean acidification's effects on marine ecosystems and biogeochemistry: Ocean carbon and biogeochemistry scoping workshop on ocean acidification research: La Jolla, California, 9-11 October 2007. Eos, Transactions American Geophysical Union, 89, 143.

Falconer, D.S., & Mackay, T.F. (1996). Introduction to quantitative genetics (4^{th} edn). Trends in Genetics, 12, 280.

FAO (2010). The state of the world fisheries and aquaculture. Food and Agriculture Organization of the United Nations.

Feely, R.A., Sabine, C.L., Lee, K., Berelson, W., Kleypas, J., Fabry, V.J., Millero, F.J. (2004). Impact of anthropogenic CO_2 on the $CaCO_3$ system in oceans. Science, 305, 362-66

Feely, R.A., Okazaki, R.R., Cai, W.J., Bednaršek, N., Alin, S.R., Byrne, R.H., & Fassbender, A. (2018). The combined effects of acidification and hypoxia on pH and aragonite saturation in the coastal waters of the California current ecosystem and the northern Gulf of Mexico. Continental Shelf Research, 152, 50-60.

Ferrari, S., Horri, K., Allal, F., Vergnet, A., Benhaim, D., Vandeputte, M., Chatain, B., & Bégout, M.L. (2016). Heritability of boldness and hypoxia avoidance in European seabass, *Dicentrarchus labrax*. PLoS ONE, 11, e0168506.

Froehlich, H.E., Runge, C.A., Gentry, R.R., Gaines, S.D., Halpern, B.S. (2018). Comparative terrestrial feed and land use of an aquaculture-dominant world. Proceedings of the National Academy of Sciences, 115, 5295-5300.

Gallardo-Escárate, C., & Del Río-Portilla, M.Á. (2007). Karyotype composition in three California abalones and their relationship with genome size. Journal of Shellfish Research, 26, 825-832.

Garibalid, L. (1996). List of animal species used in aquaculture. FAO Fisheries Circular, 914.

Gazeau, F., Paker, L.M., Corneau, S., Gattuso, J.P., O'Connor, W.A., Martin, S., Pörtner, H.O., & Ross, P.M. (2013) Impacts of ocean acidification on marine shelled molluscs. Marine Biology, 160, 2207-2245.

Gentry, R.R., Froehlich, H.E., Grimm, D., Kareiva, P., Parke, M., Rust, M., Gaines, S.D., Halpern, & B.S. (2017). Mapping the global potential for marine aquaculture. Nature Ecology & Evolution, 1, 1317-1323.

Gossner, H.M. (2018) Quantifying sensitivity and adaptive capacity of shellfish in the northern California Current Ecosystem in increasing prevalence of ocean acidification and hypoxia. Master's thesis, Oregon State University.

Griffith, A.W., & Gobler, C.J. (2017). Transgenerational exposure of north Atlantic bivalves to ocean acidification renders offspring more vulnerable to low pH and additional stressors. Scientific Reports, 7, 11394.

Gruber, N., Hauri, C., Lachkar, Z., Loher, D., Frölicher, T., & Plattner, G. (2012). Rapid progression of ocean acidification in the California Current System. Science, 337, 220-23.

Guppy, M., & Withers, P. (1999). Metabolic depression in animals: physiological perspectives and biochemical generalizations. Biological Reviews of the Cambridge Philosophical Society, 74, S00063233198005258.

Harris, K.E., DeGrandpre, M.D., Hales, B. (2013). Aragonite saturation state dynamics in a coastal upwelling zone. Geophysical Research Letters, 40, 2720-25.

Hofmann, G.E., Barry, J.P., Edmunds, P.J., Gates, R.D., Hutchins, D.A., Klinger, T., & Sewell, & M.A. (2010). The effect of ocean acidification on calcifying organisms in marine ecosystems: An organism-to-ecosystem perspective. Annual Review of Ecology, Evolution, and Systematics, 41, 127-47.

Hu, Z., & Yang, R.C. (2014). Marker-based estimation of genetic parameters in genomics. PLoS ONE, 9, e102715.

Kim, T.W., Barry, J.P., & Micheli, F. (2013). The effects of intermittent exposure to low-pH and low-oxygen conditions on survival and growth of juvenile red abalone. Biogeosciences, 10, 7255-7262.

Kroeker, K.J., Kordas, R.L., Crim, R.N., & Singh, G.G. (2010). Meta-analysis reveals negative yet variable effects of ocean acidification on marine organisms. Ecology Letters, 13, 1419-34.

Kroeker, K.J., Kordas, R.L., Crim, R., Hendriks, I.E., Ramajo, L., Singh, G.S., Duarte, C.M., & Gattuso, J.P. (2013) Impacts of ocean acidification on marine organisms: quantifying sensitivities and interaction with warming. Global change biology, 19, 1884-96.

Kurihara, H. (2008). Effects of CO_2-driven ocean acidification on the early developmental stages of invertebrates. Marine Ecology Progress Series, 373, 275-84.

Langmead, B., Trapnell, C., Pop, M., & Salzberg, S.L. (2009). Ultrafast and memory-efficient alignment of short DNA sequences to the human genome. Genome Biology, 10, 25.

Leighton, D. (2000). The biology and culture of the California abalones. Dorrance Publishing Company.

Li, C.C., Weeks, D.E., & Chakravarti, A. (1993). Similarity of DNA fingerprints due to chance and relatedness. Human Heredity, 43, 45-52.

Li, H., & Durbin, R. (2010). Fast and accurate long=read alignment with Burrows-Wheeler transform. Bioinformatics, 26, 589-595.

Lynch, M., & Ritland, K. (1999). Estimation of pairwise relatedness with molecular markers. Genetics, 152, 1753-1766.

Masonbrink, R.E., Purcell, C.M., Boles, S.E., Whitehead, A., Hyde, J.R., Seetharam, A.S., & Severin, A.J. (2019). An annotated genome for *Haliotis rufescens* (red abalone) and resequenced green, pink, pinto, black, and white abalone species. Genome Biology and Evolution, 11,431-8.

Milligan, B.G. (2003). Maximum-likelihood estimation of relatedness. Genetics, 163, 1153-1167.

Mousseau, T.A., & Roff, D.A. (1987). Natural selection and the heritability of fitness components. Heredity, 59, 181-97.

Orr, J.C., Fabry, V.J., Aumont, O., Bopp, L., Doney, S.C., Feely, R.A., Gnanadesikan, A., Gruber, N., Ishida, A., Joos, F. et al. (2005). Anthropogenic ocean acidification over the twenty-first century and its impact on calcifying organisms. Nature, 437, 681-86.

Park, J.H., Gail, M.H, Weinberg, C.R., Carroll, R.J., Chung, C.C., Wang, Z., Chanock, S.J., Fraumeni, J.F., & Chatterjee, N. (2011). Distribution of allele frequencies and effect sizes and their interrelationships for common genetic susceptibility variants. Proceedings of the National Academy of Sciences, 108, 18026-18031.

Pendleton, L.H., & Rooke, J. (2006). Understanding the potential economic impact of marine recreational fishing: California. Environment, 1-15.

Penn, J.L, Deutsch, C., (Payne, J.L, & Sperling, E.A. (2018). Temperature-dependent hypoxia explains biogeography and severity of end-Permian marine mass extinction. Science, 362, eaat1327.

Pew, J., Muir, P.H., Wang, J., & Frasier, T.R. (2015). Related: An R package for analyzing pairwise relatedness from codominant molecular markers. Molecular Ecology Resources, 15, 557-561.

Pörtner, H.O., & Farrell, A.P. (2008). Physiology and climate change. Science, 322, 690-692.

Price, A.L., Zaitlen, N.A., Reich, D., & Patterson, N. (2010). New approaches to population stratification in genome-wide association studies. Nature Reviews Genetics, 11, 459-63.

Queller, D.C., & Goodnight, K.F. (1989). Estimating relatedness using genetic markers. Evolution, 43, 258-75.

Reid, J., Rogers-Bennett, L, Vasquez, F., Pace, M., Catton, C.A., Kashiwada, J.V, & Taniguchi, I.K. (2015) The economic value of the recreational red abalone fishery in northern California. California Fish and Game, 102, 119-130.

Ritland, K. (1996). Estimators for pairwise relatedness and individual inbreeding coefficients. Genetics Research, 67, 175-185.

Rogers-Bennett, L. (2000). Serial depletion and the collapse of the California abalone (*Haliotis* spp.) fisher. Workshop on rebuilding Abalone stocks in British Columbia, 200, 11-24.

Rogers-Bennett, L., Allen, B., & David, G. (2004). Measuring abalone (*Haliotis* spp.) recruitment in California to examine recruitment overfishing and recovery criteria. Journal of Shellfish Research, 23, 1201-1207.

Somero, G.B., Beers, J.M., Chan, F., Hill, T.M., Klinger, T., & Litvin, S.Y. (2016) What changes in the carbonate system, oxygen, and temperature portend for the northeastern Pacific Ocean: A physiological perspective. BioScience 66, 14-26.

Speed, D., Hemani, G., Johnson, M.R., & Balding, D.J. (2012). Improved heritability estimation from genome-wide SNPs. The American Journal of Human Genetics, 91, 1011-1020.

Speed, D., Cai, N., Johnson, M.R., Nejentsev, S., & Balding, D.J. (2017). Reevaluation of SNP heritability in complex human traits. Nature Genetics, 49, 986-992.

Swezey, D.S., Boles, S.E., Aquilino, K.M., Stott, H.K, Bush, D., Whitehead, A., Rogers-Bennett, L., Hill, T.M., & Sanford, E. (2020). Evolved differences in energy metabolism and growth dictate the impacts of ocean acidification on abalone aquaculture. Proceedings of the National Academy of Sciences. 117, 26513-26519.

Thomas, S.C. (2005). The estimation of genetic relationships using molecular markers and their efficiency in estimating heritability in natural populations. Philosophical Transactions of the Royal Society B: Biological Sciences, 360, 1457-1467.

Utting, S., & Spencer, B. (1997). The hatchery culture of bivalve mollusc larvae and juveniles. Ministry of Agriculture, Fisheries and Food, Directorate of Fisheries Research.

Visscher, P.M., Hemani, G., VInkhuyzen, A.A., Chen, G.B., Lee, S.H., Wray, N.R., Goddard, M.E., & Yang, J. (2014). Statistical Power to detect genetic (co)variance of complex traits using SNP data in unrelated samples. PLoS Genetics, 10, e1004269.

Wang, J. (2002). An estimator for pairwise relatedness using molecular markers. Genetics, 160, 1203-1215.

Wang, J. (2007). Triadic IBD coefficients and applications to estimating pairwise relatedness. Genetical Research, 89, 135-153.

Yang, J., Benyamin, B., McEvoy, B.P., Gordon, S., Henders, A.K., Nyholt, D.R., Madden, P.A., Heath, A.C., Martin, N.G., Montgomery, G.W., & Goddard, M.E. (2010). Common SNPs explain a large proportion of the heritability for human height. Nature Genetics, 42, 565-569.

Yang, J., Bakshi, A., Zhu, Z., Hemani, G., Vinkhuyzen, A.A., Lee, S.H., Robinson, M.R., Perry, J.R., Nolte, I.M., va Vliet-Astaptchouk, J.V., & Sniedger, H. (2015). Genetic variance estimation with imputed variants finds negligible missing heritability for human height and body mass index. Nature Genetics, 47, 1114-1120.

Zhang, J., Cao, F., Liu, J., Yuan, R., & Hu, Z. (2017). Genetic parameters for growth and hypoxic tolerance traits in Pacific white shrimp *Litopenaeus vannamei* at different ages. North American Journal of Aquaculture, 79, 75-83.

Zippay, M.L, & Hofmann, G.E. (2010). Effect of pH on gene expression and thermal tolerance of early life history stages of red abalone (*Haliotis rufescens*). Journal of Shellfish Research, 29, 429-439.

FIGURES AND TABLES

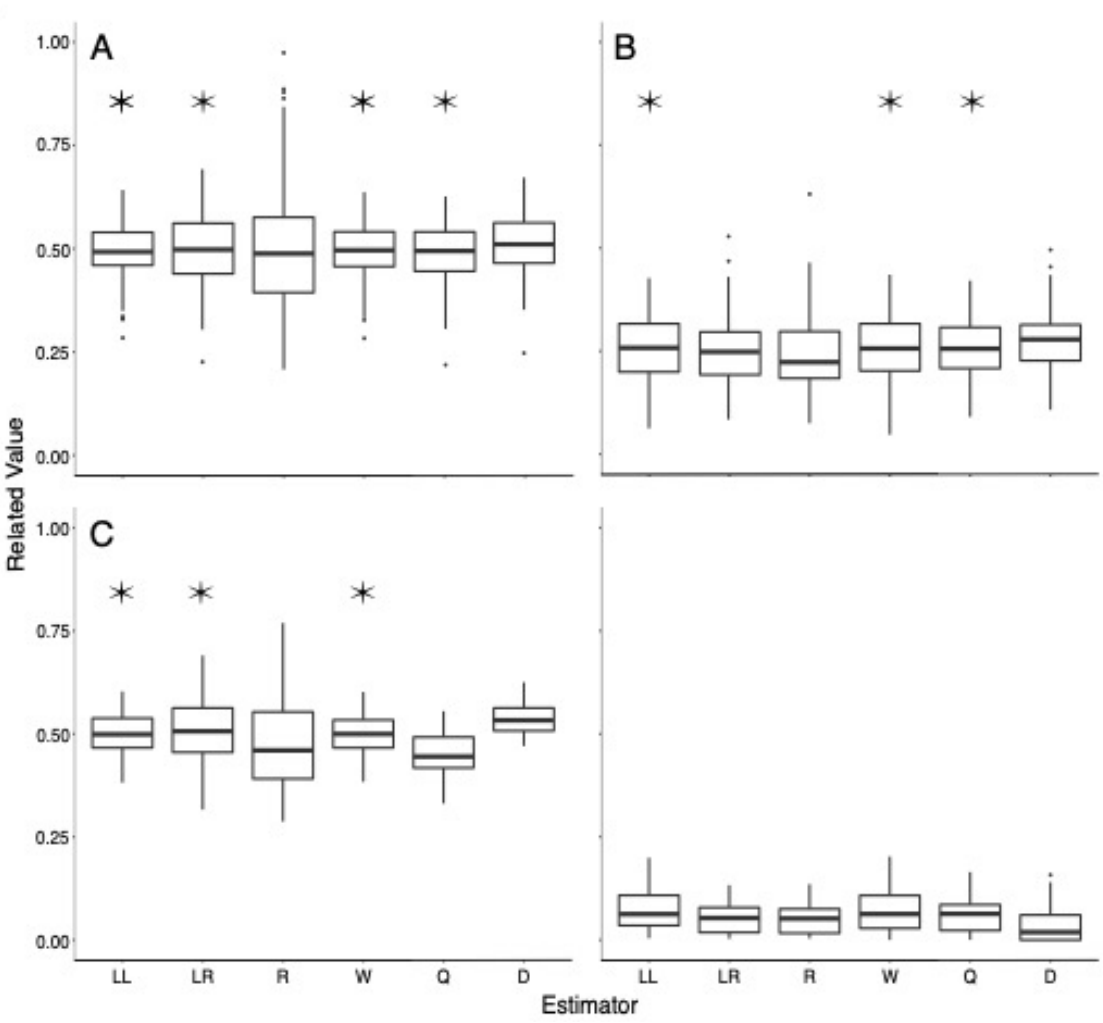

Figure 4.1: Box plots comparing relatedness estimators (LL) Lynch & Li, (LR) Lynch & Ritland, (R) Ritland, (W) Wang, (Q) Queller, and (D) Dyad, showing related values simulated for A (full), B (half), C (Parent-offspring), and D (unrelated). Best performing estimators were selected based on the difference of the relatedness estimation from the true relatedness group value (full = 0.50, half = 0.25, parent-offspring = 0.50, and unrelated = 0.00), in which relates estimates falling within 0.01 are indicated with an asterisk.

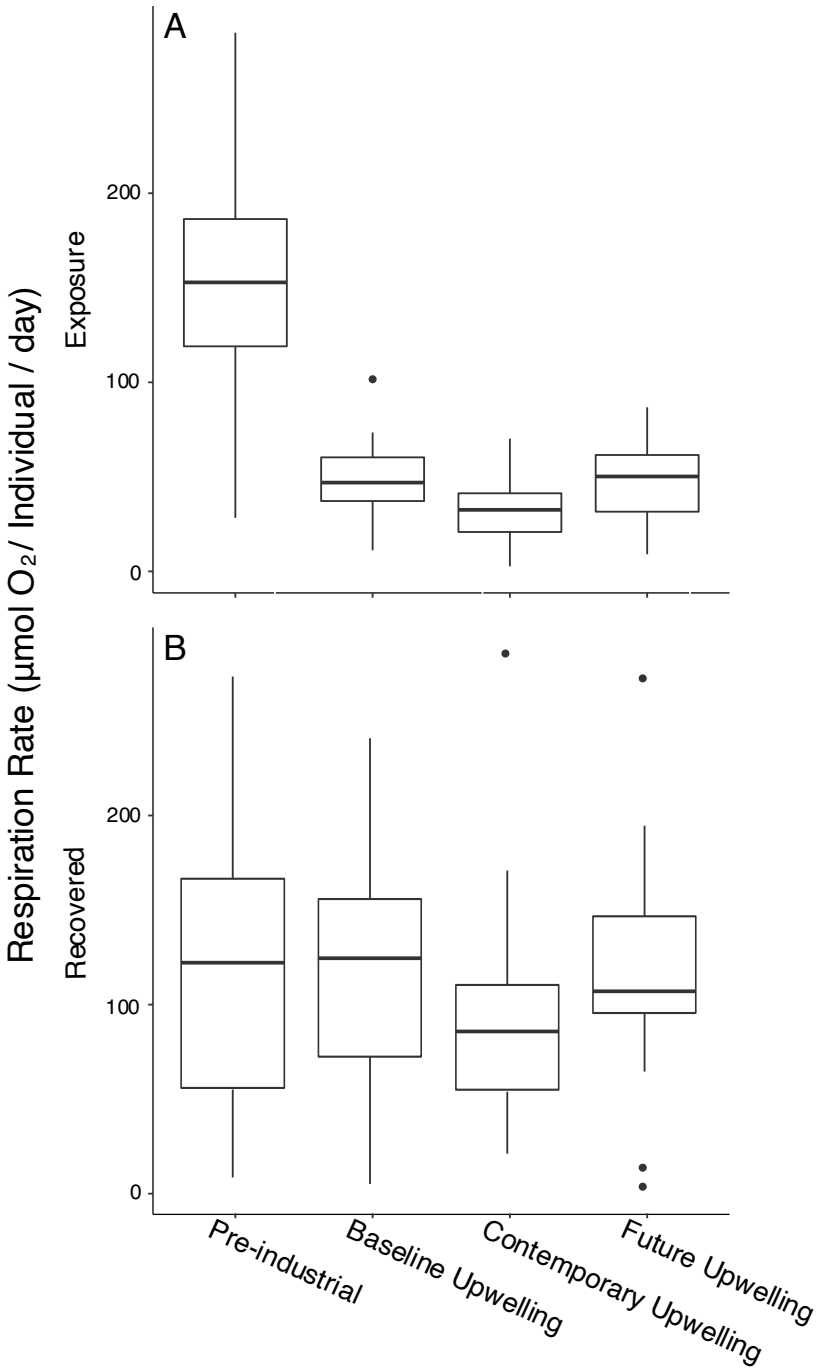

Figure 4.2: Mean respiration rates with 95% confidence intervals for each OAH treatment in the (A) exposure and (B) recovered experiment.

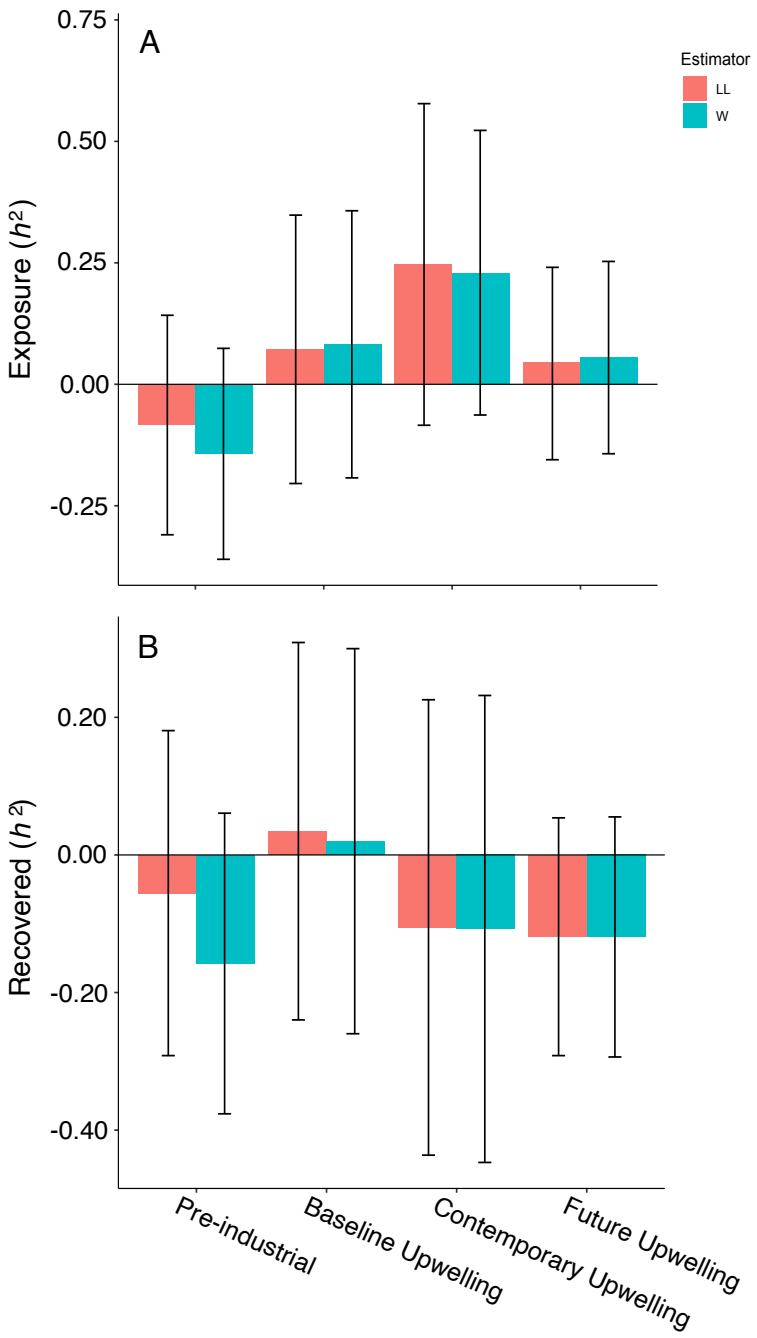

Figure 4.3: Heritability (h^2) estimates (± standard error) for each pH treatment estimated by Lynch & Li (LL) and Wang (W) in the (A) exposure and (B) recovered experiments.

Table 4.1: Target values for OAH treatments that were back calculated from the relationship between dissolved oxygen (DO) and dissolved inorganic carbon (DIC) with anthropogenic carbon load (Feely et al. 2018, Chan et al. 2017, Gossner 2018), with temperature 10°C, salinity 33.5 psu, and total alkalinity of 2250 μmol/kgSW.

Treatment	pH	pCO_2 (μatm)	TCO2 (μmol/kgSW)	O2 (μmol/L)	ΩCa	ΩAr
Pre-industrial	8.17	285	2036	297	3.60	2.27
Baseline	7.59	1238	2240	75	1.08	0.68
Contemporary	7.50	1508	2264	40	0.90	0.57
Distant Future	7.27	2628	2540	20	0.54	0.34

Table 4.2: Results from 2-way ANOVA for OAH treatment and date of experiment on respiration rates in exposure and recovered experiment.

Experiment	Term	DF	F-value	P-value
Exposure	Treatment	3	36.613	8.25e-15
	Date	1	0.332	0.566
	Treatment:Date	3	0.378	0.769
Recovered	Treatment	3	0.199	0.897
	Date	1	0.301	0.501
	Treatment:Date	3	0.22	0.882

Table 4.3: Restricted maximum likelihood model (REML) used to estimate heritability of desired respiration trait for *H. rufescens* during exposure to OAH and recovered OAH treatment within each treatment: pre-industrial, baseline upwelling, contemporary upwelling, and future upwelling. All models had respiration rate as the output (y) with PC1 calculated from principal component analyses (PCA) of allele frequencies as a fixed effect (Resp rate ~ PC). The number of individuals is shown before removal of samples that had high confidence intervals in relatedness estimates and after.

pH treatment	Exposure	Recovered	N before	N after
Pre-industrial	Pre.Exp ~ PC	Pre.Rec ~ PC	28	27
Baseline upwelling	Base.Exp ~PC	Base.Rec ~ PC	29	26
Contemporary upwelling	Cont.Exp ~ PC	Cont.Rec ~ PC	28	25
Future upwelling	Fut.Exp ~ PC	Fut.Rec ~ PC	25	24
		Total	**110**	**102**

Table 4.4: Heritability estimated (±standard error) from Lynch & Li (LL) and Wang (W) relatedness estimators. Different methods were used to estimating heritability, including before data manipulation (No adjustment), after removing samples with high confidence intervals (High CI removal), and removing loci with MAF less than 0.05 (MAF < 0.05 removed). Heritability estimates are separated based on models seen in Table 4.3. NAs indicate when estimators that were not able to estimate h^2 due to non-positive definite relatedness matrices.

Method	Experiment	Model	LL	W
No adjustment	Exposure	Pre.Exp	NA	NA
		Base.Exp	0.016 ± 0.261	0.038 ± 0.263
		Cont.Exp	NA	NA
		Fut.Exp	-0.053 ± 0.186	-0.049 ± 0.188
	Recovered	Pre.Rec	NA	NA
		Base.Rec	0.100 ± 0.261	0.093 ± 0.261
		Cont.Rec	NA	NA
		Future.Rec	-0.115 ± 0.168	-0.114 ± 0.170
High CI removal	Exposure	Pre.Exp	NA	NA
		Base.Exp	0.070 ± 0.280	0.090 ± 0.279
		Cont.Exp	0.283 ± 0.192	0.279 ± 0.194
		Fut.Exp	0.052 ± 0.193	0.043 ± 0.200
	Recovered	Pre.Rec	NA	NA
		Base.Rec	0.032 ± 0.278	0.020 ± 0.280
		Cont.Rec	NA	NA
		Future.Rec	-0.115 ± 0.174	-0.120 ± 0.166
MAF < 0.05 removal	Exposure	Pre.Exp	-0.083 ± 0.226	-0.143 ± 0.217
		Base.Exp	0.072 ± 0.276	0.082 ± 0.275
		Cont.Exp	0.247 ± 0.331	0.230 ± 0.293
		Fut.Exp	0.051 ± 0.198	0.055 ± 0.198
	Recovered	Pre.Rec	-0.056 ± 0.236	-0.158 ± 0.219
		Base.Rec	0.035 ± 0.274	0.020 ± 0.280
		Cont.Rec	-0.105 ± 0.331	-0.108 ± 0.339
		Future.Rec	-0.119 ± 0.173	-0.119 ± 0.175

CHAPTER 5 – CONCLUSIONS

General Conclusions

In this dissertation, we investigated how coastal marine invertebrates are impacted by environmental stresses and assessed their adaptive potential to stressful conditions associated with climate change. Increasing carbon emissions has resulted in shifts in marine systems, including increasing temperatures, acidified conditions, and hypoxic zones. These shifts in marine systems have created stressful conditions that are predicted to increase in severity of the next few decades. The impacts of thermal, ocean acidification (OA), and hypoxic stress has been seen in a variety of taxa, leading to concerns how these organisms will adapt as conditions worsen. Although the biological impacts of climate stressors have been well studied in a few taxa, gaps in our knowledge concerning several local species and specific life stages persist. In addition, the combined effects of OA and hypoxia (OAH) has scarcely been examined despite its high prevalence during upwelling seasons along the California Current Large Marine Ecosystem (CCLME). Using a variety of genomic techniques, we examined the current and future impacts of climate change on three economically or ecologically species of concern.

Impacts of climate stressors

Population declines due to Sea Star Wasting Syndrome (SSWS) were observed along the North American western coastline. Among sea stars decimated by SSWS, *Pisaster ochraceus*, were impacted with little evidence for tolerance. We measured little genetic variation associated with disease status between wasting and apparently normal individuals, suggesting that current populations lack genetic the basis to tolerate SSWS. Marine diseases such as SSWS are increasing due to rising sea water temperatures (Harvell et al. 2002, 2004). Predictions to why marine diseases are more prevalent relate to either the pathogens being more successful in warmer environments, host susceptibility under thermal stress, or both (Harvell et al. 2004). In either case, our study suggests that *P. ochraceus* lacks genetic composition to tolerate potential pathogen(s). Little genetic makeup for resilience to SSWS leaves *P. ochraceus* vulnerable to SSWS, especially when sea water temperatures become stressful. We did not see any similarity between genomic regions with that of previous studies conducted in California (Schiebelhut et al. 2018). Lack of similar genomic regions with previous studies suggests that sampling individuals across several geographic regions are needed.

We observed negative impacts of ocean acidification in *Crassostrea gigas* and *Haliotis rufescens*. Metamorphosis was lower in *C. gigas* under high pCO_2 conditions, while *H. rufescens* had reduced respiration rates when high pCO_2 was coupled with decreased oxygen concentrations. The threshold of metabolic processes tolerance to OAH has already been reached in *H. rufescens* (Gossner 2018), leaving them vulnerable during upwelling events. Together, these studies reiterate the impacts

of OA on calcifying organisms. However, we did not see an impact of pCO_2 condition for settlement rates or on gene expression in attached spat in *C. gigas*. Differences in metamorphosis and settlement rates underscores how life stages have dissimilar responses to OA and should be examined.

Adaptive potential

Genetic variation within a population, whether due to novel mutations or standing variation, is one necessary prerequisite for natural selection to result in adaptive change (Bitter et al. 2019). Another prerequisite is that some genetic variation is associated with nonrandom differences in fitness. In *P. ochraceus*, we found little genetic variation associated with disease status. No difference between the genetic makeup of wasting and apparently normal *P. ochraceus* suggests that this species is susceptible and lacks the genetic makeup aiding in tolerance to SSWS. Meaning there is little to no standing genetic variation to be selected upon during a SSWS outbreak. Results from our study suggests that *P. ochraceus* has little potential to adapt to future SSWS outbreaks. This is concerning as SSWS and marine diseases are correlated to rising sea water temperatures and are likely to occur in higher frequencies.

We do see some hope for *C. gigas* adaptive potential to OA. Proportion of attached spat in *C. gigas* does not appear to be impacted by OA, suggesting this stage in development are more resilient to these conditions. Earlier life stages such as metamorphosis are impacted and remain a concern, but adaptive potential of these stages was not examined in this dissertation. Having said that, knowing that not every life stages is negatively impacted by OA is encouraging as it indicates there are some individuals who will persist in acidified conditions. Further, the potential for carry over effects (Hettinger et al. 2012) to offspring may drive adaptation of the species (Takahashi 1997).

The adaptive potential of *H. rufescens* to OA was also seen when coupled with deoxygenation. Narrow-sense heritability measures the ratio of additive genetic variation to phenotypic variation for a given trait. Traits with higher heritability estimates are readily influenced by selection, which makes h^2 a common parameter for assessing the adaptive potential of a species. In *H. rufescens*, we find that metabolic processes are heritable in future upwelling conditions. However, heritability estimates power is limited by population size especially when individuals are unrelated as we observed from our data set. When utilizing heritability as a parameter for assessing adaptive potential, we suggest using larger sample sizes in related amongst unrelated individuals are used.

Conclusion

The negative impacts of environmental stressors relating to climate change are numerous. In this dissertation we see these impacts result in increased susceptibility to disease, delay specific life stages during development, and depleting metabolic processes. There are still gaps in the literature about how modern-day climate change is impacting a variety of taxa and life stages, along with how

projected conditions will impact these taxa. For instance, there is still uncertainty about the severity of SSWS outbreaks in *P. ochraceus* as sea level temperatures continue to rise. With marine diseases becoming more prevalent, preemptive measures need to be taken on how to effectively respond to disease outbreaks. Establishing a baseline of health of coastal organisms could be informative for future studies when outbreaks occur (Gravem et al. 2021). Such measures would be beneficial for other stressors such as following upwelling events as conditions increase in severity. There are still many taxa and life stages in which we know very little about the impacts of climate change associated stressors, such as OA and OAH. *C. gigas* serves as a great model organism for understanding physiological impacts of these stressors because of its commercial importance and clear phenotypic relevance (calcification), but more work is needed on how upwelling conditions impact the settlement process. Lastly, there are several understudied calcifying organisms that are economically and ecologically important in which we have little to no baseline understanding of how climate stressors impact these organisms. We discuss the advantages and limitations of assessing vulnerability and adaptive potential of understudied organisms to OAH through estimating heritability of respiration, but other stresses such as thermal stress and salinity should also be considered.

References

Bitter, M.C., Kapsenberg, L., Gattuso, J.P., & Pfister, C.A. (2019). Standing genetic variation fuels rapid adaptation to ocean acidification. Nature Communications, 10, 5821.

Gravem, S. A., Heady, W. N., Saccomanno, V. R., Alvastad, K. F., Gehman, A. L. M., Frierson, T. N., & Hamilton, S. L. (2021). Sunflower Sea Star (*Pycnopodia helianthoides*). IUCN Red List of Threatened Species.

Gossner, H.M. (2018) Quantifying sensitivity and adaptive capacity of shellfish in the northern California Current Ecosystem in increasing prevalence of ocean acidification and hypoxia. Master's thesis, Oregon State University.

Harvell, D. C., Mitchell, C. E., Ward, J. R., Altizer, S., Dobson, A. P., Ostfel, R. S., & Samuel, M. D. (2002). Climate warming and disease risks for terrestrial and marine biota. Science, 296(5576), 2158–2162.

Harvell, D., Aronson, R., Baron, N., Connell, J., Dobson, A., Ellner, S., Gerber, L., Kim, K., Kuris, A., McCallum, H., Lafferty, K., McKay, B., Porter, J., Pascual, M., Smith, G., Sutherland, K., & Ward, J. (2004). The rising tide of ocean diseases: unsolved problems and research priorities. Frontiers in Ecology and the Environment, 2(7), 375–382.

Hettinger, A., Sanford. E, Hill, T.M., Russell, A.D., Sato, K.N., Hoey, J., Forsch, M., Page, H.N., & Gaylord, B. (2012). Persistent carry-over effects of planktonic exposure to ocean acidification in the Olympia oyster. Ecological Society of America, 93, 2738-3768.

Schiebelhut, L. M., Puritz, J. B., & Dawson M. N. (2018). Decimation by sea star wasting disease and rapid genetic change in a keystone species, *Pisaster ochraceus*. Proceedings of the National Academy of Sciences, 115(27), 7069–7074.

Takahashi, F. (1997). Generation carryover of a fraction of population members as an animal adaptation to unstable environmental conditions. Research on Population Ecology, 18, 235-242.

APPENDICES

APPENDIX A: Little evidence for genetic variation associated with susceptibility to sea star wasting syndrome in the keystone species *Pisaster ochraceus*

Andrea R. Burton, Sarah Gravem, and Felipe Barreto

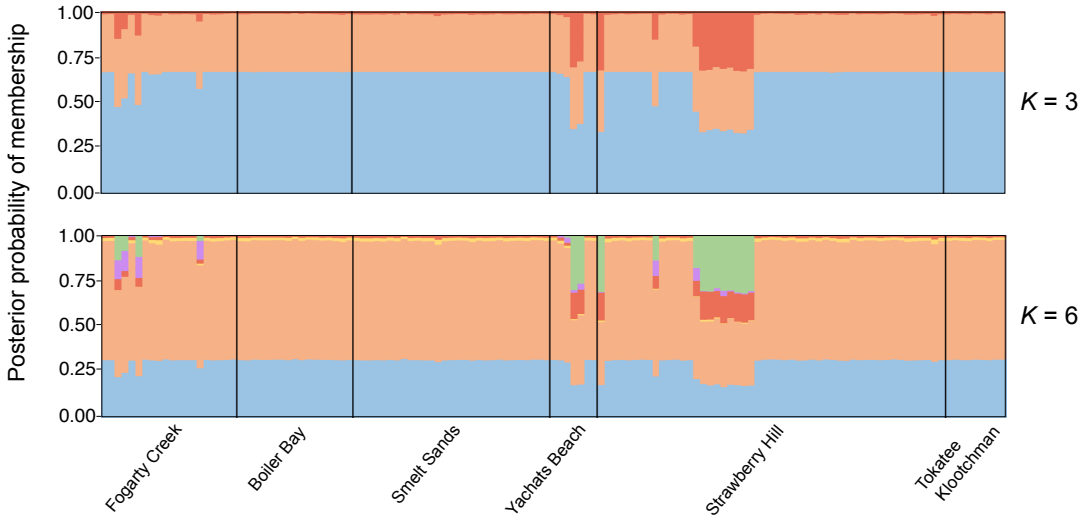

Figure S2.1. Population genetic clustering of *Pisaster ochraceus* across six sites in central Oregon. Vertical bars (y-axis) show the probability of membership of individuals (n = 133, x-axis) across 3 or 6 potential clusters, as quantified by STRUCTURE.

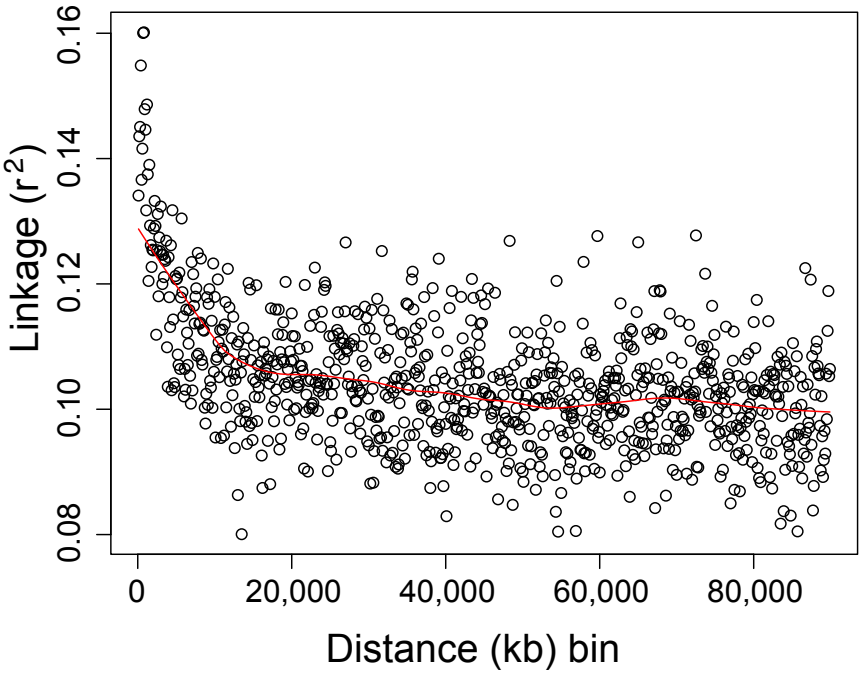

Figure S2.2: Decay of linkage disequilibrium. Plotted are average r^2 values for SNP-pair distancesin bins of 100 bp increments. Red line is a lowess smooth line, calculated in R.

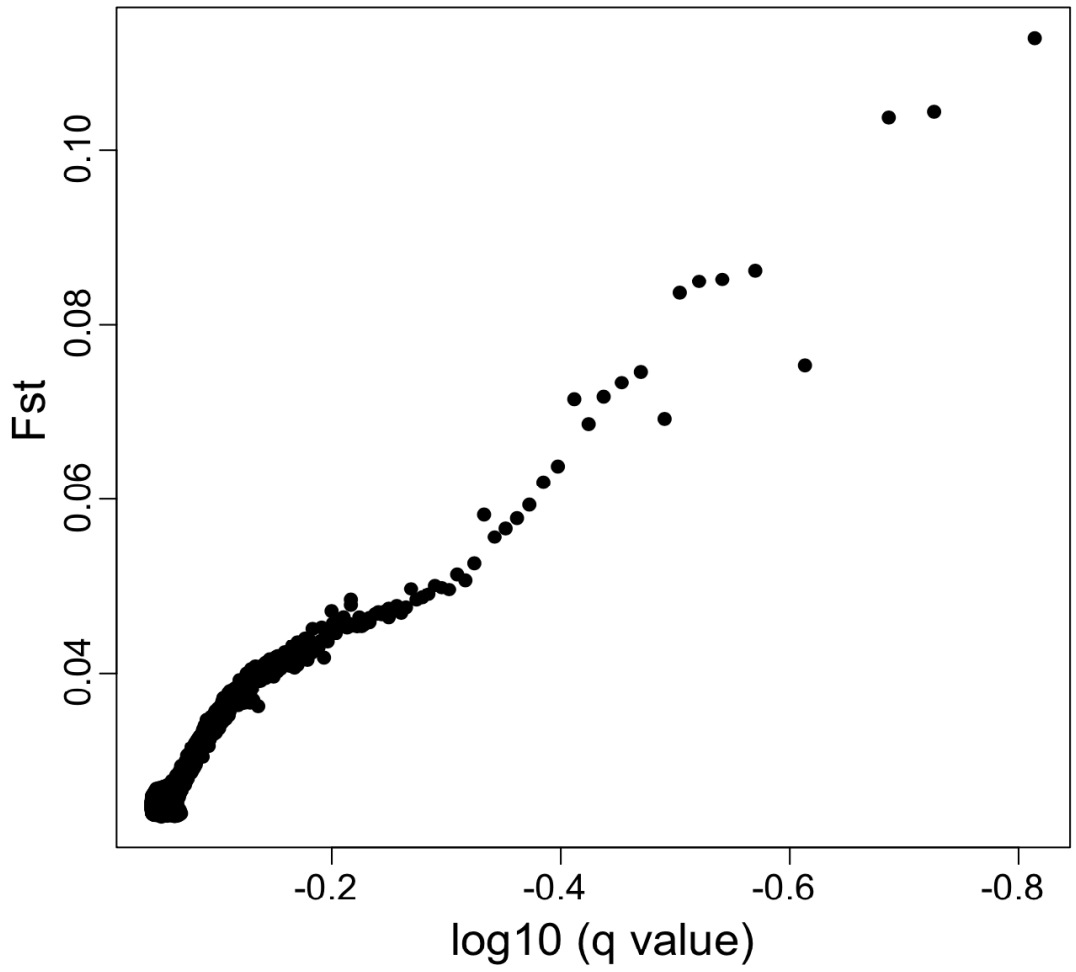

Figure S2.3. Results from Bayescan test of outliers for differentiation between wasting and apparently normal *Pisaster ochraceus*. No locus was detected as outlier.

Tables S2.1, S2.2, and S2.4 can be found from the published journal Molecular Ecology (https://doi.org/10.1111/mec.16212).

Table S2.1. List and metadata for all sea stars (*Pisaster ochraceus*) from which tissue sample was collected from six sites: Boiler Bay (BB), Fogarty Creek (FC), Smelt Sands (SS), Strawberry Hill (SH), and Tokatee Klootchman (TK). Link to document (https://onlinelibrary.wiley.com/action/downloadSupplement?doi=10.1111%2Fmec.16212&file=mec16212-sup-0002-TableS1.xlsx).

Table S2.2. Summary of final SNP loci identified post filtering and used for analyses of genetic variation. Link to document (https://onlinelibrary.wiley.com/action/downloadSupplement?doi=10.1111%2Fmec.16212&file=mec16212-sup-0003-TableS2.xlsx).

Table S2.4. BLASTP annotations of protein-coding genes located within 30 kb from the DAPC outlier SNPs. Shown are best-hit results from BLASTP searches against the Uniprot/Swissprot and against NCBI's 'nr' databases. Details about the SNPs are found on Table S3, and about loci are found on Table S2. Link to document (https://onlinelibrary.wiley.com/action/downloadSupplement?doi=10.1111%2Fmec.16212&file=mec16212-sup-0005-TableS4.xlsx).

Table S2.3. SNP loci most discriminant between apparently normal and wasting sea stars in a Discriminant Analysis of Principal Components. F_{st} estimated with GPAT (Shapiro et al., 2013) and allele frequencies and heterozygosities estimated with Stacks (Catchen, Hohenlohe, Bassham, Amores, & Cresko, 2013). Locus ID were assigned in our study (full list found on Table S2.1).

Locus ID	Chr.	Scaffold	Position	Loading from DAPC	F_{st} (WC)	P-value (F_{st})	Allele Freq (wasting)	Allele Freq (apparently normal)	Allele frequency difference	Number genotyped (wasting)	Number genotyped (apparently normal)	Heterozygosity (Symptomatic)	Heterozygosity (Asymptomatic)
10976	2	Sc28pcJ_502_HRSCAF_549	13304634	0.00022529	-0.012	4.634E-01	0.500	0.589	0.089	26	45	0.15	0.07
11591	2	Sc28pcJ_502_HRSCAF_549	16781924	0.00025183	-0.001	2.981E-01	0.650	0.579	0.071	50	63	0.42	0.30
47575	3	Sc28pcJ_1465_HRSCAF_1564	7659909	0.00020306	-0.009	9.460E-01	0.656	0.636	0.020	48	66	0.35	0.48
49004	3	Sc28pcJ_1465_HRSCAF_1564	14922132	0.00030496	-0.012	8.318E-01	0.692	0.678	0.014	52	59	0.27	0.31
49005	3	Sc28pcJ_1465_HRSCAF_1564	14922143	0.00023993	-0.007	6.361E-01	0.759	0.722	0.037	54	63	0.33	0.27
49366	3	Sc28pcJ_1465_HRSCAF_1564	17135794	0.00020361	0.040	1.239E-02	0.628	0.466	0.162	47	59	0.32	0.42
61467	7	Sc28pcJ_1840_HRSCAF_2023	6392287	0.00020981	0.071	1.862E-02	0.681	0.464	0.217	47	58	0.21	0.40
14207	8	Sc28pcJ_520_HRSCAF_571	5198014	0.00020396	0.007	1.599E-01	0.653	0.755	0.102	36	47	0.19	0.23
16394	8	Sc28pcJ_520_HRSCAF_571	17327004	0.00024693	-0.009	3.595E-01	0.650	0.600	0.050	43	49	0.23	0.36
16489	8	Sc28pcJ_520_HRSCAF_571	17814546	0.00022315	0.063	9.760E-04	0.670	0.477	0.193	47	64	0.40	0.36
41194	10	Sc28pcJ_1131_HRSCAF_1221	14619986	0.00025868	0.031	2.905E-02	0.467	0.620	0.153	46	50	0.28	0.28
30607	11	Sc28pcJ_709_HRSCAF_769	7983511	0.00025151	0.114	5.005E-04	0.594	0.825	0.231	53	63	0.28	0.25
31883	11	Sc28pcJ_709_HRSCAF_769	15433527	0.00021459	0.053	2.726E-03	0.727	0.868	0.141	55	68	0.36	0.26
69275	12	Sc28pcJ_1844_HRSCAF_2043	386791	0.00020352	0.003	3.171E-01	0.577	0.656	0.079	52	61	0.54	0.33
33938	13	Sc28pcJ_910_HRSCAF_986	7865639	0.00026851	0.109	1.250E-03	0.670	0.417	0.253	44	42	0.34	0.40
36625	14	Sc28pcJ_1028_HRSCAF_1112	5984741	0.00022481	0.027	1.653E-02	0.563	0.695	0.132	48	59	0.38	0.47
36723	14	Sc28pcJ_1028_HRSCAF_1112	6558194	0.00021546	0.004	4.959E-01	0.571	0.650	0.079	49	70	0.53	0.39
58305	20	Sc28pcJ_1837_HRSCAF_1971	1865398	0.00024904	0.006	1.837E-01	0.636	0.716	0.080	55	67	0.40	0.45

Table S2.5. Outlier SNP ranges from DAPC analyses compared from Schiebelhut et al. (2018) to ours, with distances between SNP ranges indicated.

Schiebelhut et al. 2018				This study				Distance
Locus ID	Scaffold	Chr.	Range (bp)	Locus ID	Scaffold	Chr.	Range (bP)	(bp)
Loc0087_Hap1	Sc28pcJ_649_HRSCAF_705	1	30859536-30860334					
Loc0551_Hap1	Sc28pcJ_502_HRSCAF_549	2	2274042-2274428					
Loc1088_Hap2	Sc28pcJ_502_HRSCAF_549	2	17909795-17910557	11591	Sc28pcJ_502_HRSCAF_549	2	16781924-16796924	1112871
Loc0138_Hap1	Sc28pcJ_502_HRSCAF_549	2	7266434-7267119					
Loc0855_Hap2	Sc28pcJ_502_HRSCAF_549	2	8152069-8152962					
Loc0852_Hap2	Sc28pcJ_502_HRSCAF_549	2	15241226-15241779	10976	Sc28pcJ_502_HRSCAF_549	2	13304634-13319634	1921592
Loc0930_Hap1	Sc28pcJ_502_HRSCAF_549	2	21449465-21450138					
Loc0178_Hap1	Sc28pcJ_502_HRSCAF_549	2	20421495-20422276					
Loc0953_Hap2	Sc28pcJ_502_HRSCAF_549	2	22193213-22193738					
Loc0225_Hap4	Sc28pcJ_1465_HRSCAF_1564	3	19439045-19439467					
Loc1024_Hap2	Sc28pcJ_1465_HRSCAF_1564	3	12874215-12874773					
Loc0617_Hap1	Sc28pcJ_1465_HRSCAF_1564	3	14649056-14649495	49005	Sc28pcJ_1465_HRSCAF_1564	3	14922143-14937143	257648
				49004	Sc28pcJ_1465_HRSCAF_1564	3	14922132-14937132	257637
Loc0738_Hap1	Sc28pcJ_1465_HRSCAF_1564	3	15681560-15681919					
Loc0824_Hap1	Sc28pcJ_1465_HRSCAF_1564	3	3416235-3416997					
Loc0799_Hap2	Sc28pcJ_1465_HRSCAF_1564	3	16235057-16235896	49366	Sc28pcJ_1465_HRSCAF_1564	3	17135794-17150794	884898
Loc1120_Hap1	Sc28pcJ_1465_HRSCAF_1564	3	6077067-6078049	47575	Sc28pcJ_1465_HRSCAF_1564	3	7659909-7674909	1566860
Loc0687_Hap2	Sc28pcJ_1465_HRSCAF_1564	3	15271297-15271607					
Loc0161_Hap3	Sc28pcJ_1840_HRSCAF_2023	7	9459415-9459701					
Loc0328_Hap2	Sc28pcJ_1840_HRSCAF_2023	7	1636014-1636808					
Loc0527_Hap4	Sc28pcJ_1840_HRSCAF_2023	7	9282396-9282955	61467	Sc28pcJ_1840_HRSCAF_2023	7	6392287-6407287	2875109
Loc0756_Hap3	Sc28pcJ_1840_HRSCAF_2023	7	12003949-12004675					
Loc0896_Hap2	Sc28pcJ_1840_HRSCAF_2023	7	14636614-14637170					
Loc0242_Hap1	Sc28pcJ_1840_HRSCAF_2023	7	19387027-19387901					
Loc0229_Hap2	Sc28pcJ_520_HRSCAF_571	8	523821-526539					
Loc0247_Hap2	Sc28pcJ_520_HRSCAF_571	8	18171569-18172799	16394	Sc28pcJ_520_HRSCAF_571	8	17327004-17342004	829565
				16489	Sc28pcJ_520_HRSCAF_571	8	17814546-17829546	342023
Loc0599_Hap3	Sc28pcJ_520_HRSCAF_571	8	10014159-10015204					
Loc0728_Hap1	Sc28pcJ_520_HRSCAF_571	8	1390556-1392626					
Loc0376_Hap2	Sc28pcJ_520_HRSCAF_571	8	5667809-5668767	14207	Sc28pcJ_520_HRSCAF_571	8	5198014-5213014	454795
Loc0918_Hap1	Sc28pcJ_520_HRSCAF_571	8	6020359-6020661					
Loc0135_Hap2	Sc28pcJ_520_HRSCAF_571	8	9075042-9076180					
Loc0685_Hap1	Sc28pcJ_520_HRSCAF_571	8	3700086-3700691					
Loc0970_Hap1	Sc28pcJ_520_HRSCAF_571	8	16395428-16396978					
Loc0571_Hap2	Sc28pcJ_1131_HRSCAF_1221	10	14374094-14374779	41194	Sc28pcJ_1131_HRSCAF_1221	10	14619986-14634986	260892
Loc0252_Hap2	Sc28pcJ_1131_HRSCAF_1221	10	1803663-1804414					
Loc0684_Hap2	Sc28pcJ_1131_HRSCAF_1221	10	1791911-1792400					
Loc0076_Hap1	Sc28pcJ_709_HRSCAF_769	11	16123808-16124232					

Loc0946_Hap1	Sc28pcJ_709_HRSCAF_769	11	17268706-17269706					
Loc0152_Hap4	Sc28pcJ_709_HRSCAF_769	11	3548866-3549775					
Loc1141_Hap1	Sc28pcJ_709_HRSCAF_769	11	16123655-16123807	31883	Sc28pcJ_709_HRSCAF_769	11	15433527-15448527	675128
Loc0818_Hap1	Sc28pcJ_709_HRSCAF_769	11	14339691-14340334					
Loc0494_Hap1	Sc28pcJ_709_HRSCAF_769	11	6506815-6507339	30607	Sc28pcJ_709_HRSCAF_769	11	7983511-7998511	1461172
Loc0465_Hap1	Sc28pcJ_709_HRSCAF_769	11	18238420-18239608					
Loc0634_Hap2	Sc28pcJ_709_HRSCAF_769	11	3685508-3686206					
Loc1048_Hap1	Sc28pcJ_1844_HRSCAF_2043	12	11524370-11525227					
Loc0988_Hap1	Sc28pcJ_1844_HRSCAF_2043	12	5724624-5725470	69275	Sc28pcJ_1844_HRSCAF_2043	12	386791-401791	5322833
Loc1135_Hap2	Sc28pcJ_1844_HRSCAF_2043	12	6839003-6840062					
Loc0443_Hap3	Sc28pcJ_1844_HRSCAF_2043	12	15522604-15523748					
Loc0802_Hap3	Sc28pcJ_910_HRSCAF_986	13	7559246-7559972	33938	Sc28pcJ_910_HRSCAF_986	13	7865639-7880639	290667
Loc0327_Hap3	Sc28pcJ_910_HRSCAF_986	13	14030061-14030991					
Loc0341_Hap2	Sc28pcJ_910_HRSCAF_986	13	5231561-5232383					
Loc1139_Hap1	Sc28pcJ_910_HRSCAF_986	13	3026981-3028522					
Loc0719_Hap1	Sc28pcJ_910_HRSCAF_986	13	16230004-16230976					
Loc1144_Hap3	Sc28pcJ_1028_HRSCAF_1112	14	369649-370818	36625	Sc28pcJ_1028_HRSCAF_1112	14	5984741-5999741	5598923
				36723	Sc28pcJ_1028_HRSCAF_1112	14	6558194-6573194	6172376
Loc1202_Hap1	Sc28pcJ_1837_HRSCAF_1971	20	12209158-12210675					
Loc0141_Hap2	Sc28pcJ_1837_HRSCAF_1971	20	1171135-1171569	58305	Sc28pcJ_1837_HRSCAF_1971	20	1865398-1880398	693829

APPENDIX B: Ocean acidification influence on gene expression patterns during settlement in *Crassostrea gigas*

Andrea R. Burton, Evan Durland, and Chris Langdon

Table S3.1: Water quality measurements with mean ($\pm SD$) temperature, salinity, total alkalinity (μeq kg^{-2}), total CO_2 (TCO_2), partial pressure CO_2 (pCO_2), bicarbonate (µmol kg^{-1}), carbonate (µmol kg^{-1}), pH (with pH_T = pH on the total scale), saturated calcite (Ω_{calc}), and aragonite (Ω_{rag}) for ambient and high pCO_2 treatments for filtered seawater after 48 hours of culturing (before sea water change).

pCO_2 Treatment	Temp (°C)	Salinity	Alkalinity (μeq kg^{-1})	TCO_2 (μmol kg^{-2})	pCO_2 (μatm)	HCO_3^- (μmole kg^{-1})	CO_3^{2-} (μmol kg^{-1})	pH_T	Ω_{arag}	Ω_{calc}
Ambient	24.8	30.8	2262	2112	817	1968	120.5	7.8	1.95	2.93
	(± 0.7)	(± 0.03)	(± 59)	(± 59)	(± 289.6)	(± 105)	(± 26.3)	(± 0.12)	(± 0.42)	(± 0.64)
High	24.6	30.8	2340	2302	2126	2168	71.3	7.46	1.16	1.74
	(± 0.9)	(± 0.4)	(± 115)	(± 72)	(± 969.2)	(± 67)	(± 56.8)	(± 0.26)	(± 0.93)	(± 1.4)

Table S3.2: Summary of number of up- and down-regulated genes with their associated GO terms from enriched genes from high pCO_2 and ambient for settled spat and non-attached individual cultures model.

Model	Term	GO term	# Up-regulated	# Down-regulated
Att.Spat	Eukaryotic translation initiation factor	GO:0005852	4	6
Att.Spat	Actin cytoskeleton	GO:0015629	3	8
Non.Att	Actin binding	GO:0003779	43	17
Non.Att	RNA-directed DNA polymerase activity	GO:0003964	20	31
Non.Att	Guanyl-nucleotide exchange factor activity	GO:0005085	18	29
Non.Att	Cytoplasm	GO:0005735	184	166
Non.Att	Microtubule-based movement	GO:0007018	37	12
Non.Att	ATP-dependent microtubule motor activity	GO:0008569	10	13
Non.Att	Exodeoxyribonucease III activity	GO:0008853	47	32
Non.Att	Myosin complex	GO:0016459	17	18

APPENDIX C: Methods to assess vulnerability and adaptive potential of understudied organisms to ocean acidification and hypoxia: Estimating heritability of variation in respiration rates in *Haliotis rufescens*

Andrea R. Burton, Hannah Gossner, Francis Chan

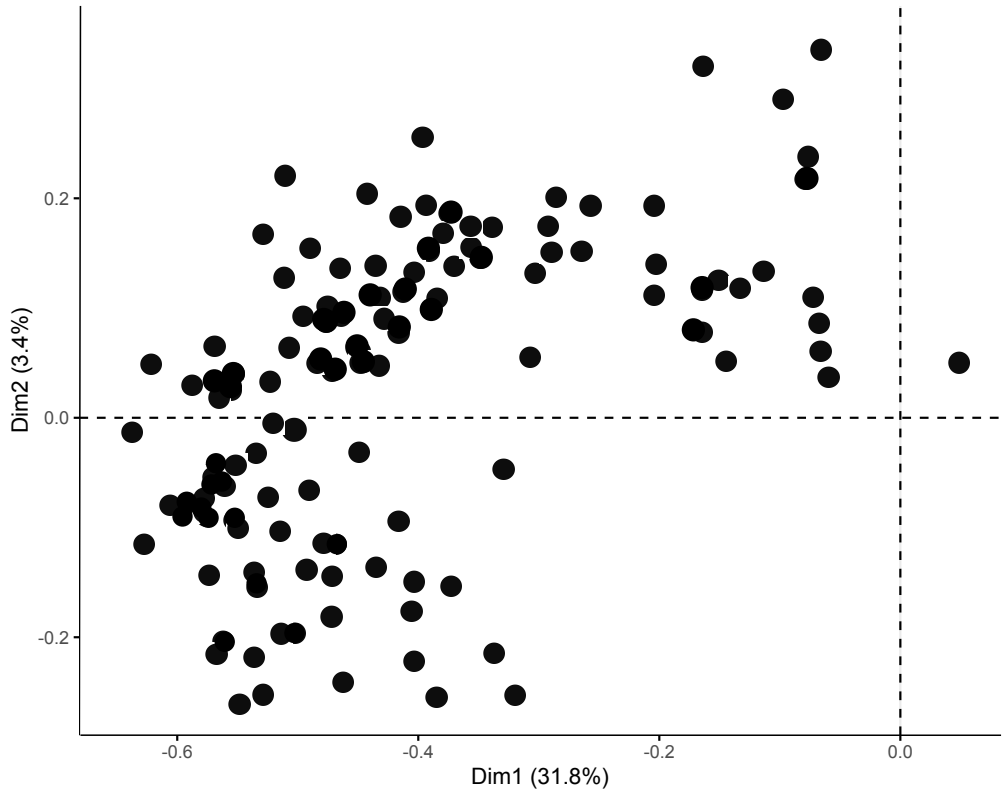

Figure S4.1: Principal component analyses of allele frequencies of each individual.

Table S4.1: Subset of first 100 relatedness estimate pairs for Wang (W) and Lynch & Li (LL) before and after correcting data set by removing individuals with confidence intervals greater than 5 in relatedness estimates and MAF < 0.5.

Pair Number	Animal 1	Animal 2	Before Corrections		After Corrections	
			W	LL	W	LL
1	HR1	HR2	0.0835	0.0293	0.8157	0.7991
2	HR1	HR3	-0.1509	-0.0606	0.7652	0.7359
3	HR1	HR4	-0.1436	-0.0576	0.6709	0.6789
4	HR1	HR5	0.0557	0.0189	0.7374	0.7509
5	HR1	HR6	0.0976	0.0215	0.5508	0.5291
6	HR1	HR7	0.2324	0.1432	0.3229	0.2837
7	HR1	HR8	-0.2225	-0.0979	1	1
8	HR1	HR9	0.2573	0.1059	0.0214	-0.0713
9	HR1	HR10	0.1843	0.0594	0.7331	0.7281
10	HR1	HR11	0.0707	0.0275	0.5898	0.5603
11	HR1	HR12	-0.1755	-0.0726	0.196	0.1529
12	HR1	HR13	-0.033	-0.0144	0.479	0.4912
13	HR1	HR14	0.0394	0.0171	0.3739	0.389
14	HR1	HR15	-0.1752	-0.0498	0.4959	0.4659
15	HR1	HR16	-0.2705	-0.0979	0.8077	0.8027
16	HR1	HR17	0.0837	0.0292	0.6295	0.5977
17	HR1	HR18	-0.1283	-0.0667	0.8775	0.8834
18	HR1	HR19	0.2192	0.081	0.3201	0.3104
19	HR1	HR20	-0.1532	-0.0559	0.5253	0.5105
20	HR1	HR21	-0.0524	-0.0198	0.1416	0.1323
21	HR1	HR22	-0.2333	-0.112	0.4454	0.4288
22	HR1	HR23	1	0.0708	0.6408	0.6212
23	HR1	HR24	0.2129	0.0678	0.4299	0.4469
24	HR1	HR25	-0.3526	-0.1712	0.6786	0.6686
25	HR1	HR26	-0.5589	-0.1699	0.2554	0.2738
26	HR1	HR27	0.304	0.1301	0.3863	0.3662
27	HR1	HR28	-0.1478	-0.0885	0.6224	0.5888
28	HR1	HR29	0.1736	0.0687	0.6276	0.6294
29	HR1	HR30	-0.0385	-0.0145	0.1665	0.0619
30	HR1	HR31	-0.0414	-0.0214	0.3098	0.3131
31	HR1	HR32	-0.2597	-0.1841	0.4479	0.4331
32	HR1	HR33	0.0839	0.0232	0.0554	0.0162
33	HR1	HR34	-0.1747	-0.0928	0.2761	0.2253
34	HR1	HR35	-0.097	-0.0404	0.0189	0.0423
35	HR1	HR36	0.0824	0.0271	0.4964	0.4903
36	HR1	HR37	-0.1245	-0.0616	0.5875	0.578
37	HR1	HR38	-0.2337	-0.1016	0.3302	0.3249
38	HR1	HR39	-0.2072	-0.086	0.414	0.4059
39	HR1	HR40	0.0977	0.0516	0.321	0.244
40	HR1	HR41	-0.0011	-5.00E-04	0.5486	0.5207
41	HR1	HR42	-0.3013	-0.1669	0.338	0.3433
42	HR1	HR43	-0.1542	-0.0696	0.6291	0.5903
43	HR1	HR44	-0.0308	-0.0098	0.6335	0.6187
44	HR1	HR45	-0.0402	-0.0199	0.4777	0.4742
45	HR1	HR46	-0.3013	-0.1364	0.2864	0.2437
46	HR1	HR47	-0.1331	-0.063	0.3645	0.2957
47	HR1	HR48	-0.2532	-0.1295	0.7537	0.7457
48	HR1	HR49	-0.2455	-0.1259	0.7381	0.7368
49	HR1	HR50	-0.2112	-0.0964	0.4898	0.4783
50	HR1	HR51	0.2408	0.0747	0.5783	0.5674
51	HR1	HR52	0.4043	0.1102	0.7909	0.756
52	HR1	HR53	-0.1951	-0.0745	0.1863	0.1309
53	HR1	HR54	0.1113	0.0513	0.8545	0.861
54	HR1	HR55	1	0.0747	0.1405	0.1436
55	HR1	HR56	-0.1983	-0.1053	0.4112	0.3997
56	HR1	HR57	0.2135	0.0604	0.8362	0.824

57	HR1	HR58	-0.1446	-0.0367	1	1
58	HR1	HR59	0.343	0.1682	0.7736	0.7424
59	HR1	HR60	0.0606	0.0098	0.5118	0.4865
60	HR1	HR61	0.0154	0.0083	0.4335	0.4276
61	HR1	HR62	0.3508	0.1062	0.708	0.721
62	HR1	HR63	0.3207	0.0749	0.5133	0.5336
63	HR1	HR64	0.0605	0.027	1	1
64	HR1	HR65	-0.0573	-0.022	0.1543	0.095
65	HR1	HR66	0.0781	0.029	0.4415	0.408
66	HR1	HR67	0.1356	0.0802	0.601	0.5841
67	HR1	HR68	0.4456	0.1596	0.4653	0.4539
68	HR1	HR69	0.108	0.0548	0.652	0.6542
69	HR1	HR70	0.2244	0.094	0.1001	0.1308
70	HR1	HR71	0.0917	0.0463	0.496	0.4723
71	HR1	HR72	0.4891	0.1566	0.5327	0.5176
72	HR1	HR73	-0.0694	-0.0363	0.6495	0.6587
73	HR1	HR74	0.1831	0.0747	0.4317	0.4136
74	HR1	HR75	-0.3363	-0.1452	0.6179	0.6194
75	HR1	HR76	-0.0497	-0.0233	0.767	0.7889
76	HR1	HR77	-0.018	-0.0085	-0.0314	-0.0664
77	HR1	HR78	-0.3018	-0.1496	0.1807	0.1309
78	HR1	HR79	-0.0694	-0.0386	0.3754	0.3795
79	HR1	HR80	0.4962	0.1803	0.2433	0.2466
80	HR1	HR81	-0.1809	-0.0842	0.3143	0.3051
81	HR1	HR82	0.3412	0.1251	0.679	0.6788
82	HR1	HR83	-0.3228	-0.1065	0.7327	0.7099
83	HR1	HR84	-0.053	-0.0218	0.7645	0.7634
84	HR1	HR85	-0.1255	-0.0756	0.2928	0.2852
85	HR1	HR86	0.4714	0.1033	0.0202	-0.0244
86	HR1	HR87	-0.288	-0.0672	-0.0075	-0.0606
87	HR1	HR88	0.5107	0.1711	0.7394	0.7376
88	HR1	HR89	0.0343	0.0116	0.7078	0.7123
90	HR2	HR3	-0.223	-0.0862	0.8901	0.8822
91	HR2	HR4	-0.0498	-0.0289	0.4446	0.4282
92	HR2	HR5	0.0814	0.0298	0.4135	0.3802
93	HR2	HR6	0.1016	0.0269	0.4478	0.4303
94	HR2	HR7	-0.1027	-0.0357	0.1131	0.0397
95	HR2	HR8	0.1659	0.0556	-0.2814	-0.4192
96	HR2	HR9	0.1032	0.0534	0.1026	0.0185
97	HR2	HR10	0.2013	0.1122	0.7258	0.7201
98	HR2	HR11	-0.1138	-0.0359	0.1261	0.1007
99	HR2	HR12	-0.5495	-0.1906	0.2826	0.2576
100	HR2	HR13	0.252	0.0844	0.1498	0.1359

Table S4.2: 95% Confidence intervals from each paired estimate of relatedness for Wang (W) and Lynch & Li (LL) with ranges of confidence intervals greater than 5 calculated by subtracting the lower from the upper limits. Individuals seen in bold were seen in more than one pair of relatedness estimates with confidence intervals greater than 5.

Pair	Ind 1	Ind 2	W: CI	LL: CI
1414	511	**532**	6.0522	5.9209
1443	583	**496**	28.7522	28.7522
1753	476	499	6.3299	6.2898
2171	**561**	**519**	7.0096	6.9934
2172	**561**	523	21.4025	21.3439
2173	**562**	**577**	13.5472	13.4515
2176	596	524	6.2684	6.2537
2204	**593**	526	8.8306	8.8003
2235	590	535	6.147	6.1072
2734	508	510	5.2157	5.216
3428	**553**	**532**	10.5017	10.6482
3859	599	**519**	12.8512	12.8213
4331	557	576	5.1831	5.1509
4436	**577**	478	6.1092	6.0904
4442	568	477	5.3033	5.2616
4553	561	517	6.6347	6.6096
4658	**593**	519	9.4645	9.4341
4798	561	518	6.6873	6.663
5753	**562**	487	10.7043	10.6851
5782	506	538	6.7055	6.7231
5868	**553**	**496**	5.8578	5.8281

Table S4.3: Heritability estimates from Lynch & Li (LL) and Wang (W) after binning MAF every 10%. NAs indicate when estimators that were not able to estimate h^2 due to non-positive definite relatedness matrices.

	LL					WW				
MAF Bin	10%	20%	30%	40%	50%	10%	20%	30%	40%	50%
N loci	172	60	36	34	33	172	60	36	34	33
Model										
Pre.Exp	NA	NA	NA	NA	NA	NA	NA	NA	NA	NA
Base.Exp	NA	NA	NA	NA	NA	NA	NA	NA	NA	NA
Cont.Exp	NA	NA	NA	NA	-0.184 $\pm$ 0.451	NA	NA	NA	NA	NA
Fut.Exp	NA	NA	NA	NA	NA	NA	NA	NA	NA	NA
Pre.Rec	NA	NA	NA	NA	NA	NA	NA	NA	NA	NA
Base.Rec	NA	NA	NA	NA	0.120 $\pm$0.262	NA	NA	NA	NA	NA
Cont.Rec	NA	NA	NA	NA	NA	NA	NA	NA	NA	NA
Fut.Rec	NA	NA	NA	NA	NA	NA	NA	NA	NA	NA